Bidirectional Propulsion of Devices Along the Gastrointestinal Tract Using Electrostimulation

Maurice Paul Burke

University College London

Department of Medical Physics and Bioengineering

Thesis submitted for the degree of Doctor of Philosophy (Ph.D)

I Maurice Paul Burke confirm that the work presented in this thesis is my own. Where information has been derived from other sources, I confirm that this has been indicated in the thesis.

Abstract

This thesis describes a method for propelling devices such as video capsule endoscopes in either direction along the small intestines using electrostimulation-induced muscular contractions. When swallowed, passive diagnostic 'one-shot' devices rely on sporadic peristaltic movement, possibly missing vital 'areas of interest'. This bidirectional propulsion method provides active control for that all-important 'second look'.

Design considerations, within the dimensional constraints, required a device shape that would achieve maximum propulsion from safely induced useful contractions produced by the electrodes and encapsulated miniature electrostimulator. Construction materials would have to produce minimal friction against the mucosal surface while having the physical properties to facilitate construction and electrode attachment.

Design investigations included coefficient of friction measurements of different construction materials and the evaluation of different capsule and electrode dimensions over a range of stimulation parameters, to obtain optimal propulsion. A swallowable 11 mm diameter device was propelled at 121 mm/min with stimulation parameters of 12.5 Hz, 20 ms, at 20 V in an anaesthetised pig. A modified passive video capsule endoscope was propelled at 120 mm/min with stimulation parameters of 12.5 Hz, 20 ms, at 10 V in an unanaesthetised human volunteer. A radio-controlled capsule incorporating an electrostimulator, voltage converter and 3 V power supply was propelled at 60 mm/min with stimulation parameters of 12.5 Hz, 20 ms, and 30 V in an anaesthetised pig.

Other possible uses of electrostimulation were investigated including propulsion of anally administered large intestine devices and introduction of the intestinal mucosal surface into a biopsy chamber. Results are presented.

The ultimate aim of the project was to provide bidirectional propulsion for wireless remote controlled devices along the gastrointestinal tract utilising contractile force produced by electrostimulation of the intestinal wall. The controllability of this system could provide clinicians with a real time view of the entire small intestines without surgical enteroscopy.

Acknowledgements

I would like to thank my supervisors: Dr. Timothy Mills for his support and guidance throughout the project; Dr. Alexander Mosse for his guidance and insight; Professor Jeremy Hebden for his support, guidance and encouragement especially during the latter stages of the project. I would also like to thank Professor Paul Swain and Dr. Annette Fritcher-Raverns for their guidance and insight, providing a clinician's point of view to the project, and also for their clinical expertise, without which testing of the equipment would not have been possible.

I would like to give special thanks to Professor Gary Royle, Dr. Nick Everdell and Dr. Julian Henty for their continued guidance, support, discussions and invaluable transfer of knowledge.

I would like to thank the staff of the Medical Physics Technical Workshop, especially Mr. Billy Raven, Mr. Denzil Booth and Mr. Stuart Morrison for their tuition, guidance and expertise.

I would also like to thank my friends and colleagues in the Department of Medical Physics and Bioengineering who provided a convivial atmosphere within which to work.

Funding for the project was provided by Given Imaging who I would like to thank along with the Department of Medical Physics and Bioengineering for giving me the opportunity to carry out this research.

I would like to thank my family and friends for all their support and encouragement throughout the project. I would especially like to thank my

Table of Contents

9

Table of Figures

11

Table of Tables

1. Introduction

Colorectal cancer is a leading cause of death in the Western World.[1] It is the second most common cause of death from malignant disease in England and Wales.[2] However, if caught early enough it is curable. A number of case control and random volunteer tests[1-12] have shown that there is a significant reduction in the risk of death from colorectal cancer when a screening programme is in operation.

Typically, the first stage of such a screening programme is a faecal occult blood test, which is used to check stool samples for traces of blood that cannot be seen with the naked eye. After this, positive diagnoses are followed up with a colonoscopy, or a double contrast barium enema (an X-ray study using a thin layer of barium sulphate as well as air to aid visualisation of the intestinal tract) where complete colonoscopy is not possible.

Colonoscopy is the 'gold standard' in clinical treatment, detecting 99% of polyps and cancers when compared with histology.[3] However, due to the nature of the procedure it remains technically difficult in 10-20% of cases.[13] It can be time-consuming for the attending clinician as well as daunting and painful for the patient. Most endoscopy units in the UK have difficulty coping with their current workload,[14] and with the introduction of colorectal cancer screening, waiting lists are sure to increase.

With advancing technology, especially in the electronics industry, new methods of imaging the gastrointestinal tract are emerging. A number of these, (such as MRI or CT virtual colonoscopy) take advantage of ever-improving

computer technologies to produce better virtual images of the gastrointestinal tract. Other methods, such as video capsule endoscopy, take advantage of miniaturisation trends within the electronics industry to produce a wireless video camera, which can be used to view the entire gastrointestinal tract.

Video capsule endoscopes such as the PILLCam capsule manufactured by Given Imaging Ltd (Israel) allow painless imaging of the gastrointestinal tract. [15-18] Using a 256 x 256 pixel colour CMOS imager and four white LEDs for illumination, approximately 50,000 images can be transmitted during an eight hour examination. [19-20]

Since gaining FDA approval in 2001, the video capsule endoscope has proved to be a useful diagnostic tool, out-performing 'push enteroscopy' in a study of patients with gastroscopy- and colonoscopy-negative gastrointestinal bleeding. [21] Although promising, these devices rely on natural peristalsis for propulsion. Their movement is therefore out of the physician's control, which is not conducive to a thorough examination.

The aims of this project are to investigate the possibility of remotely propelling a small device, such as a video capsule endoscope, within the gastrointestinal tract in such a way that it could be monitored and controlled in real time. Initially, the aim is to investigate if sufficient propulsion can be achieved, by applying electrostimulation to the mucosal membrane of the gastrointestinal tract in order to stimulate controlled muscular contractions, to propel the device in either direction with or against the natural flow.

As the gastrointestinal tract varies in diameter a range of device sizes will need to be investigated with particular interest on sizes that can be

swallowed. Although initial investigations will be conducted using the pig model, the transfer of results to the human subject will be investigated. Depending on the success of the first phase of the project, the possibility of making a control system that would not require wire leads will be investigated.

1.1   Guide to the Thesis

When designing a device it is essential to have a sound understanding of the environment within which it has to operate. With this in mind, Chapter 2 briefly describes the anatomy and configuration of the gastrointestinal tract, descriptions of the position and path of the tract, and its basic dimensions and structure. There is also a necessity to understand the extent of current procedures used to carry out observations in the gastrointestinal tract. Therefore, the final section of the chapter begins with a brief description of the history and development of various methods used in this field. This is then followed by a brief description of the current methods and procedures used for observing the gastrointestinal tract. The chapter concludes with a discussion on the merits and inadequacies of these different procedures. Due to the fact that the device uses electrostimulation to induce contractions in the intestinal muscle, Chapter 3 reviews the effects of electrostimulation within the gastrointestinal tract.

The design, construction and testing of wire connected prototype capsules are discussed in Chapter 4. The first section discusses the dimensional constraints of a swallowable device. The next section contains an investigation into both the static and dynamic coefficients of friction of different materials

with moist (intestinal) mucosal sections in order to find one that would present a minimal frictional resistive force within the gastrointestinal tract. The choice of optimal mechanical and electrical design parameters for the bidirectional driving device are discussed in the third section, which is followed by a discussion of the construction of the devices. The final section reports on the evaluation of the bi-directional devices within a pig model, and a human subject.

Chapter 5 discusses the design of the electronic circuitry used for the internal electrostimulator. The first section describes the external Grass stimulator used in the preliminary studies. The second section describes the design and development of a miniature 3 volt powered internal stimulator produced to emulate the external Grass stimulator. Details are then discussed on the use of the internal stimulator to drive the devices within the gut, and how the addition of a remote control device would enable the 3 volt powered stimulator to manoeuvre the capsule through the gastrointestinal tract and provide the possibility of developing the bi-directional capsule into a powerful diagnostic tool. Designs of the final control and stimulation circuitry are described. The final sections of this chapter describe the *in vivo* testing of the autonomous capsule in pigs.

The first section of chapter 6 describes the design requirements for a large intestine device. Although similar in design to the small intestine device, it has a larger diameter to account for the larger lumen of the large intestine. A description of the construction of the capsule is followed by a section describing a preliminary *in vivo* test. The second section describes the design and construction of a biopsy capsule are discussed. The first section describes the design of the biopsy chamber and the mechanics of the cutting device. This is

followed by a discussion of how the electrostimulation of the mucosal wall of the gastrointestinal tract can introduce enough tissue into the biopsy chamber for a sample to be taken. The final section of this chapter describes results from *in vivo* testing.

Conclusions and final remarks including a brief summary of the major achievements of this thesis are presented. Potential applications for the findings of the thesis are discussed. Future applications are discussed.

2. Medical Science Background

2.1 Introduction

The design and construction of a medical device involves an understanding of a number of different scientific fields. When designing a device it is essential to have a knowledge of the environment in which it has to operate. As the device has to operate in the gastrointestinal tract an understanding of its anatomy and physiology is required. It is important to understand how observational techniques of the gastrointestinal tract have developed to their current stage, and to evaluate the areas where the proposed device may possibly enhance these present techniques of examining the lumen. This chapter provides some insight into these topics, and in the light of the environmental constraints, an evaluation of current procedures and areas where possible improvements may be made are discussed.

2.2 Anatomy of the Gastrointestinal Tract

The alimentary canal provides the pathway for the body's digestion of food. It is essentially a musculo-membranous tube of varying diameter that extends from the mouth to the anus. This tube is subdivided into a number of different sections and subsections.

Extending some ten meters, the alimentary canal proceeds from its commencement in the mouth through the pharynx and down the oesophagus into the stomach. From the stomach it continues along the small intestine and then the large intestine to its termination at the anus. (Fig. 2.1)

Fig. 2.1 A diagram of the anatomy of the digestive system.

(www.encognitive.com 2012)

For the purposes of this project there will be a brief discussion outlining the major points of the anatomy of the oesophagus, stomach, small intestine and

large intestine. This will include descriptions of both the position and structure of these sections and their subsections. A more in depth discussion of the anatomy outlined here can be found in Appendix B.

The oesophagus is a two hundred millimetres long muscular tube that extends from the pharynx to the stomach. It is generally vertical in orientation with a few curves along its path. It passes down through the neck along a central path in front of the trachea and terminates at the cardiac orifice of the stomach.

The stomach is situated between the oesophagus and the small intestine. As well as being the principal organ of the digestive system, it is also the most dilated part of the gastrointestinal tract. The larger end, known as the fundus, is directed upwards, and the smaller end faces to the right of the body. It is positioned in the left hypochondriac and epigastric regions, placed mainly behind the wall of the abdomen and under the diaphragm.

The small intestine extends on average six metres from the pylorus (the narrowest part of the gastrointestinal tract with a diameter of about 11 mm) to the ileo-caecal valve. Gradually diminishing in size from commencement to termination (diameter of about 30 mm - 25 mm), the small intestine is contained in the central and lower portions of the abdominal cavity, surrounded by the large intestine. A portion of it passes below the brim of the pelvis to lie in front of the rectum.

The large intestine extends from the termination of the ileum to the anus. It has a length of about two metres, which is roughly a fifth of the length of the entire intestinal tract. It is at its largest diameter at the commencement of the caecum (diameter about 30 mm), gradually reducing in size, until at the rectum a dilation of considerable size, (diameter about 60 mm), occurs just above the

anus. It is larger in diameter and more firmly fixed than the small intestine. The course of the large intestine describes an arch which surrounds the small intestine.

The wall tissue of the gastrointestinal tract is mostly composed of four coats; the serous, muscular, areolar, and inner most mucous coat. (Fig. 2.2) However, the oesophagus has only three coats having no serosal coat.

Fig. 2.2 A cross-sectional diagram showing the internal structure of the wall of the gastrointestinal tract. (www.baileybio.com 2012)

The composition of all these coats changes within the different sections of the gastrointestinal tract, having a variety of thicknesses and structures. The outermost serosal coat consists of differing thicknesses of peritoneum, which loosely attaches the gastrointestinal tract to other organs of the body. The

muscular coat consists mainly of two coats of differing thicknesses, one of circumferential smooth muscle cells and another of longitudinal smooth muscle cells. The stomach has extra oblique smooth muscle cells in the cardiac region. The areolar coat joins the muscular coat to the mucosal coat. The innermost mucosal coat varies in thickness and texture, and it aids the transport of boluses along the entire length of the gastrointestinal tract. The gastrointestinal tract follows a tortuous path through the body making it extremely difficult to view endoscopically.[22,23,24]

2.2.1 Physiology of the Gastrointestinal Tract

Gastrointestinal smooth muscle tissue is constructed from small mononucleate cells. They are often considered to be spindle shaped but are generally more irregular than that. When relaxed they are between 500 - 700 μm in length and 5 μm in diameter. They are orientated so that their long axes lie in a common direction. In the gastrointestinal tract there are two layers of smooth muscle tissue. The cells within the inner layer are aligned circumferentially while those within the outer layer are aligned longitudinally.

Smooth muscle cells are many times smaller than skeletal muscle cells, which means they have a very much higher surface to volume ratio. This causes additional problems in maintaining the intercellular content. To overcome this, smooth muscle cells have a membrane resistance per unit area of approximately five times that of skeletal muscle cells.

The peristaltic controlled progression of the contents along the gastrointestinal tract performs an essential function in food digestion. Different patterns of gastrointestinal movements are involved in the progression of the contents along the digestive tract and they are the result of the interplay between activity of gastrointestinal smooth muscle and the enteric neural circuits.[25]

Small intestine peristaltic contractions have been categorised into phasic type I and tonic type III waves. Type I waves are responsible for the propulsive movement, and have a duration of between 2.6 and 5 seconds with an amplitude of between 3 and 75 mm Hg. Type III waves are responsible for the motility, and consist of an elevation of 30 mm Hg. They act as a base-line on which type I waves are superimposed. They have a duration of between 10 seconds and a few minutes.[26,]

2.3   Pathologies of the Gastrointestinal Tract

The pathologies of the gastrointestinal tract are diverse and numerous. They range from inflammatory diseases to tumours, which occur within the lumen of the tract. This section will present an overview of the major types of the pathologies that can be identified by using a video capsule endoscope.

Oesophagitis occurs in many different forms, which can be grouped into four main categories: reflux, columnar-lined (Barrett's), infective, and other. The most common of these occurs due to reflux of material from the stomach, although some occur as a result of ingestion of injurious agents.[27]

Gastro-oesophageal reflux is commonplace in healthy individuals to some degree, occurring usually after meals and also during pregnancy, with heartburn occurring weekly in approximately 20% of individuals.[28,29, 30]Contact and injury of the oesophageal epithelium by acid, and persistent or transient loss of tone of the lower oesophageal sphincter is generally accepted as the major determinant of reflux.[31] A number of factors influence the occurrence of inflammation or reflux change including the number and nature of refluxate,[32, 33] the efficiency of secondary peristalsis to clear the reflux material from the oesophagus,[34] the resilience of the oesophageal epithelium to injury and the neutralising effects of bicarbonate rich saliva and secretions of the oesophageal glands.[35,36,] Several grading systems exist to define the macroscopic appearances of reflux oesophagitis, which are observable endoscopically.[37]

Reflux changes consist of basal cell hyperplasia occurring in a layer of more than 15% of the thickness of the oesophageal epithelium. This has been found with a random distribution over the distal 80 mm of the oesophagus.[38] However, these appearances can occur normally in the lower 20 mm of the squamous-lined oesophageal mucosa as a result of physiological reflux.[39-41]

There are cases where, some individuals with reflux oesophagitis, for reasons which are still unknown, have part of the stratified squamous epithelium replaced with columnar epithelium. This condition was first described by Barrett,[42] who mistakenly thought it was a consequence of a congenitally short oesophagus. Since its discovery, there have been a number of reports of dysplasia and carcinoma complicating this condition,[43-49] with a risk of development of adenocarcinoma. [48, 50-54] Barrett's oesophagus causes the mucosal lining of the lower oesophagus to be velvety red-orange in

appearance,[55] and the wall is hypotonic and no longitudinal folds are present. (Fig. 2.3)

Fig. 2.3 Barrat's oesophagus seen as reddening from the oesophageal sphincter replacing normal paler oesophageal tissue. (www.patient.co.uk 2012)

The oesophagus is usually very resistant to infection. However, oesophagitis can occur during infectious diseases such as measles, scarlet fever, diphtheria, and typhoid. Candidal oesophagitis is the most common form of infectious oesophagitis and is characterised by creamy white patches in the middle or lower oesophagus. (Fig. 2.4) In chronic cases the mucosa shows warty lesions with central ulceration. Perforation and fistula can occasionally occur and oesophageal stricture can result in chronic cases. [56, 57]

Fig. 2.4 Candidal oesophagitis characterised by creamy white patches.

(www.ganfyd.org 2012)

Crohn's oesophagitis may be the presenting feature of Crohn's disease, and can occur without the presence of the intestinal disease. Its oesophageal presence is now well recognised and appears to be more prevalent in children than adults.[58-61] Depending on the stage of the disease erosive oesophagitis, with or without stricture formation, occurs with shallow and irregular ulcers in the mucosa, in a cobblestone pattern.[62] (Fig. 2.5)

Fig. 2.5 Crohn's oesophagitis showing irregular ulcers in the mucosa in a cobblestone pattern. (1.bp.blogspot.com 2012)

Benign epithelial tumours are usually small with a warty surface and usually occur in the lower third of the oesophagus.[63] These have to be differentiated from inflammatory polyps which are smooth in appearance and occur due to oesophageal reflux.[64, 65] The only true adenomas occur with Barrett's oesophagus.

There are 310,000 cases of oesophageal cancer per year worldwide.[66] At least 90% of these are squamous carcinomas, with the rest being adenocarcinomas, small cell carcinomas and malignant melanomas. Squamous carcinomas appear in the top third of the oesophagus as exophytic, ulcerating or infiltrating lesions, or a combination of these and often results in an irregular, friable or haemorrhagic stricture.[67-69] Nearly all adenocarcinoma of the oesophagus and gastro-oesophageal junction are believed to occur due to malignancy of Barrett's oesophagus. The majority of these are flat, ulcerating, infiltrative lesions associated with stenosis of the oesophageal lumen, with a minority appearing polypoid and fungating.[70,71] (Fig. 2.6) Other adenocarcinomas, which do not arise from Barrett's oesophagus are uncommon. Adenosquamous carcinomas are uncommon aggressive tumours, which occur when the adenocarcinomatus and the squamous carcinomatus components are intermingled. Most cases are associated with Barrett's oesophagus. [72,73]

Fig. 2.6 Adenocarcinoma of the oesophagus (trialx.com 2012)

Since the first description of primary small cell carcinoma of the oesophagus there have been 230 reported cases.[74, 75] In the majority of cases the tumours have been large and found in the lower half of the oesophagus.

Characteristically malignant melanoma tumours are large, polypoid and friable, which may or may not be pigmented, with adjacent mucosa showing patchy or diffuse melanosis and satellite lesions in some cases.[76-78] These are more likely to develop as secondary rather than primary melanomas.[78-81]

Oesophageal carcinomas spread to other parts of the body using two major methods; directly, or through metastasis. The most common and extensive form of direct spread is in the wall of the viscus, particularly in the submucosa and submucosal lymphatics,[82,83] However, spread along the ducts of the oesophageal glands is not uncommon.[84] By the time the diagnosis of symptomatic oesophageal carcinoma is confirmed, metastases have occurred in 50-80% of cases. The most common sites for metastasis are the regional lymph nodes. Another potentially important pathway for tumour spread is intramural metastasis.[85] Visceral metastasis most commonly spreads to the lungs, liver and the adrenal glands, and is found in 70% of all cases.[86-89]

Secondary tumours are rare in the oesophagus, with direct spread occurring usually from the stomach into the lower end of the oesophagus, and less commonly from the bronchus or thyroid.[89-91] Lymphatic spread occurs from carcinoma of the breast,[89, 90, 92, 93] and visceral metastasis from primary tumours in the testis, prostate, kidney, endometrium and pancreas.[89, 90, 94-98]

Fig. 2.7 Hyperplastic polyps (gastrolab.1g.fi 2012)

Gastric adenomas are uncommon and a lot less frequent than hyperplastic polyps which they resemble on gross appearance. (Fig. 2.7) They are usually solitary and occur mainly in the antrum or on the boundary of the antrum and gastric body. Their importance is their significant potential for turning malignant. Synchronous carcinoma coexist in a significant number of cases of gastric adenomas so close inspection of the surrounding mucosa is required.[99,100]

Fig. 2.8 Gastric adenocarcinoma (trialx.com 2012)

Gastric adenocarcinoma (Fig. 2.8) was reported to be the most common form of cancer in 1980, but by 1990 it had been surpassed by carcinoma of the lung. [101, 102] It is generally a condition that occurs in the middle aged and older generations. Carcinomas of the distal stomach are most common in the prepyloric, pyloric antrum, and lesser curvature regions. Tumours in the cardia region are generally of a smaller size. Gastric cancers may be ulcerating, nodular, fungating or infiltrative. Ulcerated malignant tumours tend to be larger than their benign counterparts, whereas the other tumours consist of friable masses, which project from a broad base into the cavity of the stomach. Many gastric tumours, independent of type, secrete mucin giving them a gelatinous appearance.[103]

Gastric carcinomas spread by four distinct methods: direct, lymphatic, haematogenous and transperitoneal spread. Gastric carcinomas are highly infiltrative, the majority of which infiltrate through to the subserosa. Penetration of the serosa may lead to direct spread to the pancreas, liver, spleen, transverse

colon and omentum. Lymph node metastasis is reported to have been present in 90% of autopsies and 70% of surgical resections, although, the latter figure of 70% may now be reduced due to lesions being discovered at an earlier stage of the cancer. The incidences of lymph node metastasis is related to the increase in depth of penetration of the tumour through the stomach wall. Metastasis through the blood stream occurs by invasion of the tributaries to the portal venous system and can affect any organ, but most commonly the liver, then the lungs, peritoneum, adrenal glands, skin and ovaries. The latter can also be infected through a transperitoneal route. [104]

Crohn, Ginzberg, and Oppenheimer described the condition of regional enteritis, the terminal ileal presentation of Crohn's disease, in 1932,[105] although it was first described by Dalziel in 1913.[106] Until the 1960's it was believed that Crohn's disease only affected the small intestine, but it is now known that it is pangastrointestinal making differentiation between it and the other major inflammatory bowel disease, ulcerative colitis, very important. Crohn's disease can also manifest itself outside the gastrointestinal tract, in the skin, eyes and joints.[107-111] The disease within the small intestine appears initially as ulceration, with strictures and fissures occurring as the disease progresses producing a cobblestone pattern within the mucosa in about a quarter of cases. (Fig. 2.9)

Fig. 2.9 Crohn's disease of the small intestine. (www.medgadget.com 2012)

Epithelial tumours are rare in the small intestine in comparison with their occurrence in the large intestine. Although the small intestine contributes 75% of the mucosal surface area of the gastrointestinal tract, malignancies of the large intestine are 50 times more numerous.[112] The small intestine is the site of only 1% of all gastrointestinal carcinomas.[113, 114] Carcinomas, lymphomas (Fig. 2.10), and sarcomas occur most frequently in the distal small intestine and least frequently in the duodenum; the opposite is true for adenomas and adenocarcinomas.[115, 116] Most small intestine carcinomas are annular and constricting, although a minority are polypoid or fungating.

Fig. 2.10 Small intestine lymphoma (www.gastrointestinalatlas.com 2012)

The overall appearance of colorectal Crohn's disease is fundamentally the same as that seen in the small intestinal disease. Adenomas are more common in males, but are more likely to become malignant in females.[117-119] Adenomas are uncommon before the age of thirty, with prevalence increasing with age reaching a plateau by seventy, yet adenoma frequency is less age dependent than carcinoma frequency.[120] The malignancy potential of adenomas is determined by their size, growth pattern and grade of dysplasia. Up to 40% of all large intestinal cancers occur in the rectum and rectosigmoid area. The sigmoid colon accounts for a further 25%. Most cancers of the large intestines remain relatively small in comparison with tumours found in the stomach.

The pathologies of the gastrointestinal tract are numerous and varied. The anatomy of the gastrointestinal tract makes visualization of mucosal surface and therefore the diagnosis of these pathologies difficult. The next section reviews the development of gastrointestinal visualization by presenting descriptions of the historical and current methods.

2.4   Methods of Observing the Gastrointestinal Tract

This section begins with a brief description of the development history of the various techniques used for the examination of the gastrointestinal tract. This is then followed with a review of the current methods available which includes a comparison of the merits and limitations of these procedures.

2.4.1 Contrast Enema

In the year following the discovery of X-rays by Roentgen in 1895,[121] attempts were made to obtain an X-ray visualization of the gastrointestinal tract with the use of contrast agents. Becher[122] used a lead salt, which was administered orally to guinea pigs.

During the period 1897 - 1901, Rumpel and Hilderbrand[123] instilled air into the rectum several days after the oral administration of a bismuth salt. This research produced a visualization of the transverse colon.

In 1904, Rieder[124] reported that the rectal instillation of bismuth salt was superior to its oral administration.

In 1910 Bachem and Guenter[125] used a suspension of barium sulphate to replace bismuth subnitrate. This new suspension had similar properties to the bismuth subnitrate but was cheaper to produce and safer to use. The introduction of barium sulphate made the wide spread use of the contrast enema procedure possible.

. In 1923, Fischer[126] performed the first double contrast enema. He succeeded in the visualization of the intestinal contours by using the administration of a barium sulphate suspension along with air, which also overcame the problem of interference from adjacent superimposed intestinal loops. In 1927, Bouwers[127] developed the rotating anode X-ray tube

In 1955 the convincing results produced by Andren, Frieberg and Welin[128] with their refinements to the double contrast examination of the colon led to its acceptance as a standard method. The colon was initially filled to the splenic flexure, then evacuated for visualization of the mucosa and finally insufflated with air for double contrast visualization. This method was particularly good for detecting small polyps and inflammatory changes.

In 1971, Sellink[129] introduced the small bowel enema (enteroclysis). In 1973, Hamelin and Hurtubise[130] angulated the overhead tube for visualization of the sigmoid colon. In the following year Miller, Chemish, Skucas, Rosenak, and Rodda[131] proposed the use of pharmacologically induced hypotonia of the colon (using glucagon), for use in double contrast enemas

2.4.2 Endoscopy

In 1806 Bozzini[132] used a tin tube, illuminated with a candle through mirrors, to inspect body cavities. Sixty-two years later (1868), Kussmaul[133] developed the first gastroscope. It was a rigid metal tube that was inserted using a previously placed flexible obturator as a guide.

In 1881 von Mikulicz-Radecki[134] used a tube 65cm in length, and 13mm in width, with its distal quarter slightly angulated.

In 1923 Schindler[135] introduced gastroscopy into Europe and also the USA. Nine years later, Schindler[136] constructed the flexible gastroscope.

In 1952 Hopkins, Kapani, and van Heel[137] suggested using flexible optic fibres for the sigmoidoscope. Five years later Hirschowitz, Curtiss, Wilbur Peters, and co-workers[138] developed the prototype of a fibre optic gastroscope. Six years after this in 1963, Oshiba, Watanabe, Niwa, Kanazawe, and Tanaka[139] constructed the prototype of a fibre optic scope.

2.5 Current Methods and Techniques of Observing the Gastrointestinal Tract

When the purpose of designing a device is to aid observation of the gastrointestinal tract, it is essential that there is an understanding of the current methods that are being used. There are a wide range of techniques available to the medical profession, from contrast enema to virtual colonoscopy.

This section discusses the variety of different tools and techniques used for these observations, reviewing both their merits and inadequacies as diagnostic tools.[140]

2.5.1 Radiological Examination of the Colon Procedures

The radiological methods for examination of the colon can be divided into two categories; those that involve a barium enema visualization procedure and those that involve an antigrade visualization procedure.

2.5.1.1 Precursory Visualization of the Colon

In preparation for a barium enema, the abdomen is flouroscopically screened. Radiographs are then obtained if abnormal findings are encountered (e.g. residual contrast medium, foreign bodies, calcifications, toxic megacolon, ileus, faeces, pneumoperitoneum). [140]

2.5.1.2 Single Contrast Enema with Single Suspension

The single contrast enema examination requires a fully cleansed colon. The cleaning of the colon is of paramount importance as any faecal residue may lead to diagnostic misinterpretations. Preparation of the colon consists of dietary restrictions, hydration, laxatives and cleansing enemas. A preparation enema is administered 1-2 hours before the examination to those patients who have not followed the usual prerequisite dietary regime.

This technique is used in order to gain a visualization of an overall profile view of the large intestine and can also be used to detect possible obstructions. Single contrast enema is used as the first part of a biphasic colon examination.[140]

2.5.1.3 Double Contrast Enema

The double contrast enema is the current standard technique for radiological examination of the colon. (Fig. 2.11) This method uses a thin barium coating of the mucous layer to outline the colon together with simultaneous luminal air distension to open and separate adjacent loops. The method requires a cleansed colon, good barium preparation, a relaxed colon, and a good radiographic technique. This examination requires the same type of preparation as that for the single contrast examination. The colon must be totally cleansed of faecal material.

Colonic segments such as the caecum and the ascending colon are fully accessible with this procedure. There is also partial accessibility to the transverse colon, descending colon, and the sigmoid colon with the aid of palpation, (a simple technique in which a doctor presses lightly on the surface of the body to feel the organs or tissues underneath).

Pathological changes are demonstrated in two projections, the orthograde and the tangential projections, which are used primarily in the visualization of diverticula, polyps, carcinomas, fistulas, and the appendix. Additional projections at different angles may also be used.

The double contrast examination has many advantages over the single contrast examination. The double contrast examination offers an improved evaluation of the mucosal surface by identifying fine ulceration, granular mucosal patterns, follicular hyperplasia and small polyps. Superimposition of

adjacent intestinal loops is less problematic as the colon is "transparent". The double contrast examination gives a good demonstration of impaired distensibility, and the evacuation reflex is also reduced.[140]

Fig. 2.11 Double contrast radiograph of large intestine.

(http://www9.biostr.washington.edu/hubio511/RadAbdo/frames.htm 2012)

2.5.1.4 Biphasic Colon Examination

This examination combines both the single and double contrast examinations. The single contrast enema is performed first, followed by the double contrast enema which is performed with the instillation of air after evacuation of the barium salts.

During the single contrast enema component of this biphasic examination, spot films of various colonic segments are obtained during the retrograde flow of the barium, with the patient table being rotated into a viewing position that excludes overlapping colon loops. Compression views of the caecum, a survey radiograph, and a post evacuation film are also taken. During the double contrast enema component of this biphasic examination the patient's table is required to make three rotations.[140]

2.5.1.5 Instant Enema

This is an examination that is performed without prior preparation. It uses a double contrast examination for colitis and a single contrast examination for distal obstruction, using barium sulphate solution or water-soluble contrast agents.

A preliminary radiograph of the abdomen is taken to exclude a toxic megacolon or perforations. Barium sulphate suspension is then administered. Instillation, the same as that for the double contrast examination, is undertaken

by initially filling the colon to the splenic flexure, followed by air insufflation, and drainage of the rectum. Adequate visualization of the affected colonic region is possible (as there is now no faecal matter present) without attempting to produce visualization of the remaining normal colon.[140]

2.5.1.6 Air Enema

The air enema examination is used in the case of acute colitis. There is no need to cleanse the colon before this procedure because the colon is free from faecal matter as a result of this condition. Air is gently insufflated into the patient under fluoroscopic guidance and radiographic images are taken of the abdomen.[140]

2.5.1.7 Water Enema

A water enema is used to verify a suspected lipoma of the colon. This examination method, which makes use of the difference in the absorption energy of water and fat, manifests the lipoma as a radiolucent region. This method has not found widespread use with lipomas, which are usually diagnosed by endoscopic, CT or MRI examinations.

The cleansing preparation for this procedure is the same as that for the double contrast enema examination. Retrograde filling of the colon with water is

performed through a rectal tube. Radiographical images of the area under investigation are taken from different projections and with compression.[140]

2.5.1.8 Antegrade Examination of the Intestines

There are two distinct procedures for performing this examination. The first is the small bowel series, and the second is enteroclysis.

The small bowel series procedure consists of 800-1200 ml of barium suspension being administered orally. When the ileo-caecal region and the ascending colon have filled with barium, double contrast visualization is possible. Effervescent powder is administered orally and a waiting period is required for the gas to progress to the desired region. Air is also insufflated into the rectum through a rectal tube to enhance visualization.

The enteroclysis procedure commences with the duodenum being intubated with a Bilbao-Dotter tube and the tip advanced to the duodeno-jejunal junction with a guide wire. Then an infusion of 700 ml of barium suspension is administered. An injection of air, or water with a 5% methylcellulose solution, when passed through the tube results in excellent visualization of the entire small intestine. Rectal insufflation of air, after the barium suspension has reached the ascending colon, also creates suitable conditions for a good visualization of the region.[140]

2.5.2 Virtual Colonoscopy

Virtual colonoscopy is a non-invasive method of examining the entire small and large intestines. There are two different methods of performing such virtual colonoscopies. The first method uses images produced from a number of Computer Tomographic (CT) scans, and the second method uses images produced from a number of Magnetic Resonance Imaging (MRI) scans.[141,142]

2.5.2.1 CT Colonoscopy

Effective CT colonoscopy (CTC) has grown out of the rapid increase in computer technology. Since 1994, when the Vining group produced the first 3D images of the colon, both 2D and 3D images of the colon have been of beneficial use in colonic diagnoses.[143,144]

This method of colorectal imaging offers rapid visualisation of the complete colorectal area allowing for greater patient comfort and convenience. There is no need for sedation of the patient or risk of perforation as the only invasive component of the procedure is the introduction of an enema tip for insufflation of the colon. A great deal of preparation is required, however, followed by adequate distension of the colon. This can produce discomfort for the patient as well as being time consuming for the attending radiologist.

Before the screening can take place the patient has to undergo adequate preparation of the colon. This preparation, similar to that required for the contrast enema procedure, consists of two prerequisite parts. The first is that the

patient limits their oral intake, to clear liquids or to a low residual diet, during the 24 hours before screening is due to begin. The second is that the patient ingests a cathartic or laxative to promote the evacuation of the colonic content.[145, 146, 147]

Cleansing is essential because of the detrimental effects that any faecal matter or excess fluid remaining in the bowel can have on the CT images. Faecal matter appears as areas of possible interest in the scans resulting in a false positive diagnosis, whereas excess fluid can obscure actual areas of interest, resulting in a false negative diagnosis.

Adequate distension of the colon is just as important as proper cleansing for the success of CT colonoscopy. Collapsed portions of the colon may cause some polyps to remain undetected there by leading to a false negative diagnosis, or they could suggest possible carcinomas, which narrow the lumen, resulting in a false positive diagnosis.[145,147]

When the colon has been adequately prepared and distended a number of CT scans of the abdomen are taken. The resulting images are used, together with computer software, to reconstruct a virtual colon for examination by the attending radiologist.[148]

The scanners can produce two-dimensional and three-dimensional images (Fig. 2.12) providing the opportunity for different diagnostic techniques to be exploited. Using this stored data and dedicated computer software, the virtual colonoscopies can then be regenerated at any future time.

Fig. 2.12 CT colonography showing both the external and internal surfaces of

the large intestines. (http://www.mtbakerimaging.com 2012)

The introduction of multidetector array computed tomography, (MDCT), in late 1998 provided the capability of producing thinner reconstruction scan widths. The scanning acquisition times were comparable to those of the single detector array computed tomography, (SDCT). Additionally these new systems produced images more rapidly than the SDCT, and consequently images of comparable quality could be acquired with decreased radiation dosage.[149]

2.5.2.2 MRI Colonoscopy

In recent years MRI colonography (Fig. 2.13), has evolved as a potential colorectal cancer screening strategy, but it still requires further development. With continued improvements in multi-slice CT colonoscopy, now enabling the combination of lung and colon imaging during one pause in breathing with automated dose optimisation, MRI colonography has largely been superseded. However, the main potential role for MRI colonography is still colorectal cancer screening, but it can also play an important role with patients who have undergone incomplete endoscopic colonoscopy. MRI colonography can achieve an examination of the entire colon in these patients.[150,151]

Currently MRI colonography patients undergo a bowel cleansing similar to that used in other methods of colonic observation. It has been found recently that MRI imaging is a useful non-invasive tool when used for patients with Crohn's disease, as it can be used to assess disease activity. MRI colonography can also be used to demonstrate the nature and extent of a Crohn's disease stricture if the small intestine is ante-retrograde filled and distended by the enema. A resected ileum facilitates retrograde filling of the small intestine.

Fig. 2.13 MRI colonography showing exterior and interior view of large intestine (http://www.mr-tip.com/exam_gifs/mr_colonography_gadolinium_per_rectum_1.gif, http://radiology.rsna.org/content/223/1/248/F2.small.gif 2012)

Motion artefacts can interrupt this procedure when data acquisition per slice takes the complete imaging time. This means that 2D and 3D gradient echo images are sensitive to motion artefacts. In contrast, the half-Fourier acquired, single-shot, turbo spin-echo/single-shot, fast spin echo (HASTE/SSFSE) technique allows sequences to be performed while patients are breathing, because of the serial acquisition nature of the device which takes fewer than 300 ms to acquire a slice. However, natural peristaltic movement of the colon also produces motion artefacts. These are decreased with the use of muscle relaxants. [152, 153]

Just as the double contrast enema procedure requires an optimally distended colon, the MRI colonography also requires this, in order to obtain the maximum mass detection. To achieve this, a positive contrast liquid or gas enema is usually used, although in some cases a negative contrast liquid or gas enema, such as water or air, can be used.

2.5.3 Endoscopy (Push Enteroscopy)

There are five types of conventional endoscopic instruments for inspecting the gastrointestinal tract; the proctoscope, proctosigmoidoscope, colonoscope, gastroscope and double-balloon enteroscope. (Fig. 2.14)

The proctoscope is used for examinations of the anus and anal conditions and as part of a cancer screening program (beginning at the age of 45 years for those deemed to be at risk). It is also used for an initial examination before the use of either a proctosigmoidoscope or a colonoscope. Generally, it is not necessary to prepare the colon, as normal bowel movement prior to the examination is usually adequate, but if the distal rectum is still full, a Fleet enema is given.

Proctosigmoidoscopy is performed on all patients with intestinal complaints and is part of the physical examination of any patient older than 35 years. As with anal proctoscopy, proctosigmoidoscopy can be used to examine anal conditions such as pain, pruritus, perianal bleeding, passage of mucous, or haemorrhoids. It can also be used to investigate intestinal haemorrhage, positive guaiac test, diarrhoea or constipation.

Colonoscopy is performed if areas of concern are radiographically found or suggested, or if there has been an inconclusive radiographic examination. It is also used as a follow-up examination of a precancerous condition, as a follow-up of an anastomosis, or used in cases of observed bleeding. Colonoscopy is also a therapeutic tool, used to perform, polypectomy, coagulation of bleeding sites, or removal of foreign bodies.[154]

Proctosigmoidoscopy and colonoscopy require a similar preparation of the colon as that used for radiographic examinations although no dietary restrictions are necessary. The colon is considered to be clear when the evacuant is clear of faecal matter.

Fig. 2.14 Images of a proctoscope, sigmoidoscope, colonoscope, gastroscope and a double balloon enteroscope.

(http://www.rbmedical.co.uk, http://www.generalmanual.com , http://www.zgrum.com/, http://img.medicalexpo.com, http://www.suatozden.com/ 2012)

Gastroscopy is performed by oral approach and allows a physician to endoscopically view the oesophagus, stomach and the proximal small intestine.

The procedure requires the patient to follow a controlled diet up to twenty four hours before the procedure.

Total enteroscopy is performed initially using double balloon endoscopy by anal approach, where a tattoo is injected at the most proximal site reached by the endoscope. Double balloon endoscopy is then carried out by oral approach to examine the remaining area. Double balloon endoscopy by oral approach is performed within two days after the anal approach. Before both approaches, intestinal looping is checked fluoroscopically. The anal approach is performed after bowel preparation with an oral electrolyte lavage, the same as that used for regular colonoscopy. The oral approach is performed after overnight fasting. Patients are sedated if necessary, with blood pressure, heart rate, and oxygen saturation monitored during the procedures.[154]

2.5.4 Video Capsule Endoscopy

Research and development of the video capsule endoscope was initiated in 1995, by Dr. Paul Swain's (London, UK) group and Dr. Gavriel Iddan (Israel) both working independently. In 1996 these two groups collaborated and by 1999, working prototypes were produced.[155,156] This research and development culminated in the introduction of the M2A video capsule endoscope produced by Given Imaging Ltd (Israel), and it has provided a new method of endoscopy, which allows painless endoscopic examination of the entire small intestines.[157]

The patient is required not to eat any food for ten hours before the examination is to take place. The patient is then asked to wear a special belt, which receives and records the transmitted images, which come from the M2A. The M2A capsule is then swallowed with the aid of a glass of water. Video images and positional data are acquired as the M2A passes through the digestive system. This information is then transmitted via an array of sensors secured to the abdomen, to the DataRecorder attached to the belt worn around the patient's waist. The eight-hour examination can be conducted while a patient continues their normal daily activities. The patient returns the DataRecorder for processing on the RAPID workstation. The RAPID application enables the physician to view and analyze the Patient Rapid Report (PRR), save individual images or short video clips and add comments for consultation and reports.[158]

Fig. 2.15 Images of the PillCam ESO 2, SB 2, and COLON video capsule endoscopes. (www.givenimaging.com 2012)

Given Imaging Ltd (Israel) first received FDA approval for their M2A wireless video capsule endoscope in 2001, and rebranded it PillCam. Since 2005 there have been several technological advances, both in the capsule itself and the associated hardware and software, that have greatly improved image quality and battery lifespan. Video capsule endoscope systems consist of a capsule, a sensing system, and a workstation. Portable external viewers for direct monitoring of the images received during the examinations are also available. Currently, capsule endoscopy systems are manufactured by four companies. Video capsule endoscopy devices available from Given Imaging Ltd (Israel) include the PillCam SB for the small intestine, the PillCam ESO for oesophageal imaging and PillCam COLON for the large bowel. (Fig. 2.15) Olympus (Japan), IntroMedic (Korea) and Chongqing Jinshan Science and Technology Group (China) have entered the sector and produced the EndoCapsule, MiRo-Cam and the OMOM respectively, all for use specifically in the small bowel. The different companies have approached the video capsule endoscope system in slightly different ways. The four capsules differ with regard to the type of sensor used, the capsule dimensions, image acquisition frame rate, field of view, and recording duration, which can be seen in more detail in Table 2.1.

	PillCam SB2	EndoCapsule	MiRo-Cam	OMOM capsule
Length, mm	26	26	24	27.9
Diameter,mm	11	11	11	13
Weight, g	3.4	3.8	3.4	6
Frame rate, frames/second	2	2	3	0.5-2
Image sensor	CMOS	CCD	CCD	CCD
Field of view	156°	145°	150°	140°
Illumination	6 white LEDs	6 white LEDs	6 white LEDs	NA
Antennas (body leads), n	8	8	9	14
Real-time (RT) view	RT viewer	VE-1 viewer	Miro-Viewer	RT monitoring
Recording time, hours	8	9	11	7-9

Table 2.1 Comparison of available small intestine video capsule endoscopes.

Video capsule endoscopes allow patients to continue daily activities throughout the endoscopic examination, although patients are advised not to undergo heavy exercise. Water can be consumed two hours after capsule

ingestion and food eaten after four. Patients are asked to make a record of any abdominal symptoms and check a blinking light on the belt pack to confirm signal reception. [158] Originally designed to image the entire gastrointestinal tract, video capsule endoscopes have for the first time allowed non-invasive visual observation of the mucosal surface of the entire small intestine. The full range of indications within the small intestines is becoming apparent as these devices get more clinical exposure. The main indications are obscure gastrointestinal bleeding, iron deficiency anaemia, non-stricturing small intestine Crohn's disease, celiac disease, hereditary polyposis syndromes and small intestinal tumours.[159]

The major adverse event associated with video capsule endoscopy is the retention of the capsule due to intestinal obstructions such as stricture, stenosis, diverticula and fistulas. To investigate the possibility of retention, Given Imaging Ltd (Yoqneam, Israel) have produced a patency system consisting of a self-disintegrating AGILE capsule without a camera but containing a radio-frequency identification (RFID) tag and a RFID scanner. The AGILE capsule is identical in size to the small-bowel PillCam. This solid, biodegradable capsule contains the small RFID tag (2×12 mm) within a radio-opaque lactose and barium body. This body is coated with an impermeable membrane of parylene except for two small windows that allow luminal fluid access to paraffin timer plugs to bring about disintegration of the capsule within 30 hours. The capsule remnants can pass through even small orifices. Detection of a radio-frequency signal by the scanner indicates that the capsule is still in the gastrointestinal tract. The radio-opaque capsule can be detected by plain abdominal X-ray.[160]

54

Functional patency is verified by this test if the AGILE capsule is egested intact without any change in its original dimensions, irrespective of the time of expulsion, or, if the RFID tag is not detected when the patient is scanned at 32–38 hours. Patients at high risk who develop pain during the AGILE capsule test are not eligible for video capsule endoscopic examination.[161]

In 2004, Given Imaging Ltd (Israel) developed the PillCam ESO as a non-invasive device for the examination of the oesophagus. The video capsule endoscope, although similar in size to the intestinal capsule, was equipped with a camera at each end, allowing the capture of 14 images/second, 7 from each. The operating time was 20 minutes. A new version, the PillCam ESO 2, was released in 2007. It has almost twice the field-of-view, a 50% increase in depth-of-view, a frame rate of 15 frames/second, and better image quality with a wide dynamic range, and illumination that can be adjusted in real time to provide optimal images.

A specific ingestion protocol is required to slow down the transit of the capsule in order to increase the examination duration of the oesophageal mucosa. Patients lie down on their right side, and following ingestion of the capsule, swallow sips of water every 15 seconds over 3 minutes. The main indications for oesophageal video capsule endoscopes are screening of Barrett's oesophagus and of oesophageal varices.[162]

A recent addition to the number of video capsule endoscopes on the market was the PillCam COLON capsule. The device has some technical aspects that are different from those of the small intestine capsule. It is approximately 6 mm longer and like the PillCam ESO it has dual cameras that enable the device to acquire video images from both ends. The optics allow

more than twice the coverage area than that of the small intestine capsule, and it has automatic light control with a video capture frame rate of four frames per second. After initial capsule activation and 5 minutes of image transmission, the capsule enters a delay mode of approximately 2 hours, after which it spontaneously restarts the transmission of images for approximately 10 hours. This enables the device to pass a long way towards the large intestine before the precious battery lifetime expires.[162]

2.5.5 Evaluation of Current Methods of Observing the Gastrointestinal Tract

For the patient, the requirement of having their gastrointestinal tract examined is an extremely daunting prospect, and this is understandable. Significant discomfort is involved in the entire procedure, from the cleansing of the intestines, to the actual examination of the patient. Due to the nature of most of the conventional methods of examination there is a requirement for totally clean intestines. Therefore, the patients are given a diet of low residual foods or clear liquids for anything up to 48 hours (for the less invasive methods), before the procedures take place. In addition, they then have their intestines cleansed with laxatives just before the procedures begin. After the preparation follows the examination itself, which is an intimidating experience and can also be

dangerous sometimes when using the more invasive techniques. Although there are a great number of techniques open to the medical profession for observing the bowels, none of them are completely satisfactory. This section, therefore, discusses the merits and inadequacies of these techniques, and looks to the future and new methods of observing the gastrointestinal tract.[143]

2.5.5.1 Intestinal Preparation Evaluation

With the non-invasive methods such as virtual colonoscopy, it is essential that the entire colon is fully cleansed, dry, and distended. Faecal matter in small quantities can produce false positive results because it can mimic polyps, while in large amounts it can produce false negative results by obscuring polyps completely. Residual fluid can also obscure polyps thus giving false negative results. A poorly distended intestine, can obscure polyps and also appear to resemble carcinomas that narrow the lumen.[143]

Radiological screening of the gastrointestinal tract also requires complete cleansing of the intestines before the examination can be performed. If the intestines have not been cleansed properly the patient has to undergo a preparatory enema. A contrast medium is introduced into the intestines, which is then fully distended. As with virtual colonoscopy, faecal matter and inadequate distension can be misinterpreted by the attending radiologist. With both non-invasive colonoscopy and radiological examinations, it is essential that the

patient's intestines are not over distended, as this can lead to perforations in the intestinal wall.

Pre-procedural preparation of the intestines for video capsule endoscopy is a controversial issue. Some favour the bowel preparations and prokinetics. However, according to data from the international conference on capsule endoscopy, it was suggested that there was no need for routine use of intestinal preparations.[163] The manufacturers suggest patients fast overnight for at least twelve hours before taking the capsule. During the procedure patients can drink clear liquids two hours after capsule ingestion and eat a light meal a further two hours after that.

Summarizing these findings it appears that virtual colonoscopy and radiological screening require long preparation times and unpleasant preparation procedures. However, the preparation procedures for video capsule endoscopy are less unpleasant and less time consuming.

2.5.5.2 Comparison of Small Intestinal Investigation Techniques

2.5.5.2.1 Obscure Gastrointestinal Bleeding

Several studies have compared video capsule endoscopy with push enteroscopy in the evaluation of patients with obscure gastrointestinal bleeding.

They have shown a significantly better diagnostic yield for video capsule endoscopy (63 %) compared with push enteroscopy (23 %). In a recent randomized study first line exploration of obscure gastrointestinal bleeding identified a bleeding source with video capsule endoscopy in 50% and push enteroscopy in 24% of patients. Furthermore, it was shown that video capsule endoscopy detected a source of bleeding in a greater proportion of patients (72 %), than computed tomography angiography (24 %), or standard angiography (56 %) and gave positive findings in more than half of the cases that were negative at computed tomography or angiography. When using intraoperative endoscopy as a reference, video capsule endoscopy had sensitivity, specificity and positive and negative predictive values of 95%, 75%, 95%, and 86% respectively. [164]

Ell et al performed a study comparing video capsule endoscopy to push enteroscopy on 32 patients with a history of GI bleeding. The patients had been previously examined by a variety of imaging techniques, which failed to identify the source of pathology. The results of their investigation revealed that push enteroscopy detected a definitive source of bleeding in 28% compared with 66% by video capsule endoscopy. The most common aetiologies encountered were irritable bowel syndrome, angiodysplasia and tumours.[164]

The use of video capsule endoscopy and push enteroscopy were also compared in a group of 50 patients with a history of chronic gastrointestinal bleeding and negative screenings in the past. The results of this study also showed that video capsule endoscopy was found to be superior in diagnosing a source of bleeding located within the small intestine (68% versus 32%). The total diagnostic yield, which took into account pathology both within and

outside of the small intestine, also demonstrated the superiority of video capsule endoscopy over push enteroscopy (76% (38/50) versus 38% (19/50)).[165]

The diagnosis of bleeding by video capsule endoscopy has also been compared with that of barium imaging. A study by Costamagna et al examined the use of video capsule endoscopy in a total of 20 patients with a variety of small intestinal diseases, including gastrointestinal bleeding, irritable bowel syndrome, suspected sarcoma recurrence, familial adenomatous polyposis, chronic diarrhoea and small bowel polyps. Several procedures, including push enteroscopy, gastroscopy, colonoscopy, angiography, intraoperative enteroscopy and radionuclide scanning, had been performed before the study. The diagnostic yield of video capsule endoscopy in their investigation was 45% (9/20), while that of barium follow through was only 20% (4/20). The most common sources of bleeding detected were angiodysplasias followed by suspected irritable bowel syndrome and polyps.[165]

It has been shown that the diagnostic yield for video capsule endoscopy is higher compared with that of double-balloon enteroscopy, with the agreement between video capsule endoscopy and double-balloon enteroscopy at about 74% for angioectasias, 96% for ulcerations, 94% for mucosal and sub mucosal polyps, and 96% for large tumours. Two studies investigated the yield and the outcomes of double-balloon enteroscopy following video capsule endoscopy in patients with obscure gastrointestinal bleeding. Patients first underwent video capsule endoscopy and then double-balloon enteroscopy. The overall detection rates for both techniques were similar. Therefore, for this condition, these two techniques may be considered complementary. However, double-balloon enteroscopy may permit endoscopic treatment of the bleeding lesion. [164]

Video capsule endoscopy is a cost-effective investigation tool in patients with obscure gastrointestinal bleeding. The diagnostic yield of video capsule endoscopy compared with other imaging procedures has been evaluated as a measure of efficacy. The mean cost of a positive diagnosis with video capsule endoscopy was only 55% of that for other procedures.[165]

2.5.5.2.2 Coeliac Disease

Two studies of patients with suspected coeliac disease and positive coeliac serology, compared the diagnostic performance of video capsule endoscopy, with that of conventional upper gastrointestinal endoscopy with duodenal biopsies. Using duodenal histology as the gold standard, both studies showed that video capsule endoscopy had good sensitivity (85.0%–87.5 %) and specificity (90.9 % –100 %) for the diagnosis of coeliac disease. In a more recent study carried out in untreated patients with biopsy-proven coeliac disease, video capsule endoscopy had 92% sensitivity and 100% specificity for the detection of villus atrophy. [164]

In a study of 47 patients with complicated coeliac disease video capsule endoscopy had a high diagnostic yield, by identifying mucosal abnormalities and by excluding adenocarcinoma. In another study of 14 patients with refractory coeliac disease, video capsule endoscopy identified signs of ulcerative jejunoileitis or intestinal T-cell lymphoma in 2/7 patients with type II refractory coeliac disease. In one of these, video capsule endoscopy was the only method by which the diagnosis could be made.[165]

2.5.5.2.3 Small Intestinal Tumours

A small series of studies showed that video capsule endoscopy is more effective than barium contrast radiological procedures in detecting small intestinal polyps in patients with familial adenomatous polyposis or Peutz–Jeghers syndrome.[164]

The accuracy of video capsule endoscopy has been shown to equal that of MRI in detecting small intestinal polyps bigger than 15 mm, but the detection rate for polyps 5–15 mm in size was much higher for video capsule endoscopy and polyps smaller than 5 mm were visualized only by video capsule endoscopy. However, it provided only partial views of large polyps, while MRI provided a better estimation of the site and the size of the detected polyps. Available published data suggests that now video capsule endoscopy may replace enteroclysis for surveillance in Peutz–Jeghers syndrome patients. Video capsule endoscopy is indicated in familial adenomatous polyposis patients with duodenal polyps, because these patients may develop small intestinal polyps.[165]

The diagnosis of small intestinal tumours has, often been delayed when traditional techniques are used. The majority of patients with small intestinal tumours usually undergo multiple investigations prior to video capsule endoscopy without any definitive diagnosis. The average number of previous negative procedures prior to video capsule endoscopy has been reported to range between 3.6 and 5 per patient.[164]

Virtual colonoscopy methods suffer from movement artefacts. This means it is imperative that the patient lies completely still during the scanning procedure. As this takes a relatively long time for each position, discomfort may be felt by the patient during the entire procedure. Sensitivity is also an issue with virtual colonoscopy. Dachman[150] wrote an article reviewing the diagnostic performance of virtual colonoscopy. He stated that Fletcher et al[152] found that in 180 high risk patients the sensitivity and specificity were 75.2% for the detection of polyps 10 mm or larger, and 47.2% for polyps 5-9 mm in size. He also stated that Rex et al[153] in a screening population study found that CT colonoscopy identified 75% of patients with adenomas larger than 20 mm, 83% of patients with adenomas that were 10-19 mm, and 43% of patients with adenomas that were 6-9 mm.

Video capsule endoscopy provides a satisfactory estimation of tumour location when compared with surgery or autopsy, and it appears to have an influential role in therapeutic screening, providing information on the location, dimension, and appearance of the lesion.[164]

2.5.5.2.4 Crohn's Disease

The diagnostic yield of video capsule endoscopy for Crohn's disease when compared with all the other available procedures showed significant incremental diagnostic yields for all the patients examined. Small-bowel follow through showed 40% (9 studies) while colonoscopy and ileoscopy 15% (4 studies), CT enterography 38% (3 studies), push enteroscopy 38% (2 studies)

and magnetic resonance imaging (MRI) 22% (1 study). There was no significant difference seen between video capsule endoscopy and alternate modalities for diagnosing small intestinal Crohn's disease in patients with a suspected initial presentation.[164]

Subgroup analysis of patients with established disease and suspected small intestinal recurrence revealed a statistically significant difference in diagnostic yield in favour of video capsule endoscopy compared with all the modalities mentioned. In a small retrospective study in known or suspected Crohn's disease, the sensitivity of video capsule endoscopy for active small intestinal Crohn's disease was not significantly different from computed tomography, ileocolonoscopy or even small-bowel follow through. However, it was concluded that lower specificity, and the need for preceding radiography due to the high frequency of retention, may limit its use as a first-line test. Video capsule endoscopy was found to be more effective in finding recurrences than colonoscopy and intubation of the neoileum after surgery for Crohn's disease. Out of 24 patients retrospectively studied, recurrence was demonstrated in 15 (62 %) with the video capsule endoscopy and only in 6 (25 %) with colonoscopy. Video capsule endoscopy should also be considered in ulcerative colitis patients with atypical clinical features, particularly after colectomy and in cases of indeterminate colitis.[165]

Several recent studies sought to compare the use of video capsule endoscopy to barium studies in diagnosing Crohn disease. Eliakim et al looked at 20 patients with a history of recurrent abdominal pain, weight loss, or chronic diarrhoea. Each one underwent evaluation by barium studies followed by video capsule endoscopy and CT enteroclysis. The diagnostic yield of video capsule

endoscopy was determined to be 70% and that of the radiologic procedures 37%. Furthermore, video capsule endoscopy detected all of the lesions located by small bowel follow through and CT enteroclysis and detected additional lesions in 47% of the cases. In another study by Eliakim et al looking at 35 patients, the diagnostic yield of video capsule endoscopy was reported to be 77%, while that of barium and CT studies were 23% and 20%, respectively. In a recent retrospective study of 31 patients documented to have terminal ileac involvement with Crohn's disease using colonoscopy, which included retrograde ileoscopy, the diagnostic yield of video capsule endoscopy was significantly superior to enteroclysis (89% versus 37%).[165]

2.5.5.2.5 Oesophageal Investigations

The main indications for oesophageal video capsule endoscopy are screening of Barrett's oesophagus and of oesophageal varices. Since 2006, the accuracy of oesophageal video capsule endoscopy for detecting lesions related to gastro-oesophageal reflux has been evaluated in several studies comparing the diagnostic yields of video capsule endoscopy and gastroscopy. In these studies, oesophageal video capsule endoscopy appeared feasible, safe, well tolerated, and always preferred by patients to unsedated gastroscopy. However, the sensitivity of oesophageal video capsule endoscopy was quite variable between studies, ranging from 60% to 100% for Barrett's oesophagus and from 50% to 89% for erosive oesophagitis. In addition, in a recent study, a quite low diagnostic agreement was found between oesophageal video capsule endoscopy

and gastroscopy in a heterogeneous group of patients undergoing gastroscopy because of suspicion of a range of various oesophageal diseases.[164]

A large, multicenter retrospective study compared gastroscopy and oesophageal video capsule endoscopy for the detection of oesophageal varices, and showed very good positive and negative predictive values (92% and 77%, respectively) and an overall fair agreement with gastroscopy. Moreover, in discriminating between medium/large varices requiring treatment and small/absent varices requiring surveillance, the positive and negative predictive values for video capsule endoscopy were 87% and 92%, respectively, with a substantial overall agreement of 91% on treatment decisions based on variceal size. Two recent studies have compared the cost-effectiveness of oesophageal video capsule endoscopy versus gastroscopy and/or systematic prescription of prophylaxis by beta-blocking agents. Neither of these studies demonstrated any advantage in using oesophageal video capsule endoscopy over the other approaches.[164]

Both in the screening of Barrett's oesophagus and of oesophageal varices, the usefulness of oesophageal video capsule endoscopy must be weighed against the wide availability of gastroscopy, its good tolerability and relatively low cost. Moreover, gastroscopy allows a complete examination of the stomach and duodenum during the same procedure and also enables biopsy sampling to be performed.

2.5.5.2.6 Colon Investigations

For colon video capsule endoscopy the recommended preparation regimen consists of conventional colonoscopy preparation plus ingestion of domperidone before capsule ingestion, and boosts of sodium phosphate purge and bisacodyl suppositories during the examination.[164]

This non-invasive examination has been evaluated in two pilot studies, in one large European trial, and in a meta-analysis as an alternative modality for colon neoplasia screening. Data from these two studies suggests that the colon capsule was expelled within 10 hours post ingestion by 74% of patients in one study, and by more than 90% in the other, allowing sufficient battery lifetime for the examination of the entire colon in the majority of patients. However, intestinal cleansing is an issue. In the two pilot studies there was poor intestinal preparation in 1%–3% of cases, but in the large European trial the proportion of cases with fair to poor intestinal preparation was 29%. No examination-related adverse events have been reported to date. According to the meta-analysis, the sensitivity and specificity of colon video capsule endoscopy for the detection of significant colon adenomas and carcinomas are 69% and 86%, respectively, suggesting that although it is a promising diagnostic tool, colon video capsule endoscopy requires improvements to be made before it can be used as an alternative to colonoscopy for colon cancer screening.[164]

Colon video capsule endoscopy might also have potential, firstly as a complement to incomplete colonoscopy, and secondly where conventional colonoscopy is either refused by patients or poses substantial risk to them. A

small case series did not show encouraging results for the first proposition, and there are no published data regarding the second.[164]

2.5.5.2.7 Technique Comparison Summary

In comparing the techniques, it is pertinent to evaluate the advantages and disadvantages of using one modality over the other. Push enteroscopy provides excellent visualization of the mucosal surface, which often contains abnormalities of interest that are too subtle to be detected by radiography. Similarly, video capsule endoscopy allows viewing of the mucosal surface but accomplishes this through a less invasive process when compared with push enteroscopy. It is consequently the preferred examination for patients. The overall time to perform push enteroscopy ranges from 15–45 minutes. In addition, patient sedation is required, as well as recovery time to relieve the effects of the sedation. Small intestinal video capsule endoscopy does not involve patient sedation, and therefore no recovery time is needed. However, even though the patient can continue with normal activities, video capsule endoscopy takes up to 10 hours to complete.[165]

With regards to length of the small intestine that it is possible to investigate, push enteroscopy can visualize approximately 80–120 cm beyond the ligament of Treitz, while video capsule endoscopy has the potential to examine the entire small intestine. It is, however, important to note that failure of video capsule endoscopy to reach the caecum during the eight hours of recording has been reported in approximately 15% of patients undergoing the study.[165]

Despite this statistic, multiple studies have reported video capsule endoscopy to be more sensitive than push enteroscopy in detecting causes of obscure gastrointestinal bleeding. (Table 2.2) A limitation of video capsule endoscopy is the inability to obtain biopsies and provide therapeutic intervention, a capability possessed by push enteroscopy. Potential complications of push enteroscopy include intestinal perforation and acute pancreatitis, as well as the rare occurrence of bleeding and infection. Many authors have described the two examinations as being complimentary to one another and suggest that video capsule endoscopy be the initial diagnostic procedure in order to select the patients most likely to benefit from the therapeutic capability offered by push enteroscopy studies (i.e., those patients with lesions identified in the proximal small intestine).[165]

Author	Capsule endoscopy (%)	Push enteroscopy (%)
Ell (N 32)	66	28
Mata (N 42)	74	19
Mylonaki (N 50)	68	32
Saurin (N 58)	69	38
Hartmann (N 33)	76	21
Brown (N 32)	66	28
Pennazio (N 100)	59	29

Table 2.2 Comparison between the diagnostic yields of capsule endoscopy and push enteroscopy in studies of patients with obscure GI bleeding Diagnostic yield.

2.5.5.2.8 Limitations and Risks of Intestinal Observation Techniques

While invasive methods such as colonoscopy allow the attending physician to see the lumen of the intestines directly in real time, there are many complications that can occur. Complications occur in about 3-4 per 1000 in diagnostic colonoscopies, and about 23 per 1000 therapeutic colonoscopies. Perforation can be caused by the motion of the instrument, air insufflation, or after a biopsy is taken from diverticula or from a diseased intramural area. Bleeding can be caused by mechanical contact abrasions, after biopsy, or after polypectomy. There is a possibility of internal explosion occurring during polypectomy when cauterising, in particular when methane explodes in the unprepared colon. Temperature elevation can increase so much that burns occur after polypectomy. Peritoneal irritation, meteorism, and mild ileus can occur after biopsy. Sometimes infections can also be transmitted during procedures. Also myocardial infarction, pulmonary embolism, ruptured aortic aneurysm, and splenic rupture can occasionally occur but they are very rare.[164]

A disadvantage in using radiological examination techniques is the exposure of the patient to radiation. In addition, these types of techniques do not permit close examination of the mucosa and therefore have a low sensitivity for flat, small, infiltrative, or inflammatory lesions. In addition to this they have poor diagnostic sensitivity during the early stages of a disease process. Although the sensitivity of enteroclysis has been reported to be superior to that of small

bowel follow through, the procedure is relatively invasive and may require patient sedation.[164]

Small intestinal video capsule endoscopy has some limitations and risks, of which those practicing video capsule endoscopy examinations will be aware. MRI examination, if needed, should not be carried out before the capsule is expelled from the gastrointestinal tract. Video capsule endoscopy should also not be used in patients with swallowing disorders, due to the risk of aspiration. Pregnancy is regarded as a contraindication for video capsule endoscopy examination because of the microwaves transmitted by the capsule. However, there are two case reports of video capsule endoscopy examination during the first trimester of pregnancy. Video capsule endoscopy is not contraindicated in patients with a cardiac pacemaker or implantable cardiac defibrillator as there is no interference between either of the two devices and the video capsule endoscope. [165]

Capsule retention risk is high in patients with known Crohn's disease, NSAID stricture, radiation enteritis and small intestinal tumours. The capsule retention rate ranges from 0% to 13%. The rate of retention in patients with obscure gastrointestinal bleeding is 5% and in suspected Crohn's disease 1.4%, and it can be as high as 8% in patients with known Crohn's disease. Interestingly, no capsule retention was reported in healthy volunteers. The overall frequency of capsule retention is usually 1%-2%.[164] Therefore, a novel method now being evaluated is the precursory use of a patency capsule, which, in the event that it cannot be naturally excreted, will begin to disintegrate and therefore avoid the need for invasive removal of the capsule. However, others think that the retention of the capsule in patients with Crohn's disease should be

seen as potentially diagnostic in and of itself, as it most likely represents stricture or stenosis associated with the patient's disease. Using radiological imaging as a mechanism to evaluate patients with suspected risk factors for capsule retention has been proposed. The theory behind this is to help identify strictures or other anatomical derangements that would impede the capsule's course. The problem with this role for small bowel follow through is that a negative study does not completely exclude the presence of structural defects.[165]

Another limitation of video capsule endoscopy that has been encountered is the quality of visualization provided by the capsule. Some studies have reported that the duodenum is not effectively visualized. Mylonaki et al thought that the quality of images obtained from push enteroscopy were superior to those of video capsule endoscopy. This was due in part to several factors, including the light intensity, which can be manipulated during push enteroscopy to match changing environmental requirements, but is fixed in video capsule endoscopy. However, recent improvements in technology in the PillCam COLON and ESO 2 have included controllable lighting and better image quality which may improve this situation. Likewise, the lesions that are discovered by video capsule endoscopy cannot be washed or examined repeatedly, biopsies cannot be obtained, or therapeutic intervention cannot be delivered, which are all possible with push enteroscopy.[165]

2.5.5.2.9 Conclusion Summary

Video capsule endoscopy is a safe and well-tolerated procedure for patients, with very low complication rates. It outperforms most of the conventional methods for observing the mucosal surface of the small intestine showing greater sensitivity than virtual and radiological procedures, and the ability to see more of the small intestine than other endoscopic procedures. It also reduces the patient's exposure to radiation in the case of virtual and radiological procedures, and sedation in the case of endoscopic procedures.

However, observation of the data from the procedure is a time-consuming process, as even at the optimal review rate of fifteen images per second it takes over one hour to re-examine a full eight hour procedure. The reliable interpretation of the video capsule endoscopic procedure requires experienced readers with experience of reading at least 20 studies. [164]

Technical problems related to the battery lifetime and failure of images to download also occurs, with an overall technical failure rate of around 9%. Incomplete study occurs due to delayed gastric emptying, previous small intestine surgery, hospitalisation and poor intestinal cleansing. Real time viewers of video capsule endoscopy may help to identify prolonged gastric transit in such cases. However, higher video capture rate and longer battery lifetime could resolve these obstacles.

Video capsule endoscopes would benefit from a radio-controlled self contained propulsion system, which would allow them to be moved with or against the natural peristaltic flow of the small intestine, or be held in a

stationary position to provide clearer real time observations. This project investigates how electrostimulation applied to the mucosal surface of the small bowel via a pair of electrodes, and hence inducing adjacent circular muscle contraction, would be used to propel a small capsule device to travel forwards or backwards along the small intestines safely and painlessly.

Such a propulsion system could enable the attending physician, while viewing real time images, to propel the capsules quickly through areas of non-interest, conserving the all-important battery lifetime. It would also provide the physician with the resources to reverse the capsule direction and return it to re-examine more closely areas of particular interest that had only been briefly seen, or were totally missed during the first transit. A propulsion system such as this could turn a passive diagnostic tool, which relied solely on peristalsis to propel it past areas of interest, into a manoeuvrable and completely active diagnostic tool, giving real time control to the attending physician.

However, to produce such a propulsive device, a knowledge of its electrical interaction with the surrounding gastrointestinal environment is essential. Therefore, the next chapter begins with a review of the electrophysiology of the gastrointestinal tract.

3. Electrostimulation Considerations

3.1   Introduction

As was shown in Chapter 2, devices such as video capsule endoscopes would benefit from an electrostimulation propelled radio-controlled system to allow real-time control. Using electrostimulation of the adjacent enclosed lumen to propel itself along the gastrointestinal tract, the device will have to maintain an electrical interaction with it. Therefore, an understanding of the electrophysiology of the gastrointestinal tract, how current methods of functional electrostimulation are being used to manipulate muscle, and the electrical safety requirements for such devices, is essential.

3.2   Electrophysiology of the Gastrointestinal Tract

3.2.1 Cell Membranes

The membrane wall of an excitable muscle cell which separates the ionic concentrations in the intracellular and extracellular regions, can be modelled in terms of the transmembrane potential difference (electrical gradient) and the relative ionic concentrations across the membrane. The model considered is the Nernst model of the cell membrane for a single species of ion.

For a dilute solution of ions, in the absence of an electrical potential gradient across a cell membrane there would be no electrical force produced. The ions would then produce a force by diffusing across the membrane at a rate proportional to the concentration gradient. The algebraic sum of these two forces is known as the electrochemical potential gradient, and it is used to calculate the net flow of ions across the membrane. If this gradient is zero there is ionic equilibrium and the chemical gradient opposes the electrical gradient equally. This allows the membrane potential at equilibrium to be calculated for particular ions by equating the electrical gradient and the opposing ionic concentration gradient.

The electrical gradient force is given by the following equation:

$$\text{Electrical gradient force} = ZFE \qquad\qquad [3.1]$$

where Z = ion valency

                    F = the Faraday constant

                    E = potential gradient

The concentration gradient force is given by:

$$\text{Concentration gradient force} = RT \ln\left[\frac{[C]\,\text{outside}}{[C]\,\text{inside}}\right] \qquad [3.2]$$

where R = gas constant

                    T = absolute temperature

                    C = ionic concentration

At equilibrium these forces are equal and opposite and equating [3.1] and [3.2] gives the Nernst Equation for E:

$$E = \frac{RT}{ZF} \ln\left[\frac{[C]\,\text{outside}}{[C]\,\text{inside}}\right]$$

[3.3]

The wall of an excitable muscle cell is made from an extremely thin membrane consisting of phospholipids that is waterproof and resistant to Na^+, K^+ and Ca^{2+} ion transport. However, there are proteins embedded in the membrane, through which ions can diffuse. These form ion selective channels that are species specific and can be rapidly opened or closed. This gate mechanism is controlled by chemical messenger molecules or by the electric potential difference across the region of membrane. Ion pumps within the cell use this to pump K^+ into the cell while pumping Na^+ out.

Under resting conditions when the cell is in a non-excitable state, some of the channels are open and allow K^+ that had previously been pumped into the cell to now move out along the chemical gradient, increasing the electronegativity of the inside of the cell. In contrast, most of the Na^+ channels are closed during these resting conditions so that only a small amount of Na^+ flows into the cell to counteract its electronegativity. On its own, the relatively free flow of K^+ out of the cell would continue until a potential difference of -90 mV was achieved in order to balance the ion concentration gradient established by the pumps. However, this is partially offset by the restricted flow of Na^+ into the cell, creating a 'resting potential' of approximately -70 mV and the cell is said to be 'polarized' with respect to the surrounding extracellular fluid.

77

When a chemical or electrical stimulus is introduced, which is capable of opening the Na^+ channels, (i.e. it must be sufficiently positive to raise the potential of one area of the membrane to at least +20 mV with respect to the inside of the cell), positive charge flows in making the nearby membrane more positive, which in turn opens more channels, allowing more Na^+ to enter. Spreading like an avalanche, the entire inside of the cell membrane rapidly becomes positive, reaching a peak potential of about +50 mV 'depolarizing' the cell with respect to the surrounding extracellular fluid.

Na^+ channels only remain open for about a millisecond and then close. During this time extra K^+ channels open, allowing extra K^+ to flow out of the cell, producing a negative 'refractory' period, which prevents the positive charge from neighbouring areas retriggering another action potential in an area that has just fired.[166,167]

3.2.2 Muscle Contraction

Smooth muscle contains spindle-shaped cells, each possessing a single, central nucleus. Surrounding the nucleus and throughout most of the cytoplasm are the thick (myosin) and thin (actin) filaments. (Fig. 3.1) Tiny projections that originate from the myosin filament are believed to be cross bridges. The ratio of actin to myosin filaments, which is twice that observed in striated muscle at approximately 12 to 1, may provide a greater opportunity for a cross bridge to attach and generate force within smooth muscle. This may, in part, account for

the ability of smooth muscle to generate a comparable or greater force than striated muscle, with far less myosin.

Fig. 3.1 Change in smooth muscle during contraction.

(http://faculty.etsu.edu 2012)

Differing from striated muscle, smooth muscle lacks any apparent organisation of the actin and myosin contractile filaments into sarcomeres. A similar structure may nonetheless exist in smooth muscle, composed of the actin filaments that are anchored to dense, amorphous bodies in the cytoplasm as well as dense plaques on the cell membrane. These dense areas are composed of actinin, a protein, also found in the Z lines of striated muscle, to which actin filaments are known to attach. Thus, force generated by myosin cross bridges attached to actin is transmitted through actin filaments to dense bodies and then through neighbouring contractile units terminating on the cell membrane which causes the cell to contract. (Fig. 3.2)

79

Fig. 3.2 Interaction between actin and myosin filaments during muscle

contraction (http://www.ncbi.nlm.nih.gov 2012)

Relaxed smooth muscle cells possess a smooth cell membrane appearance, but upon contraction, large membrane blebs (or eruptions) form as a result of inwardly directed contractile forces that are applied at discrete points on the muscle membrane. These points are presumably the dense plaques on the cell membrane to which the actin filaments attach. As an isolated cell shortens it does so in a helical manner. The contractile proteins in smooth muscle are helically oriented within the muscle cell. Such an arrangement of contractile

proteins could contribute to the slower shortening velocity and enhanced force-generating ability of smooth muscle.[166,167]

3.2.3 Smooth Muscle Contraction

The interaction of sliding actin and myosin filaments is similar in smooth muscle to that of cardiac or skeletal muscle. However, smooth muscle does not contain troponin, but contains the thin filament protein tropomyosin and other notable proteins caldesmon and calponin. Contractions are initiated by the calcium-activated phosphorylation of myosin.

A nerve impulse or electrostimulation ultimately results in muscle cell contraction when it produces an action potential at the sarcolemma, the membrane that surrounds the muscle cell. This is a process of depolarizing the sarcolemma and extracellular Ca^{2+} entering through calcium channels, and intracellular Ca^{2+} release predominately from the sarcoplasmic reticulum. Ca^{2+} release from the sarcoplasmic reticulum is from Ryanodine receptor channels by a redox process and Inositol triphosphate receptor channels by the second messenger inositol triphosphate. The intracellular Ca^{2+} binds with calmodulin, which then binds and activates myosin light chain kinase.

Within a few minutes of initiation, the Ca^{2+} level markedly decreases, the myosin light chains' phosphorylation decreases, and energy utilization decreases. However, force in tonic smooth muscle is maintained. During contraction of muscle, rapidly cycling cross bridges form between activated actin and phosphorylated myosin, generating force. It is hypothesized that the

maintenance of force results from dephosphorylated "latch-bridges" that slowly cycle and maintain force.

As the stimulation of the muscle cell continues, the terminal cistemae continue to release Ca^{2+}. At the same time, however, some of the Ca^{2+} are being removed from the sarcoplasm by another portion of the sarcoplasmic reticulum, the longitudinal tubules. Once the Ca^{2+} are inside the lumen (cavity) of the longitudinal tubules, many of them slowly diffuse back to the terminal cistemae, where they are bound to a protein, calsequestrin, as a storage site. The removal of Ca^{2+} ions from the sarcoplasm by the sarcoplasmic reticulum requires energy. The breakdown of ATP is the chemical reaction that supplies the energy, and two Ca^{2+} ions are apparently removed from the sareoplasm for each ATP molecule that is split, resulting in the dissociation (release) of Ca^{2+} from the tropomyosin system. The tropomyosin system is then transformed back to its original state, preventing myosin and actin from interacting and thus causing relaxation of the muscle cell.[166,167]

3.3 Functional Electrical Stimulation

This brief section has been included for completeness in order to show some of the extensive applications where electrostimulation is used in medicine. However, these application use electrostimulation parameters which are not directly applicable to the project.

Functional Electrical Stimulation (FES) can be classified into three types according to its specific purpose: the restoration of skeleto-motor functions; the

restoration of sensory functions; and the restoration of autonomic functions.[168]
FES aims to generate movement or functions which mimic those found naturally. It is therefore necessary that FES is under the subject's control and available when required. If successful it may be required that the system performs successfully for the lifetime of the patient. This section will briefly describe the different uses of FES.

Skeleto-motor FES is used to restore a variety of motor functions with stimulation being applied in a number of different ways. Phrenic stimulators are used for ventilatory pacing. Electrodes are surgically implanted and stimulation is applied to the phrenic nerve in a train of stimulation pulses of increasing strength followed by a pause. The stimulation causes contraction of the diaphragm, (a purely inspiratory muscle) and the pause in stimulation allows expiration to occur.

Electrical stimulation of the nerves associated with the bladder can have two main purposes: to restore continence, or to achieve efficient voiding. Continence may be promoted by either activating the sphincter mechanism or by inhibiting the detrusor reflex. Efficient voiding may be achieved by stimulation of the conus medullarus, the sacral arterial roots, the sacral nerves or the detrusor muscle.[169,170,171]

Most of the work done with upper-limb stimulators has been to restore upper-limb function in patients with injuries to the cervical spinal cord. There is scope for restoring hand grasp function in suitable patients. These patients usually have voluntary control of the shoulders, elbow flexion movements and wrist extension. This treatment is only really suitable for patients with equal

damage to both arms, as they have much to gain from an implanted device which restores grasp in one hand.

Lower-limb stimulators have a range of uses for paraplegic patients, being used for both standing and stepping. Paraplegic standing was first demonstrated in 1963 using surface stimulation of the quadriceps femoris.[172] Several problems have to be overcome with this type of stimulation. Firstly, muscle training for fatigue resistance is required, after which the endurance of the continuously stimulated quadriceps is still limited. Secondly, the hips must be stabilised in extension, which is most commonly achieved by stimulating the gluteus maximus as well. Thirdly, control mechanisms must be introduced which allow safe stand up and sit down transitions.[173] Stepping can be initiated by first transferring the weight onto the stance leg, and moving the centre of gravity forward. The swing leg must then be brought forward through a sequence of hip and knee flexions, followed by knee extension and ankle dorsiflexion. This can be achieved with surface FES activating the flexor withdrawal reflex, strongly stimulating the common peroneal nerve.[174] However, this method does not allow for a well controlled or dynamic gait.[168]

Foot drop, where the toe catches in the early swing stage and slaps to the ground on heel strike, is often a gait limiting factor in patients with stroke or incomplete spinal cord injuries. It may be relieved using surface FES of the common peroneal nerve at the fibular head. The main difficulty with this method is successful placement of the electrodes as they have a tendency to move. Also they tend to malfunction during use. Implanted electrodes can solve the problem of accurate electrode location.[168] A two-channel implant achieves

balanced dorsiflexion by stimulating the tibialis anterior and peroneal nerves separately.[175]

FES is also used in a variety of ways for cardiac assistance. Trained skeletal muscle can be used, usually the latissimus dorsi, which is transplanted with its nerve tissue and blood vessels intact into the thoracic cavity. In a procedure called cardiomyoplasty, the transplanted muscle is wrapped around the heart in patients with progressive cardiac failure due to a dilated heart. In a slightly different procedure the transplanted muscle is wrapped around the ascending or descending aorta. A third procedure uses a skeletal muscle ventricle, where the muscle is fashioned into a ventricle shape forming its own chamber, and is then located in series or parallel with the aorta. With all these procedures the muscle is stimulated in time with the cardiac cycle so that contraction occurs with every beat or every alternate beat. These procedures improve cardiac output and reduce the work load on the already damaged heart.[168]

FES can also be used to aid with sensory dysfunction. There are two types of sensory stimulator devices, cochlear and visual cortex stimulators. Cochlear implants have progressed considerably since their first demonstration with a single electrode device in 1957.[176] Multichannel stimulators with multiplexed digital signals are now used in conjunction with either intracochlear or extracochlear electrodes to enhance performance.

3.3.1 Electrostimulation of Smooth Muscle

The majority of the current work using electrostimulation of the bowel is to determine its usefulness for increasing motility, or for incontinence prevention procedures. There is a wide variety of different methods available. This section reviews some of the more relevant methods.

Gastroparesis is a chronic disorder of gastric motility and many cases are unresponsive to anriemetic and prokinetic drug treatments. This has promoted a search for nonmedicative therapies for this challenging condition, one of which is the use of Gastric Electrical Stimulation (GES).[177] Electrically stimulating the stomach to treat gastroparesis has been proposed by investigators for decades. With the development of techniques for implantable pacing devices and electrodes, and the promising preliminary results in chronic pacing studies, GES has received increasing attention recently among researchers and clinicians.[178]

Investigations of how GES at the proximal stomach induced gastric relaxation, using four pairs of electrodes implanted along the greater curvature of the stomach in seven dogs obtained measurements randomly during control, proximal and distal stimulation, using stimulation parameters of 4 mA, 375 ms and 0.1 or 0.3 Hz.[179]

Within human subjects, the first evidence that implantable gastric neurostimulators, reduced nausea and vomiting, and decreased the need for supplemental nutrition in subjects with gastroparesis from a variety of causes was presented. The study used stimulation parameters of 5 mA, 330 µs, and 0.2 Hz.[180]

Constipation is a common coloproctologic problem that may be attributed to recognisable causes, one of which is colonic inertia, which is a disorder of colonic motility, and may be total or segmental. Investigations into the pacing parameters required for rectal evacuation of normal and constipated subjects have been carried out.[181]

Rectal electric activity was recorded before (basal activity) and during electric stimulation with a constant electric current of 5 mA at 200 ms. From this study it would appear that this method could be applied for rectal evacuation of patients with inertia constipation.[182]

The use of electrostimulation for colonic pacing to treat patients with Irritable Bowel Syndrome (IBS) has also been investigated.[183] The optimal parameters used for pacing were 6 mA, and 150 ms with a frequency 25% higher than that of the basal colonic waves. It was found that colonic pacing succeeded in normalizing the tachyarrhythmic pattern and relieving the symptoms of the IBS.

Although useful in providing an idea of the electrostimulation parameters being used within the bowels, these investigations all use electrostimulation to aid motility by enhancing natural peristalsis. This is not what the device being constructed for this project will do. It will use electrostimulation to produce a direct contraction of the walls of the gastrointestinal tract, local to the electrodes, with enough force to propel the device.

A small amount of work has also been carried out into the usefulness of electrostimulation of the small bowel in preventing incontinence. Electrostimulation in some cases is used to control a neosphincter, formed from

a wrap of gracilis muscle around the anal canal.[184,185] This method uses contraction of striated muscle to produce the neosphincter, and does not represent direct contraction of the smooth muscle of the bowel.

The control of intestinal reservoirs in dogs has been investigated by implanting four pairs of stainless steel electrodes into the serosal surface of jejunum and ileum pouches. Pressures of 80 mm Hg were produced with pulses of 100 ms, 3 Hz, and 50 ms, 6 Hz, with currents of 10-25 mA. Pressure increases were also observed when using 1 ms, 330 Hz, and 1 ms, 10 Hz, stimulation. A constant current generator produced pouch contraction and reservoir emptying with stimulation at 50 ms, 6 Hz, with currents between 15-25 mA[186]. A pressure increase of 50-80 mm Hg was induced in the jejunum using 50 mA, 500 μs, and 910 Hz currents, with a threshold current of 25 mA. In long term studies, the average pressure observed in 10 trials using 25 mA, 500 μs, 910 Hz was 26 mm Hg. When using 25 mA, 200 μs, 1.67 kHz, the average pressure was 28 mm Hg. Continued contraction was also observed following termination of the stimulation and produced an average pressure of 48 mm Hg.[187]

Although these methods produce direct contraction of pouches within the bowel to aid their emptying, the electrodes used were not attached to the mucosal surface. This may lead to different stimulation parameters being required to produce a comparable pressure. Therefore, although these and the other methods discussed above show how electrostimulation can be used to provide a therapeutic tool for a variety of gastric complaints, they only give background knowledge of the electrical parameters that are being used to

manipulate the muscles of the gastrointestinal tract, and are only partially relevant to the project. The only publication found that was totally relevant to the project, described the only recorded use of electrostimulation which was applied directly to the mucosal surface of the small intestines and oesophagus to propel objects. In this paper the use of electrostimulation for the propulsion of five different ovoid capsules, with various diameters and taper angles, within the oesophagus and small intestine of pigs was investigated. The threshold for movement of the capsules was achieved at 12 mA, with 15 Hz, 30 ms pulses, and the device moved readily at 20 mA.[188]

The initial concept of the using electrostimulation to propel a video capsule endoscope was adapted from devices described in the PhD thesis of Mosse[189] from the Department of Medical Physics and Bioengineering at University College London, who investigated methods of improving conventional colonoscopy. He describes preliminary designs of devices using electrostimulation to tow the tip of a conventional colonoscope along the large intestines.

Fig. 3.3 Devices developed during the PhD of Mosse (Mosse 1999)

A few experiments were conducted by Mosse using the devices shown if Fig. 3.3 to determine their effectiveness to aid the propulsion of an endoscope tip along the length of the gastrointestinal tract. Initial electrostimulation experiments were carried out *in vitro* on excised porcine colon in Kreb's solution. These were followed by *in vivo* experiments in the oesophagus, small intestine and large intestine in two pigs.

The results show that within the oesophagus smooth movement of the capsule was achieved with stimulation parameters of 30 V 15 Hz and 18 ms. Contraction but no movement was observed with the same frequency and pulse duration at a voltage between 20 V and 30 V, and no contraction was observed below 20 V. Changing the frequency to 10 Hz caused a slower trembling movement and 6 Hz produced a slow juddering movement with little progress. Within the small intestine it was found that movement could be achieved with

voltages as low as 12 V and a larger range of frequencies and pulse durations were examined. The best movement was achieved with stimulation parameters in the ranges of 12-30 V, 15-25 Hz and 15-30 ms. Within the large intestine the stimulation parameters 15 V, 15 Hz, and 30 ms were used, but the contractions produced completely engulfed the device, preventing movement.[189]

3.4   Electrical Safety

3.4.1 Introduction

When constructing electromedical equipment, patient safety is of paramount importance and must be the major concern. Therefore, rigorous examinations of any potential hazards which may be embodied in a new system have to be investigated, and guidelines for their avoidance have to be reported and discussed.

This section begins with a review of the current safety regulations and precedents, with a discussion of their relevance to the project. This is then followed by a discussion of the effects and potential hazards that may occur during electrical stimulation of a patient. This includes the effects that charge has on electrodes during stimulation, the effects that electrical stimulation has on the gastrointestinal tract and the surrounding area, and the safety issues that are relevant to an *in vivo* electrical stimulator. Finally, conclusions are presented.

3.4.2 Safety Regulations and Precedents

Safety and constructional standards are contained within documents produced by the European Committee for Electrotechnical Standardisation (CENELEC). The BS EN 60601-1 : 1990[190] contains an extremely detailed general safety standard for the construction of medical electrical equipment.

This standard discusses the safety issues for all medical electrical devices, which come into contact with humans. The stimulator used during the initial experimental stages was powered using a mains driven external power supply. Earth leakage currents were minimised by the use of medical grade isolation transformers.

Of greater relevance to the final design is the current limit quoted for electrical devices positioned across the heart. This limit is very low, being only 10 μA.

3.4.3 Effects and Potential Hazards of Electrical Stimulation

Currents that are passed between a pair of electrodes placed on tissue have at least three major effects that may be harmful to the patient. These effects are electrolysis, heating and neuromuscular contraction. Accidental nerve stimulation is considered to be the most dangerous of these, as the nervous system controls two vital systems; blood circulation and respiration.

If two electrodes with an applied direct current are placed on tissue electrolysis occurs by the iontophoresis mechanism at the electrode tissue

interface. If the current is applied at 100 µA for a few minutes ulceration occurs beneath the electrodes. 'Direct current' is defined as current with a frequency of less than 0.1 Hz.[190] At frequencies above this the movement of ions that occurs when the applied current is flowing in one direction is balanced by the movement of the ions when it is flowing in the other, resulting in a net effect of no electrolysis. The safety limit for 'direct current' that flows between two electrodes is defined as being 10 µA.[190]

The normal potential found across a nerve membrane is about 80 mV. In the frequency range of 10 Hz – 10 kHz neural stimulation can occur. If the potential is reversed for 20 µs or more, the neurone will be stimulated, propagating an action potential along the nerve fibre. If a motor nerve has been stimulated a muscle will be caused to contract. The major hazard with neural stimulation is the activation of motor nerves which could affect the skeletal or heart muscle, interrupting breathing or more dangerously causing fibrillation of the heart.

A 100 µA current can cause ventricular fibrillation if it is applied directly to the ventricular wall of the heart. This is well below the pain sensation threshold, so fatal currents can be passed through the body without sensation. The current delivery directly across the heart is limited to 10 µA with a maximum of 50 µA for a single fault condition.[190]

At higher frequency, 10-100 kHz, the current does not stimulate neural tissue, but it does produce heating of the tissue. As the devices used in this work have operational frequencies well below those where heating becomes the dominant biological effect, it will not be discussed within this safety report.

3.4.4 The Effects that Charge has on Electrodes During Stimulation

At low frequencies an electrode must establish ohmic contact with tissue. Most electrodes achieve this through an electrolyte. Much is known about the properties of electrode-electrolyte-tissue interfaces, but it is not possible to predict the electrical characteristics of such interactions with accuracy.

Several charge distribution types have been proposed, with the simplest being that conceived by Helmholtz in 1879.[191] It was postulated that there exists a layer of charge tightly bound to the electrode and a layer of opposite charge in the immediately adjacent electrolyte. In 1964 Parson[192] described electrodes in terms of the reactions at the double layer (gap between the two layers). It was stated that when no net flow of charge occurs across the interface, the electrodes are described as 'perfectly polarized', whereas those electrodes which allow unhindered flow of charge are described as 'perfectly non-polarizable'.

In a conceptual sense, this electrode-electrolyte interface can be represented by a voltage source and a capacitor, requiring any electrical model of the system to include a resistance, capacitance, and a potential. Now that these elements have been identified, modelling the system requires calculated magnitudes which are dependent upon the electrode metal and its area, the electrolyte, the temperature, current density, and the frequency of the signal.

With stimulating electrodes the impedance of the electrode-electrolyte interface can become very important due to the combined reactive and resistive

nature with both being dependent on current density. This along with the nature of the stimulator output circuitry can result in the production of different voltage and current waveforms. In addition, the current density distribution is often non-uniform across the surfaces of the stimulating electrodes.

The measurement of the capacitive and resistive nature of a single electrode-electrolyte interface is difficult. Warburg[193] describes a model that represents the interface as a resistance and capacitance in series, whose magnitudes are selected to emulate the conditions produced by the variables described earlier.

The impedance of the electrode-electrolyte interface decreases with an increase in current density. There is also a non-uniform distribution of current density under the electrode, being higher around the perimeter than at the centre, since all the current that flows to areas beyond the electrode must flow through the perimeter. Stimulation occurs at the regions where the current density is highest. Therefore the determination of the average current density of the stimulus by dividing the current by the electrode area is not an accurate method.

When determining electrode properties it is also essential to know what type of voltage signal is being applied: DC, unidirectional pulses, and AC waveforms all affect the properties of the electrode-electrolyte interface. The type of current source is also important, as constant-current and constant-voltage supplies also affect the interface properties.

The main considerations when determining the current flow using low current densities are the area of the electrode, the electrode-electrolyte circuit and the type of current source. As the current density is increased on the other hand, electrolysis will occur, forming gas bubbles at the surface of the

electrodes. The gas expelled is dependent on the electrolyte and the polarity of the electrode. [194]

3.4.5 The Effects of Electrical Stimulation

Biological tissue contains 'free charge carriers', so it can be meaningfully considered as an electrical conductor. 'Bound charges' also exist so dielectric properties are also present. In addition to these passive properties, a mechanism for active ion transport is present, which acts as an important mechanism in neural function and membrane absorption processes, such as those found in the gastrointestinal tract. Conductivity is the dominant factor at frequencies less than 100 kHz.

There are a variety of stimulation methods, some mechanical, some electrical and some chemical, which can be used to stimulate tissue. The most controllable of these is electrical stimulation. An effective stimulation alters the environmental conditions to produce a characteristic and reversible response in the tissue.

To stimulate a cell, it is only required that the transmembrane potential is reduced by a critical amount. The current delivered by the active electrodes reduces the transmembrane potential. The amount by which it is reduced is dependent on the current density. Therefore with a high enough current density the threshold (action) potential will be achieved.

When this action potential is reached, a regenerative process occurs within the cell. The transmembrane potential is caused to drop to zero

(depolarizes) by the influx of sodium ions into the cell combined with the exit of potassium ions, and after reversing slightly it then recovers (repolarizes) to the resting membrane potential. Stimulation can occur when the transmembrane potential is reduced by one third.

Physiologically initiated muscular contractions occur when motor nerves transmit electrical signals which overcome a number of muscle fibre's action potentials. When stimulating electrodes are used to stimulate muscle fibres directly, the induced force produced is only dependent on the number of muscle fibres which are stimulated past their action potentials. Increasing the intensity of the stimulating current will increase the number of contracting muscle fibres until all the fibres within the region are stimulated. Beyond this point no more force can be produced.

Intramuscular electrodes do not directly stimulate major nerve trunks, but they do excite peripheral local nerve fibres. Any damage to the neural tissue would be expected to be small, because of the physical separation between the electrodes and the nerves. [194]

3.4.6 *In Vivo* Electrical Stimulator

When using electrostimulation within the gastrointestinal tract one must investigate the effects that the stimulating current will have on the surrounding organs. The most important from a safety point of view is the effect this current will have on the heart. The oesophagus and proximal stomach lie very close to the heart, so much so that electrostimulation through the oesophageal wall is

sometimes used to pace the heart. This is called transoesophageal pacing and employs electrodes that are placed on the mucosal surface of the oesophagus.

The thresholds for transoesophageal atrial pacing has been investigated by a number of groups. [195,196,197] The minimal pulse width and current required for capture were within, or very close to, the ranges under investigation for this project. There was also no correlation between current and pulse width on the one hand and age, height, weight, or body surface area on the other. Likewise neither electrode type nor the existence of structural heart disease influenced the threshold required for capture.[198] These results suggests the proposed propulsion device should not be used in the oesophagus.

Another potential hazard when using electrostimulation within the gastrointestinal tract is inadvertently affecting the heart rate by stimulating vagal nerves. The vagal nerve which controls the pace of the heart remains in close proximity with the gastrointestinal tract as far as to the distal stomach, and in some cases can reach the proximal small intestine.

Using stimulation parameters within a range similar to those proposed for this study it has been shown that simultaneous bilateral stimulation of the vagus nerve in intact and sympathectomised rats of various ages significantly reduced heart rate. Stimulating the left cervical vagus nerve in pigs was also sufficient to reduce the heart rate by 20 ± 4 beats per minute.[199] Similar results were found with humans, when stimulating the left vagus nerve proximal to the origin of the cardiac vagal bunch.[200] This suggests that the proposed propulsion device should not be used in the proximal small intestine.

Within the rest of the tract the safety question is: what is the stray current value induced in the heart by the devices when used within the small and

large intestines? To investigate this, a very simple finite element representation of the tissues was constructed by Dehghani using the TOAST software program.[201] This was then used to examine the distribution of current arising from a locally placed stimulator.

Initially the heart and torso were given the same electrical conductivity as blood, the two 1 mm^2 electrodes of the electrostimulator were separated by 10 mm and the device was placed 50 mm from the heart. The maximum stray current induced in the heart by a 15 mA flow of current between the electrodes was found to be 0.65 µA. The heart and torso were then given the same electrical conductivity as fat, and it was found that the maximum stray current induced in the heart was 0.07 µA. Therefore, whether the electrical conductivity of the heart is chosen to be that of blood (worst case) or that of fat (best case), the maximum stray current induced in the heart by the electrostimulator was calculated to be at least one order of magnitude less than the maximum current of 10 µA deemed to be safe.[190]

Another concern when using electrostimulation is adverse tissue surface effects such as blistering and burning, which can occur due to irreversible faradic electrolysis between the electrode and tissue surfaces. This happens when the 'reversible charge injection limit' is exceeded. For a given electrode material, there is a limit to the charge which can be injected in either direction to produce reversible surface processes.[202] To ensure chemical reversibility, the current must be reversed before the limit is reached. The main factors which affect this are, the electrode material and its shape and size, the electrolyte and the parameters of the stimulation wave form.

The type of cyclic waveform used with the equipment in this project is a monophasic pulsatile waveform, which consists of periodic trains of short pulses of equal amplitude interspersed with longer 'off' periods.

The inverse relationship between the frequency and period is the same as for sinusoidal waves. However, the short pulse duration and therefore the charge per cycle is independent of the frequency, permitting greater control over the individual stimulation parameters.

The least damaging of these waveforms are those which have no net direct current with charge density levels below those that cause H_2, O_2, or Cl_2 evolution. Any net direct current, even a few $\mu A/cm^2$, can lead to irreversible electrolytic reactions.

Simple monophasic waveforms with single polarity deliver a direct current signal, resulting in water hydrolysis and both electrode and tissue damage. The requirement for charge retrieval can be overcome through the use of a series capacitor, which delivers a reverse current through the electrodes between pulses preventing the accumulation of charge upon the stimulating electrodes.

The safe injectable charge that an electrode can deliver is limited by the capacitive nature of the electrode-electrolyte interface, and its breakdown voltage. Beyond this voltage limit most currents produce an irreversible electrochemical process which is harmful to tissue.

In particular, a pulse generator with constant output resistance (R_0) and a series capacitor (C), coupled to the cathode to enable the electrode potential between pulses to 'slide back', could provide a charge density per pulse within the region of the maximum safe possible, ~350 $\mu C/cm^2$ pulse. The series

capacitor inhibits a flow of net direct current in the event of the electrode potential (φ) being accidentally driven beyond the safe operating range (φ_{max} - φ_{min}), thereby eliminating the danger of tissue damage from the products of chloride oxidation. The inclusion of such a series capacitor would therefore seem to be worthwhile.

The capacitor (C) should be sufficiently large to pass the stimulation pulse without excessive 'sag'. Extensive 'sag' indicates a wasteful loss of charge and its associated large 'overshoot' reduces the effect of the stimulating charge that has been delivered.

However, C must be sufficiently small for the time constant CR_0 to be a small fraction of the time interval between pulses in order to enable the electrode (cathode) to exhaust fully. [202]

However, the project stimulation device will be moving through the gastrointestinal tract, thus allowing any gaseous products of water electrolysis to readily escape from the electrode-tissue interface. Also, the device will take a matter of hours to pass through whole gastrointestinal tract, with intermittent stimulation lasting only for minutes. Therefore, the need to achieve charge balancing may be unnecessary.

3.5   A Model for Electrode Impedance

Impedance characterization of the electrode-electrolyte interface is of paramount importance. During stimulation a certain current density is necessary to generate activity. To supply this through a high interface impedance would

require a large applied electrode voltage leading to undesirable electrochemical reactions that may be harmful to cellular cultures. A well characterized, fully understood interface impedance leads to an optimized electrode-electrolyte interface design.[203]

Equivalent circuit models have long been used to model the interface impedance. The first model of the electrode-electrolyte interface was suggested by Helmholtz[191] in 1879, who proposed that a double layer of charge existed at the interface.

The significance of this concept is that such a layer resembles a charged capacitor, thereby indicating that any model for the interface must include capacitance. However, direct current passes through the interface, so resistance must also be a component of any model.

In 1901 Warburg[193] proposed that the interface could be represented by a polarization resistance in series with a polarization capacitor. For a low current density, the polarization capacitance (C_w) varies inversely with the square root of frequency and that the phase angle is constant, being 45 degrees. This model however, does not take into account the behaviour of direct current at the interface.

Observing the limitations of the Warburg model, Fricke[204] reported in 1932 that for low current density and for a frequency range from 100-3500 Hz, the electrode capacitance value was $C_w = k/\omega^m$, and the phase angle (ϕ) remained constant with varying frequency and was equal to $m\pi/2$. The value of k and m depend on the metal. Therefore, the reactance $X_w = 1/\omega C_w = 1/k\omega^{1-m}$, and as $\tan \phi = X_w/R_w$, the resistance $R_w = X_w/\tan(m\pi/2)$. In a series of experiments he found that m varied between 0.15 and 0.32. Fricke's model, like

Warburg's, does not consider the passage of direct current. Experimental findings soon revealed that the polarization capacitance exhibited a frequency dependency leading to the introduction of Fricke's law, and the use of a constant phase angle impedance to represent the impedance of the interface capacitance.

Physical chemists have studied the properties of the electrode-electrolyte interface. Zimmerman[205] investigated the effect of temperature and electrolyte concentration on the capacitance and resistance of the electrode electrolyte interface over a frequency range from 60-4000 Hz. Measurements were made from 0-95°C. For a range of electrolyte concentrations, the capacitance increased and the resistance decreased with increasing temperature and concentration.

In 1947 Randles[206] synthesized a circuit model consisting of a double-layer (Helmholtz) polarization capacitance (C_p) in parallel with a series resistance (R) and capacitance (C). This model although popular, does not account for the passage of direct current through the interface.

In 1968 Geddes[207] proposed two circuit models for the electrode-electrolyte interface, which both contained a half-cell potential (E). In the first model the Warburg capacitance (C_w) is shunted by the Faradic resistance (R_f) to account for the direct current carrying property of the interface. The second model places the half-cell potential (E) in series with the Warburg components (R_w, C_w), and the Faradic resistance (R_f) was placed in parallel with the Warburg components to account for the direct current property of the interface.

A more complex electrochemistry model was described by Sluyters-Rehbach[208] in1970. This model places the Warburg impedance (R_wC_w) and a resistance (R_s) in series with a parallel resistance (R_p) capacitance (C_p) circuit;

this combination is shunted by a capacitance (C_d). Once again however, this model does not account for the direct current property of the interface.

In 1982 using low current density for a 0.085 cm^2 electrode, Onaral[209] found that the resistance and capacitance components of a platinum/0.9% saline interface both decreased with increasing frequency from 0.001-1000 Hz. In general, they found that the Warburg model was a fair approximation in this frequency range. Their low-frequency data strongly suggested the presence of a resistance in parallel with the Warburg equivalent that would accommodate the ability of the interface to pass direct current. Of particular importance to biomedical applications is Schwan's limit of linearity: the voltage at which the electrode system's impedance becomes nonlinear, which is often exceeded during stimulation.

McAdams et al,[210] extensively studied the platinum pacing electrode (90% platinum and 10% iridium) in physiological saline, successfully interpreting the frequency-dependent nonlinear interface impedance. Kovacs[211] has presented an equivalent circuit model based on the Randles model, with an additional Warburg impedance due to the diffusion of faradic current.

In 2005, Franks et al,[203] produced an equivalent circuit model consisting of an interface capacitance, shunted by a charge transfer resistance, in series with the solution resistance. The model parameters were fitted to the experimental results and confirmed with theoretical equations, validating the model.

When a metallic electrode comes in contact with an electrolyte, an ion exchange occurs with metal ions entering solution and ions from the electrolyte

combining with the metallic electrode. The net result is a charge distribution that produces unique properties within the electrode-electrolyte interface.[212]

As discussed earlier, many models have been developed to describe the behaviour of the electrode-electrolyte interface. The Warburg model for low current density states that the capacitive reactance, namely $X_c = 1/2\pi fC$, is equal to R and both vary inversely as the square root of frequency (f)[193]. Expressing R and X_c as A/f^α and B/f^β respectively, the Warburg model states that A = B and $\alpha = \beta = 0.5$. Because the phase angle ϕ is given by $\tan \phi = X_c/R$, the Warburg model states that $\tan \phi = 1.0$ and is constant with frequency. This means that ϕ is constant with frequency and is equal to $\pi/4$ radians or 45°.

Although the Warburg equivalent is useful as a conceptual model of the electrode-electrolyte interface, the accuracy of this model has been questioned. Fricke[204] concluded that R and X_c did not vary inversely as the square root of frequency. He proposed a constant-phase model in which $X_c = B/f^\beta$ and $\phi = 0.5\pi\beta$. Expressing R and X_c as A/f^α and B/f^β respectively, the Fricke constant-phase model states that $\alpha = \beta$ and $B/A = \tan(0.5\pi\beta)$. Schwan[213] examined Fricke's constant-phase model for platinum electrodes and reported that ϕ varied by only a factor of 2 over a 4 decade range of frequency (20 Hz to 200 kHz). Geddes[214] showed that β ranged from 0.38-0.78 for several common electrode metals. Onaral[209] studied the platinum/0.9% saline interface and found that Fricke's constant-phase model was valid from 10-400 mHz and above 10 Hz. Onaral noted that electrodes can be expected to deviate from constant-phase behaviour toward both extremes of these frequency ranges. A discussion of the history and applicability of the constant-phase model was presented by MacDonald,[215] who also discussed several other models for the electrode-

electrolyte interface presenting both empirical and theoretical models of various complexity.

However, as MacDonald[215] noted, that real data are usually subject to a less-than-perfect fit. Therefore, it is usually easiest to fit the data with the simplest model and then relate the results to more complex models as necessary. As a result, the Ragheb model, where $R = A/f^{\alpha}$ and $X_c = B/f^{\beta}$ was chosen because it is a more general representation of the electrode-electrolyte interface than the Warburg or Fricke models, but is simpler than many other models which could be used.[212]

Although the series RC equivalent is a sound basic model for the electrode-electrolyte interface, this equivalent does not account for the very low-frequency behaviour of the interface as electrodes can pass direct current. Therefore, placement of a Faradic resistance (R_f) in parallel with the series RC model produces this equivalent circuit. The value of R_f is high in the low frequency region and is very dependent on current density, decreasing with an increase in current density. To give a complete model of a single electrode-electrolyte interface, it is necessary to add the half-cell potential (E) to the equivalent circuit. The value of E depends on the species of metal and the electrolyte (species, concentration and temperature).

However, if one focuses attention on the nature of the electrode-electrolyte impedance at frequencies above 10 Hz and is not concerned with measuring DC electrode potentials, the series equivalent circuit provides a reasonable basis for quantitative determination of electrode polarization impedance over a wide frequency and current density range.[212]

The term polarization impedance is used to describe the impedance of the electrode-electrolyte interface because this quantity is not constant, but is altered by the passage of current and varies with both frequency and current density. Ragheb[212] characterized the polarization impedance at the interface of several common metals with 0.9% saline, to provide a useful reference for calculating the impedance of such electrodes.

When representing an electrode-electrolyte interface as a series RC circuit, it is not generally true that R and X_c both vary as $1/\sqrt{f}$ as stated in the Warburg model. This is because the values of the constants A and B and the exponents α and β depend on the species of metal, concentration, and temperature of the electrolyte and on electrode area.

Although it may not be generally true that $\alpha = \beta$ as proposed in the Fricke constant-phase model, it is a better representation of electrode behaviour than the more restrictive Warburg model. Onaral[209] suggested that Fricke's constant-phase rule may be valid over limited frequency ranges. The frequency range examined by Ragheb[212] (100 Hz to 20 kHz) may not have been sufficient to allow identification of a transition between regions of constant-phase behaviour. Nonetheless, Fricke's additional constraint that $\phi = 0.5\pi\beta$ or $B/A = \tan(0.5\pi\beta)$ was not valid for the metals examined in that study.

The exponents α and β are expected to be independent of electrode area because, at low current density, the manner in which R and X_c vary with frequency depends mainly on the electrode material, the species and concentration of the electrolyte, and the temperature. Therefore, a valid comparison between the exponents α and β determined in both the Ragheb

studies and the literature is possible. The constants A and B, however, reflect the absolute magnitudes of R and X_c and not the manner in which they change with frequency, therefore their values vary with electrode area, decreasing as area increases.

Therefore, values of A, B, α, and β for a stainless steel electrode with surface area 0.005 cm^2 in contact with physiologic 0.9% saline as presented by Ragheb[212] can be used to model stainless steel electrodes of any surface area (S). The electrode-electrolyte impedance is given by:

$$Z = \sqrt{R^2 + X_c^2} \qquad [3.4]$$

and because it is inversely proportional to the electrode surface area, the impedance of an electrode-electrolyte interface operated at low-current density may be calculated as:

$$Z = \frac{0.005}{S} \sqrt{(Af^{-\alpha})^2 + (Bf^{-\beta})^2} \qquad [3.5]$$

where S is the surface area of the electrode in cm^2 and A, B, α, and β are constants.

Taking the values of A (989), B (1849), α (0.760), and β (0.734) presented by Ragheb[212], and applying them along with results produced from the work described in the following two chapters to the above model, a range of electrode-electrolyte interface impedances (Z) at a stimulation frequency of 12.5 Hz for different electrode types are shown in Table 3.1.

	A/f^{α}	B/f^{β}	Z (k Ω)
Capsule electrode	145.1	290.0	1.799
11 mm bidirectional device electrode	145.1	290.0	1.205
15 mm bidirectional device electrode	145.1	290.0	0.862
20 mm bidirectional device electrode	145.1	290.0	0.504

Table 3.1 Electrode-electrolyte interface impedances for a range of electrodes.

Taking these values for Z, the current at the electrode-electrolyte interface can be determined for a given voltage. Table 3.2 shows currents for a range of voltages with various electrode types used during the work presented in the next two chapters.

	Z (kΩ)	Current at 5V (mA)	Current at 10 V (mA)	Current at 15V (mA)
Capsule electrode	1.8	2.8	5.5	8.3
11 mm bidirectional device electrode	1.2	4.1	8.3	12.4
15 mm bidirectional device electrode	0.9	5.8	11.6	17.4
20 mm bidirectional device electrode	0.5	9.9	19.8	29.7

Table 3.2 Impedance and current values for a range of electrodes

As the objective of the project was to produce a swallowable device, the model is now compared with the results obtained during the Human trial for validation.

Supply Voltage (V)	Experimental (measured) Current (mA)	Model (calculated) Current (mA)	Experimental Impedance (kΩ)	Model Impedance (kΩ)
5	2.5	2.8	2.0	1.8
8	3.7	4.4	2.1	1.8
10	4.9	5.5	2.0	1.8
12	9.0	6.6	1.3	1.8
15	12.0	8.3	1.3	1.8

Table 3.3 Comparison of model and experimental data for a range of voltages.

Table 3.3 shows that for 5 V, 8 V and 10 V pulses, the values of the current calculated with the model give a reasonable approximation to the values measured during the experiment. It would seem however, that as voltage increases, the current calculated by the model begins to differ from those measured during the experiment. The parameters of the model indicate that they could be used in the range below 10 V to model the impedance for a stainless steel electrode/0.9% saline interface.

3.6   Aims of the Project

The anatomy and many pathologies of the gastrointestinal tract offer many problems for diagnostic medicine. Methods of visualization of the gastrointestinal tract's mucosal surface are both a daunting and sometimes dangerous experience for the patients. Video capsule endoscopy is a safe and well-tolerated procedure for patients, with very low complication rates. It outperforms most of the conventional methods for observing the mucosal surface of the small intestine. It also reduces the patient's exposure to radiation in the case of virtual and radiological procedures, and sedation in the case of endoscopic procedures.

However, observation of the procedure is a time-consuming process, and technical problems related to the battery lifetime and failure of images to download also occur. However, these obstacles could be resolved. Video capsule endoscopes would benefit from a radio-controlled self contained propulsion system, which could allow them to be moved with or against the natural peristaltic flow of the small intestine, or held in a stationary position to provide clearer real time observations.

This project investigates how electrostimulation applied to the mucosal surface of the small bowel through a pair of electrodes, and hence inducing adjacent circular muscle contraction, could be used to propel a small capsule device to travel forwards or backwards along the small intestines safely and painlessly.

However, it is apparent that to produce such a device, thought must be given to how it will interact mechanically and electrically with its surrounding environment. Therefore, the aim of this project is to devise a method of remotely propelling a small device, such as a video capsule endoscope, within the gastrointestinal tract which could be monitored and controlled in real time. As the device is to be ultimately used in a human subject the device and the electrodes have to be modelled within constrained anatomical and electrical safety parameters.

For a human subject the maximum diameter an FDA approved capsule can have, to safely pass through the pylorus, is 11 mm. Electrical safety guidelines for devices used in medicine include the following constraints which apply to the electrical stimulation of tissue. If direct current (frequency less than 0.1 Hz) is applied for a few minutes at 100 μA, ulceration occurs under the electrodes due to electrolysis. Within the frequency range of 10 Hz − 10 kHz, neural stimulation can occur if the potential is reversed for 20 μs or more, which could lead to fibrillation of the heart. The direct application of a direct current of 100 μA across the heart can cause fibrillation. Therefore, the guidelines limit the current directly delivered across the heart to a direct current of 10 μA with a maximum single fault of 50 μA. At frequencies in the range 10-100 kHz the heating of tissue is the main concern.

Initially for development purposes, the pig model will be used because the anatomy and physiology of the pig's small intestine is similar to that of the human. As a starting point, the stimulating parameters in the range of 12-30V, 15-25 Hz and 15-30 ms, found by Mosse[189] to produce movement of a device along the small intestine of an anaesthetised pig by electrostimulation of the

adjacent mucosal membrane, will be used to replicate the results using a redesigned device. The second phase of the development will be to design, construct and test a bidirectional device capable of travelling along the small intestine with or against the direction of peristaltic flow. The third phase of development will be to investigate the effects of reducing the device diameter to 11 mm, so that it can safely pass through the human pylorus, allowing it to travel along the entire gastrointestinal tract after being swallowed. The fourth phase will investigate stimulation parameters to determine those which produce optimal propulsion in the small intestines. The penultimate phase of development will be to design and build a miniature radio-controlled stimulation device based on the stimulation parameters found in the previous phase. The final phase of development should culminate in a device with a radio-controlled self-contained propulsion system which could be evaluated in a human subject.

4. Design, Construction and Testing of a Wire Driven Electrostimulation Induced Propulsion Device

4.1 Objectives and Strategies

In designing the device one must consider the environmental constraints within which the device must operate. The human gastrointestinal tract is a convoluting tube of varying diameters, which means there will be limiting dimensional constraints on the device diameter. At the narrowest point of gastrointestinal tract, the pylorus has a maximum diameter of about 11 mm, the maximum diameter of the small intestine is about 25 mm and the diameter of the large intestine ranges from about 30 mm at its narrowest to about 60 mm at its widest in the colon.

There are also dimensional constraints imposed on the device length as it has to be short enough to pass through the gastrointestinal tract's many tight loops but long enough not to tumble end over end, i.e. changing camera position front to back and vice versa, in the areas of interest. This has been simply achieved by making the video capsule endoscopes slightly longer than the diameter of a specific region of the gastrointestinal tract in which they are to be used. Therefore, the PillCam SB capsule with a length of 27 mm has been successfully used to pass through and observe the small intestine, which has a maximum diameter of 25 mm, without tumbling. Also, the PillCam COLON capsule with a length of 33 mm has been successfully used to pass through and

observe the large intestine, which has a maximum diameter of 30 mm, without tumbling, which was a possibility for the PillCam SB.

The gastrointestinal tract is essentially a tube of smooth muscle with a mucosal inner coating to reduce friction of the peristaltic propelled bolus. For the purposes of the project the natural bolus will be replaced by a device made from plastic. The device will need to have a smooth surface and there will be constraints on its diameter and length as indicated above. Initially in order to select an optimal material for the construction of the device, the coefficient of friction μ between the mucosal surface and a variety of plastics will need to be investigated.

Electrostimulation is the stimulation of muscle and neural tissue by an external electrical source provided by the placement of electrodes. It can be used to activate the local adjacent smooth muscle tissue of the gastrointestinal tract causing it to contract in a manner that produces the propulsion to propel an enclosed device. Electrostimulation of the intestinal wall has been shown to produce sufficient contractile force to evacuate a jejunal pouch of a dog and to pull an endoscope along the gastrointestinal tract. Part of the initial design process will be to verify Mosse's stimulation parameters.[189]

The propulsive force exerted on the device produced by contraction of the adjacent smooth muscle tissue will depend on the force of the contraction. This will depend on the electrode dimensions and placement, the parameters of the electrical stimulation, the angle of the sloping face of the device and the frictional forces. All of these will need to be investigated.

For initial experimental investigations using the pig model, device dimensions required to fill enough lumen of the small intestine to ensure

electrical contact would need to be explored. The diameter of the capsules with FDA approval is limited to 11 mm to allow them to safely pass through the pylorus. However, access to the gastrointestinal tract is possible through the mouth or anus.

Investigations will include:

Selection of optimal plastic material for device construction.

Investigate how angle of sloping face affects propulsive force in order to find optimal angle.

Investigate how change in shape of bidirectional device may affect movement and compare movement in both directions.

How the diameter of the device relative to the small intestine diameter may affect device propulsion.

How stimulation parameters may affect device propulsion in order to find the optimal set.

How the device may have to be finally adapted for human trial from the pig model device.

4.2 Introduction

The aim of this section of the project is to produce a device which ultimately uses electrostimulation to propel small devices like video capsule endoscopes primarily along the small intestine, although some of the initial tests occur in the oesophagus. When designing such a device there are many issues which have to be taken into account. As well as the issue of electrical safety which was discussed in the previous chapter, there are a number of questions relating to the optimal dimensions of the device. There are also the questions of how best to convert the contraction of the intestine into a propulsive force for the device.

This chapter describes the design and evaluation of physical properties of the device, which includes a description of the path followed in an attempt to obtain the optimal design. This commences with a report of the experimental investigations into the coefficient of friction between porcine intestinal tissue and a range of possible materials from which the devices could be constructed.

Using these results, the design criteria of the device are discussed. This includes a description of the dimensions of the device and an investigation into the optimal angle design for the tapered section.

The chapter then describes how the devices were constructed, tested and presents analysis of the results. The chapter concludes with a description of how the device was tested *in vivo* with a human subject and an analysis of these results.

4.3 Design Considerations

As the device has to move as freely as possible through the gastrointestinal tract, the material chosen for its construction should have a low coefficient of friction with the mucosal lining. The material needs to be easily machined and work well with adhesives. The device has to gain maximum propulsion from the contractile force, therefore the optimal tapered angle will be investigated.

4.3.1 Selection of Materials for Device Body

Before the device can move, it must overcome static friction which is greater than the dynamic friction it will experience while moving. In order to utilize the propulsion force produced by the induced intestinal muscular contractions a value for both the static and dynamic coefficients of friction between the mucous surface of the small intestines and the capsule surface had to be determined. These properties were investigated for different materials which might be used to construct the device. The chosen materials not only needed to have a low coefficient of friction, but they also had to be easily machined. Thus, Acrylic, Delrin, and PTFE were selected for the test.

For the simplest case shown in Fig. 4.1 the coefficient of friction is calculated from the limiting equilibrium equation:

At the point of slipping, $\qquad F = \mu N \qquad$ [4.1]

Resolving parallel to the slope, $\qquad F = Mg\sin\theta \qquad$ [4.2]

Resolving perpendicular to the slope, $\qquad N = Mg\cos\theta \qquad$ [4.3]

Substituting [4.2] and [4.3] into [4.1] gives, $Mg\sin\theta = \mu Mg\cos\theta$ [4.4]

Which simplifies to give, $\qquad \mu = \tan\theta \qquad$ [4.5]
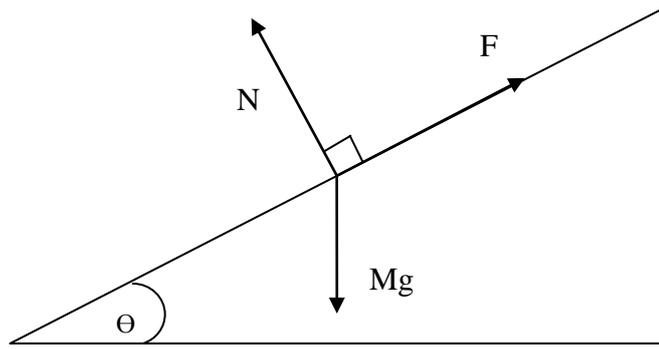
Fig. 4.1 Simple force diagram to aid in the resolution of the coefficient of friction $\mu = \tan\theta$

4.3.2 Equipment Used to Determine Coefficients of Friction

The rotation equipment used to determine the coefficients of friction was produced by HASS Automation (Oxnard, California). A platform attached to a HASS SC5 rotation indexer (Fig. 4.2) could be rotated to an angle with a precision of 0.001°. This rotation could be continuous with a slow steady rotating motion, or direct to a designated angle, using the programmable keypad. The platform could be rotated through 360° in either a clockwise or anti-clockwise direction enabling measurements to be taken in both directions, reducing systematic errors.
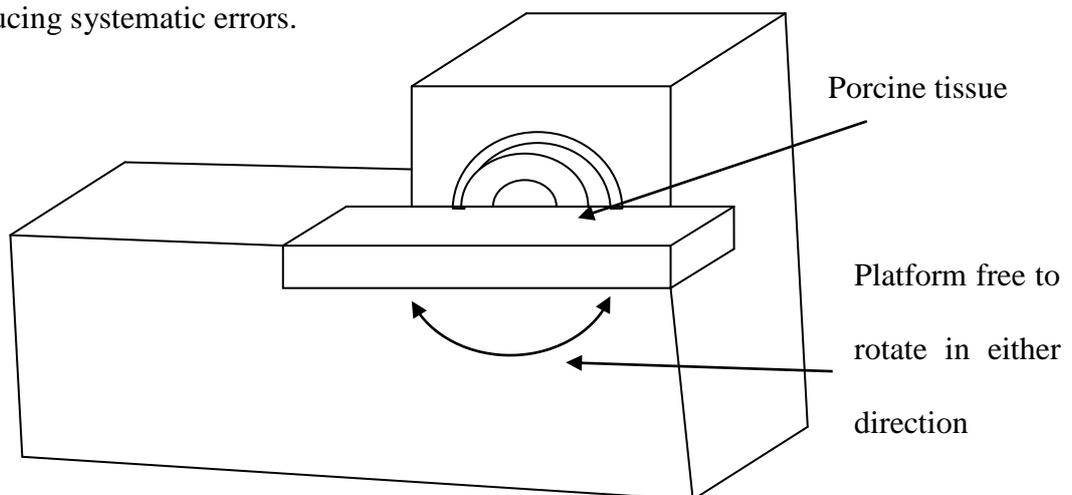
Fig. 4.2. Schematic diagram of Hass SC5 rotation indexer.

The rotation control was connected to a platform onto which post-mortem porcine small intestinal tissue was securely attached. In an attempt to imitate the moist *in vivo* conditions, the small intestinal tissue was kept moist with normal saline solution during the experiment. The platform was initially levelled with a spirit level and the control unit was set to the zero degree setting with a spirit level. The equipment was then ready to be used to measure the coefficients of friction between the porcine small intestinal tissue and a range of different materials.

The prepared samples of materials used were flat 60 x 100 x 30 mm rectangular blocks with slightly rounded edges to eliminate snags. The blocks weighed about 100 g, and there were supplementary loads of 100 g and 200 g that could be added to them.

4.3.3 Measurement of the Coefficients of Friction

To measure the coefficient of static friction for each material the platform was rotated from the zero degree position to an inclination angle at which the sample material was just about to move; the limiting equilibrium point. The platform was rotated in both the clockwise and anti-clockwise directions to eliminate any systematic error. The average values of these sets of angles, repeated ten times for each material, were found and then used to calculate the coefficient of static friction for each sample.

The measured coefficients of static friction were:-

$\mu_{\text{Delrin}} = \tan (6.37) = 0.11$ (SD 0.0069) (N = 10)

$\mu_{\text{Acrylic}} = \tan (4.59) = 0.080$ (SD 0.0080) (N = 10)

$\mu_{\text{PTFE}} = \tan (2.40) = 0.042$ (SD 0.0025) (N = 10)

To measure the coefficient of dynamic friction, the platform was set at an angle greater than the limiting equilibrium point to allow the sample to move. After the sample gained momentum the angle of the platform was reduced slowly until the sample just stopped moving. The average values of these sets of angles, repeated ten times for each material, were found and then used to calculate the coefficient of dynamic friction for each sample.

The coefficients of dynamic friction:

$\mu_{\text{Delrin}} = \tan (4.24) = 0.074$ (SD 0.0060) (N = 10)

$\mu_{\text{Acrylic}} = \tan (3.38) = 0.059$ (SD 0.0053) (N = 10)

$\mu_{\text{PTFE}} = \tan (0.67) = 0.012$ (SD 0.0021) (N = 10)

The results show that both the coefficients of static and dynamic friction for all the materials is low enough to produce a frictional force which will be negligable. Therefore, when chosing one of the materials, the major considerations are how easily they are to machine and how they work with adhesive. Acrylic proved to be the best for both of these, so it was chosen.

4.3.4 Capsule Design

At this stage, with all three materials (Acrylic, PTFE and Delrin) having such low coefficient of friction values, Acrylic was selected for the device construction because of its favourable physical properties. However the next consideration was to investigate how optimal propulsive movement could be produced from a given induced lateral contractile force and the effects that various coefficients of friction may have. To address this problem, a limiting equilibrium equation was derived by considering the forces produced during intestinal contraction.

It was assumed that the contractile force (R) would be applied to a tapered section with an angle Θ (Fig. 4.3) and that the propulsive force (P) is a function of Θ.

P = Propulsive force

R = Contractile force

N = Normal force

F = Frictional force

θ = Taper angle
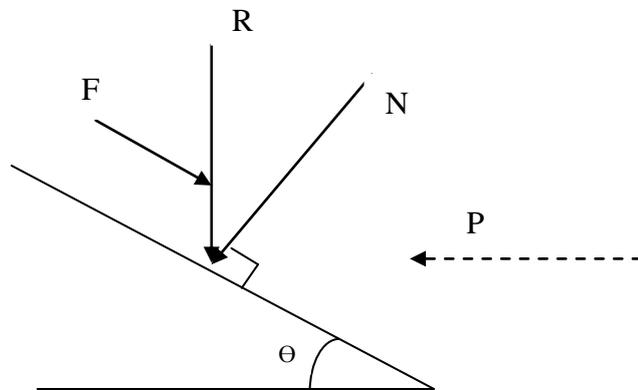
Fig. 4.3 Diagram representing the forces acting upon the taper at limiting equilibrium.

Resolving ↙ for N:

$$N = R \cos \theta \qquad\qquad [4.6]$$

Resolving ↘ for F:

$$F = \mu N \qquad\qquad [4.7]$$

Resolving ← for P:

$$P = N \sin \theta - \mu N \cos\theta = R \cos \theta \sin \theta - \mu R \cos^2\theta \qquad [4.8]$$

$$P = R \cos \theta (\sin \theta - \mu \cos\theta) \qquad\qquad [4.9]$$

Equation [4.9] shows that the fraction of contractile force that is converted into propulsive force varies with Θ. As well as showing this, Fig. 4.4 also shows that the optimal taper angle at which maximum propulsive force occurs and the maximum magnitude of the propulsive force varies with μ.
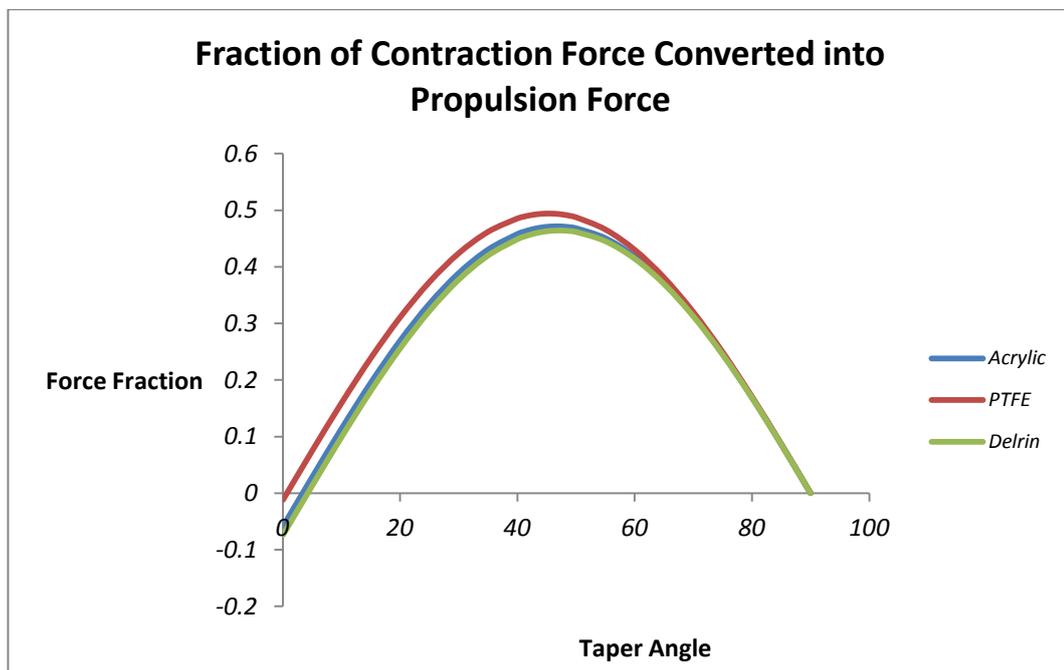
Fig. 4.4 Plot of P against Θ representing equation [4.9] using values of μ for Acrylic, PTFE and Delrin.

Fig. 4.4 shows that the maximum force for each material occurs at a taper angle between 40° and 50°. To examine this in more detail, Fig. 4.5 shows this region of the curves in more detail.
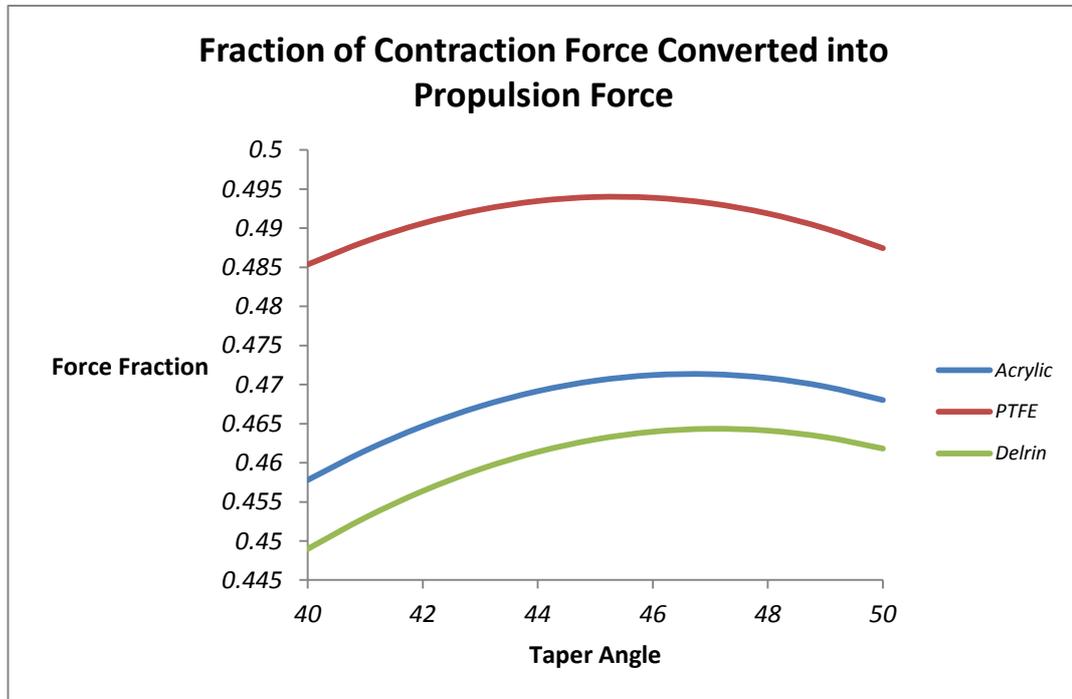
Fig. 4.5 Plot of P against Ө for values of Ө between 40° and 50° using values of µ for Acrylic, PTFE and Delrin.

From the maximum values of the curves (Fig. 4.5) it can be seen that the maximum propulsive force produced for all three materials is just under half the contractile force, (Acrylic 47%, PTFE 49.5% and Delrin 46%). The differential of the resolved force P with respect to Ө was determined and equated to zero, giving a value for Ө where the maximum value of P occurs.

Differentiating P with respect to Θ gives:

$$\frac{dP}{d\theta} = \frac{R}{2}(2\cos 2\theta) + \mu R\sin 2\theta \qquad\qquad [4.10]$$

Max P occurs when

$$\frac{dP}{d\theta} = 0 \qquad\qquad [4.11]$$

Therefore max P occurs when

$$\cos 2\theta + \mu\sin 2\theta = 0 \qquad\qquad [4.12]$$

The differential $\frac{dP}{d\theta}$ was plotted against Θ in order to determine the angle at which the maximum propulsive force occurs (Fig. 4.6 and Fig. 4.7).
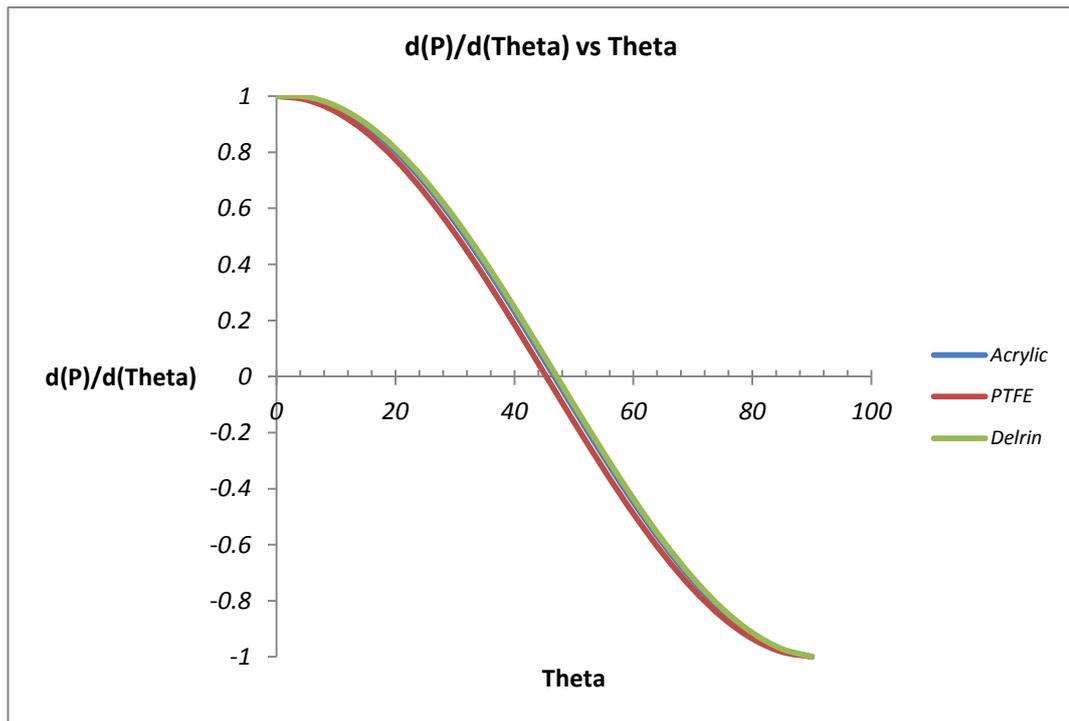
Fig. 4.6 Plot of $\frac{dP}{d\theta}$ against Θ using values of µ for Acrylic, PTFE and Delrin.

Fig. 4.6 shows that the angle at which the maximum propulsive force occurs, lies between 45° and 50° for all three materials. To examine this region more closely, Fig. 4.7 shows the trends between 45° and 50°.
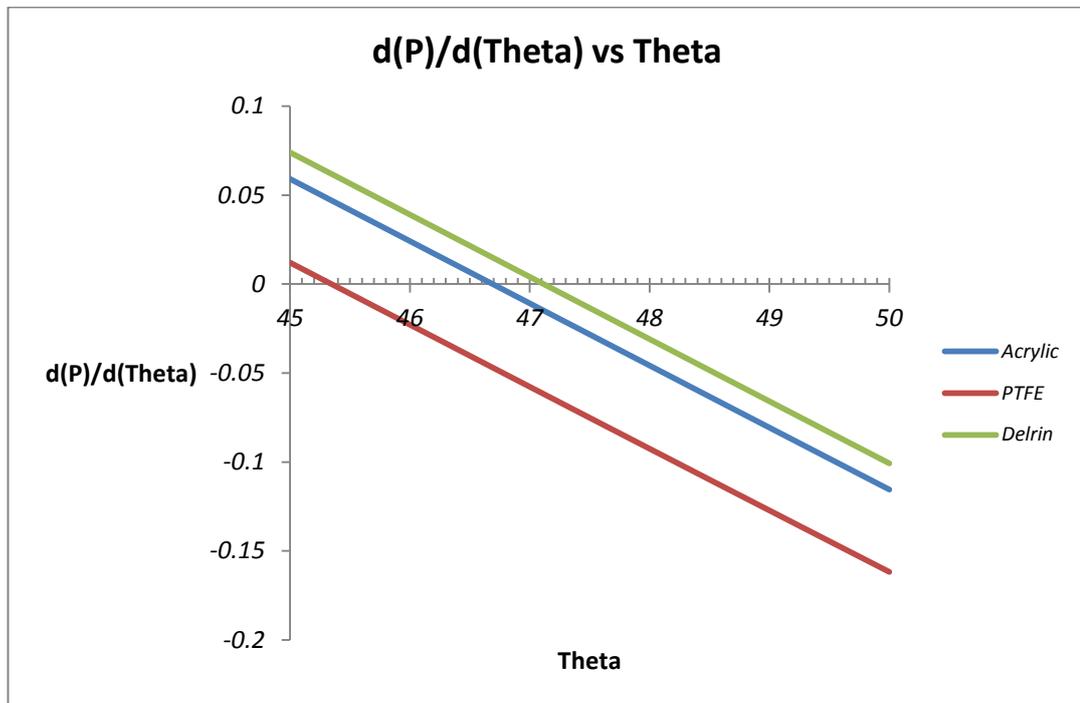
Fig. 4.7 Plot of $\frac{dP}{d\theta}$ against Ɵ between 40° and 50° using values of μ for Acrylic, PTFE and Delrin.

From Fig. 4.7 it can be seen that the optimal taper angle for PTFE is 45.3°, Acrylic is 46.6° and Delrin is 47.1°. Although Acrylic produces only 95% of the maximum propulsive force that is achievable by PTFE, the advantages of its physical properties outweigh this small loss. Therefore, Acrylic requiring a taper angle of 46.6° to achieve a maximum propulsive force of about 47% of the contractile force produced by the intestinal wall was chosen.

4.4 Initial Designs and Construction

Rationale for design

Using values compatible with those shown by Mosse[189] in the pig model of the oesophagus the range of stimulation parameters to be initially tested where:

- Voltage range of 5 - 35 V in 5 V increments. (No further increase in speed above 30 V)

- Frequency range 5 - 15 Hz in 5 Hz increments. (No increase in speed above 15 Hz)

- Pulse duration of 20 ms

From calculations in the previous section, it was shown that the optimal angle for the tapered section was 47°.

The device was constructed in a teardrop shape with a rounded front and a tapered rear section (Fig. 4.8). The initial design had a maximum outer diameter of 15 mm and the angle of the tapered section was 47° to produce the best propulsion from the contractile force. Two electrodes were placed diametrically opposite towards the widest part of the tapered rear section to provide the induced forward motion. The electrodes were constructed from 2 mm brass screw heads soldered to 2 m long insulated wires, which passed through the device and out through the rear of the tapered section.

Electrode
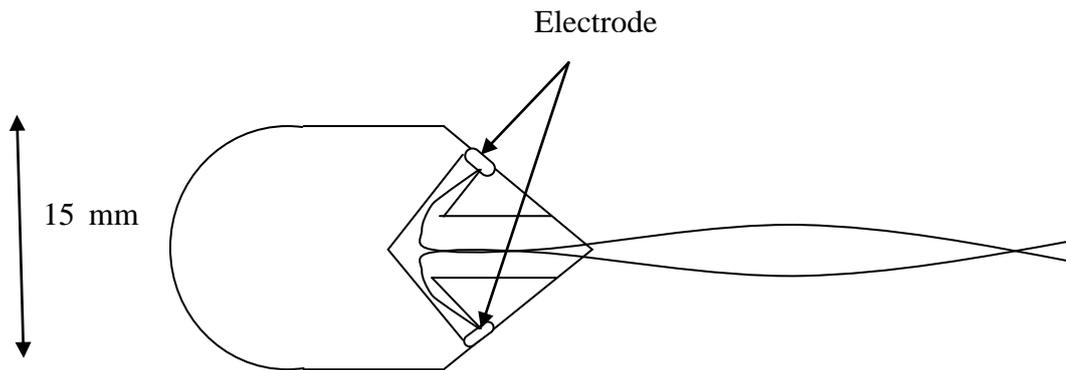
15 mm

Fig. 4.8 Schematic diagram of unidirectional device.

The body of the device was machined from a section of acrylic rod (a cylinder 50 mm long with a 15 mm diameter) using a lathe. Once the tear drop shape was achieved, the device was polished to remove the final rough surface. Two holes were then drilled in the top of the taper section using a pillar drill. They were diametrically opposite and perpendicular to the tapered section. The holes were both 2 mm in diameter and drilled so that they met on the central axis of the device. A third 2 mm hole was drilled along this axis from the centre of the rear of the tapered section to meet the other holes. This produced the pathway through which the wires would pass from the electrodes to the stimulator. Each 2 mm brass screw head was soldered to 2 m of flexible multi-strand insulated wire which had an outer diameter of 0.5 mm. (The drag effect on the device movement that the trailing wires would have was considered, and the use of smaller diameter wire contemplated. However, the devices had to be robust and it was thought that wire of smaller diameter would be too fragile. It was therefore decided that 0.5 mm multi-strand wire would be used.) Each wire was fed through its corresponding hole on the tapered section and drawn

128

through the rear hole until the electrode had reached the device. They were then fixed over the top of their holes with epoxy resin.

4.4.1 Initial Animal Tests

With permission granted from the Home Office to Swain (the attending physician) to perform a range of experiments on pigs including electrophysiological work, the initial experiment was designed to verify the findings presented in the thesis of Mosse.[189] It examined the stimulation properties required to propel the 15 mm teardrop device described previously along the gastrointestinal tract. A Grass SD9 stimulator, (Grass Technologies, West Warwick, USA) was used to supply the stimulation signal to the 2 mm diameter electrodes.

The stimulator produces a square wave stimulation signal, which can have a three decade output voltage range from 0.1 to 100 V, a three decade frequency range from 0.2 Hz to 200 Hz, and a four decade range of duration from 0.02 ms to 200 ms. It has a maximum output impedance of 1 kΩ, a peak output current of 50 mA, with a maximum power output of 2.5 W (peak).

To prevent it from entering the trachea, the device was passed through an over tube into the oesophagus of an anesthetised pig with a following endoscope. Once the capsule had been successfully placed into the oesophagus, the over tube was withdrawn. The endoscope was pulled back slightly so that the rear of the device could be clearly seen by the camera of the endoscope. Once set in this position, which was the starting position for each tested stimulation parameter, the stimulator was activated. After the effects were

observed, the stimulator was deactivated and (if movement had occurred) the capsule was returned to the starting position. This was repeated three times over a number of stimulation parameters and the results are presented in Table 4.1.

Voltage (V)	Frequency (Hz)	Pulse Length (ms)	Contraction	Movement
5	5	20	None	None
5	10	20	None	None
5	15	20	None	None
10	5	20	None	None
10	10	20	None	None
10	15	20	None	None
15	5	20	None	None
15	10	20	Very weak	None
15	15	20	Very weak	None
20	5	20	Weak	None
20	10	20	Strong	None
20	15	20	Strong	Slight, intermittent
25	5	20	Strong	Slow, intermittent
25	10	20	Strong	Slow, juddering
25	15	20	Strong	Smooth
30	5	20	Strong	Slow juddering
30	10	20	Strong	Juddering
30	15	20	Strong	Fast, smooth
35	5	20	Strong	Slow juddering
35	10	20	Strong	Juddering
35	15	20	Strong	Fast, smooth

Table 4.1. Initial oesophageal experiments

The strength was judged by observing the degree of contraction caused by stimulation and although not quantitative, the results from this initial test showed that the new design performed in such a way as to concur with results presented by Mosse.[189] (Table 4.2)

Voltage set	5V	10V	20V	25V	30V	35V
Resulting movement	Nothing	Nothing	Slow contraction no movement	Contraction no movement	Contraction rapid movement	As for 30V

Table 4.2 Results presented by Mosse showing the effect of varying voltage

across the electrodes of Device E4 placed in pig oesophagus.

The results show that smooth movement was produced by stimulation parameters of 15 Hz and 20 ms through a range of voltages from 25 V – 35 V. This showed close agreement with the results presented by Mosse.

However, as one of the aims of this project was to produce a system that would provide propulsion of the device in either direction, a prototype bidirectional capsule was devised that could fulfil this criterion.

For this design and each subsequent design change, a crude model of the charge density was used to determine the order of magnitude of the maximum charge density on the electrode. The charge density per cycle was calculated by

$$\frac{pulse\ width\ x\ current\ supplied}{electrode\ area}$$

Some values are presented in Appendix D.

4.4.2 Design and Construction of a Bidirectional Device

The bidirectional device (Fig. 4.9) was designed to have a tapered section with the same tapered angle ($\Theta = 47°$) at both the front and the rear of the device. Unlike its unidirectional counterpart it had two pairs of electrodes. One

131

pair of electrodes was placed on the rear tapered section to provide the induced forward motion and a second pair of electrodes was placed on the front tapered section to provide the induced backward motion. The electrodes were once again 2 mm diameter brass screw heads and the 2 m of insulated wires connected to each of them passed through the capsule and out through the rear tapered section.

15 mm

Electrode
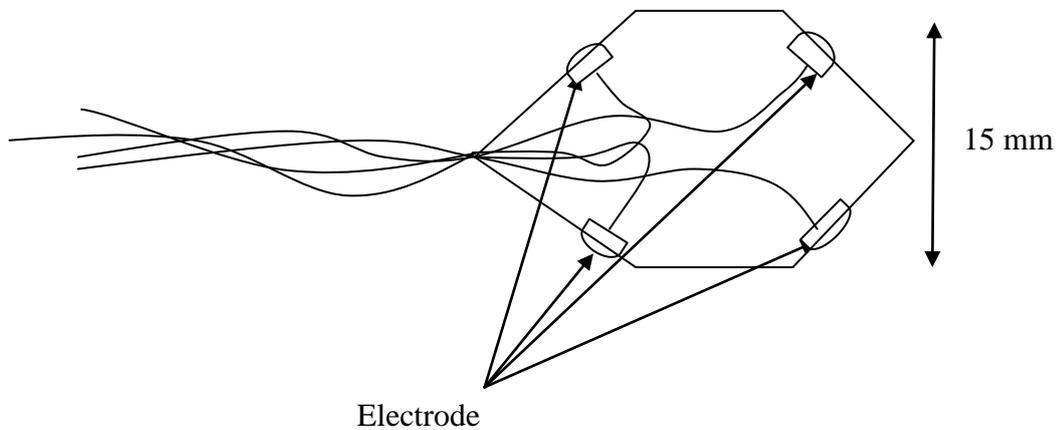
Fig. 4.9 Schematic diagram of original bidirectional device

The bidirectional device was initially constructed using a similar method to that used for the unidirectional device. The rounded section was replaced with another tapered section and holes for the extra electrodes were added. The hole from the rear of the device was drilled so that it connected to all the holes from the tapered sections. However, when the wires were fed into the holes it was extremely difficult to get them to emerge from the rear of the device. The hole through the centre was then increased to have a diameter of 3 mm. Although

132

this helped, it was not sufficient, so the construction method for the bidirectional

device was further modified.
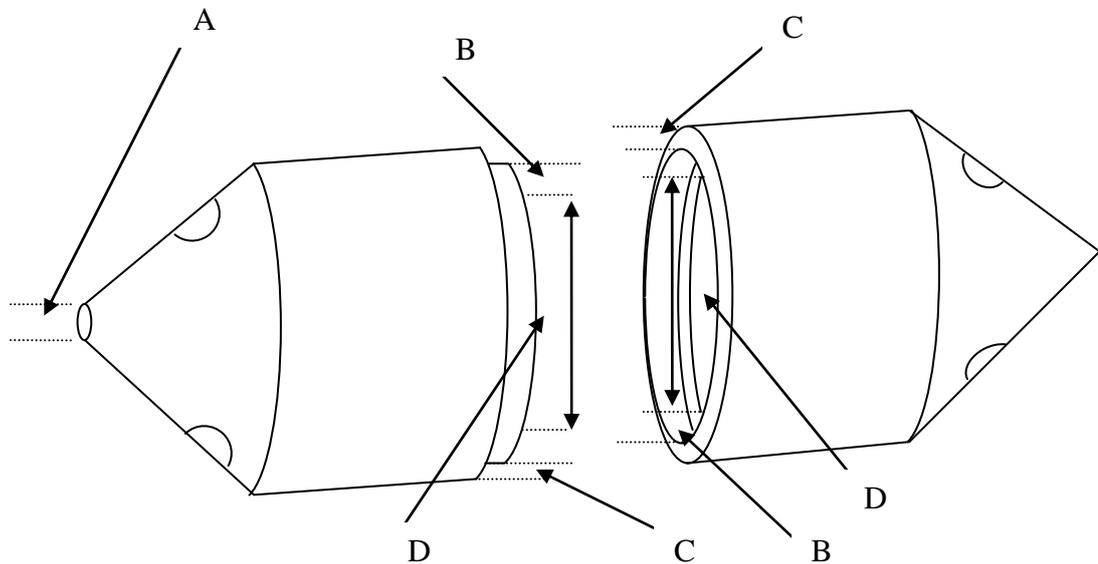
Device diameter (mm)	11	15	20
A: Wire exit hole	2	2	2
B:	3	3	3
C:	2	2	2
D: Inner diameter	6	10	15

Fig. 4.10 Schematic diagram of the second design of bidirectional devices

The modified device was constructed in two halves. Each half was

constructed from a acrylic cylinder with the same dimensions as that used for

the unidirectional device. Once the tapered section was complete the cylinder

was repositioned in the lathe so that a 10 mm hole could be drilled, thus making

a hollow device when the two halves were put together. A larger 12 mm drill bit

was used to make a 2 mm recess into one half of the the device, while the other

had a 2 mm lip with an outer diameter of 12 mm machined into it. This

produced a secure way of attaching the two halves together at the end of construction. Once polished the 2 mm holes were drilled on the tapered section to accommodate the wires, with only one hole required for the wires to pass through the rear of the device. When the wires were passed through the device the electrodes were fixed in place and the integral device was sealed with epoxy resin. Fig. 4.10 shows a schematic drawing of the second design of the bidirectional devices.

4.4.3 Initial Bidirectional Capsule *In Vivo* Experiment

The following experiments were undertaken to determine how the tapered front section of the bidirectional device affected its forward progress compared to that of the rounded front section of the unidirectional device. The experiments were also used to determine if the wires would affect the reverse progress of the bidirectional device. Therefore, the performance of the bidirectional and unidirectional devices were compared. Each device was fed through an over tube into the oesophagus of a small anaesthetised pig with a following endoscope. Once in place, the overtube was removed and the endoscope was withdrawn slightly so as not to interfere with the device, but not so far that sight of it was lost. The electrodes of the device were connected to a Grass SD9 stimulator (Grass Technologies, West Warwick, USA) using wires.

In a preliminary experiment, induced muscular contraction was observed on activation of the stimulator at 10 V, 15 Hz and 15 ms with both the bidirectional and unidirectional devices. Further experiments using a range of voltages and frequencies similar to those examined in the initial test with the

unidirectional capsule were then performed. The results showed that contraction with movement was achieved at 20 V with a frequency of 15 Hz. However, contraction with no movement was observed at 10 V and 15 V with a frequency of 15 Hz. For the unidirectional device, contraction with movement was again observed at 20 V with a frequency of 15 Hz. Once again, however, contraction with no movement was observed at 10 V and 15V.

The tests were repeated in the small intestine of the anaesthetised pig during laparotomy, where an incision is made in the abdomen of the pig to allow direct access to the intestines. Both devices moved continuously without juddering with 20 V, 15 Hz and 15 ms supplied by the Grass stimulator. The results were similar to those found in the oesophagus. In both the oesophagus and in the small intestine the two devices appeared to perform as well as each other. With this equality of performance confirmed, further investigations used only the bidirectional devices.

4.4.4 Design and Construction of Devices of Different Diameter

In order to investigate how the diameter would affect the performance of the devices, bidirectional devices of different diameters were made to be tested in the pig model. Similar in design to the original, three devices with diameters of 11 mm, 15 mm and 20 mm were constructed with 2 mm diameter stainless steel electrodes (Fig. 4.10). These devices would be used to examine how the difference between device diameter and lumen diameter would affect their

performance. The 11 mm device was of special interest as it was the only device which could safely pass through the pylorus, allowing it to travel the whole length of the gastrointestinal tract after being swallowed in the human model.

The devices were constructed using similar methods to those used for the original 15 mm bidirectional device, but there were two differences to be taken into consideration. First the diameter changes meant that the internal diameters of the hollowed sections also changed. Each of the devices was constructed to have 5 mm thick walls with the 2 mm thick attaching lip. The second change to the construction method was the soldering of the stainless steel electrodes to the wires. As the flux within solder does not aid bonding to stainless steel, ortho-phosphoric acid was used as a flux. The electrodes were then fixed in place with epoxy resin.

All three were tested separately in porcine small intestine during laparotomy. Although it was possible to fit all three devices into the small intestine, the 20 mm device was approaching the maximum diameter that the small intestine could accommodate without distension occurring. The three devices were tested using the same stimulation parameters that had been used in the initial test. Similar results were now observed for all three capsules regardless of size. Contraction, but with no movement, was observed when the stimulator produced voltages of 10 V or 15 V, and contraction with movement was observed when the stimulator produced a voltage of 20 V. These tests were performed using each pair of electrodes at separate times, producing the same results both for movement with and against the natural intestinal flow.

An interesting problem was discovered during these experiments. When the small intestine is empty it lies flat. Consequently the 11 mm capsule which

did not have an outer diameter large enough to fill the cavity left voids between itself and the lumen of the small intestine. This meant that when the 11 mm capsule was placed into the small intestine at certain orientations, with the electrodes in these areas of non-electrical contact with the internal walls, induced contractions could not be produced. The 11 mm diameter capsule is of greatest interest if the device has to be swallowed, as it is the only device with a diameter small enough to pass through the pylorus safely. With this criterion in mind a solution to the 'non-electrical contact' problem had to be found.

This left the author with an intriguing problem. The initial thought was to move the position of the electrodes to an orientation whereby the electrodes could not lose contact with the wall of the small intestines. Moving the electrodes closer to one another around the circumference of the device was the first considered as stimulation of any portion of circumference of the lumen would cause the circular muscle to contract. Although this would ensure one electrode would be in contact with the wall of the small intestine, it did not prevent the problem as a situation could still arise where the other electrode was not in contact. In fact any orientation of the 2 mm electrodes could lead to a situation where electrical contact between at least one of the electrodes and the small intestines was lost. It was at this moment the author thought of a design for the electrodes which would allow both of them to remain in contact with the small intestinal wall no matter how the device was positioned. If the electrodes covered almost all of the tapered section leaving only a small gap between them, they would remain in contact with the lumen of the small intestine no matter how flat it became. Resulting from this, large area electrodes were designed,

each to cover half of the entire tapered section except for a small insulating gap between them.
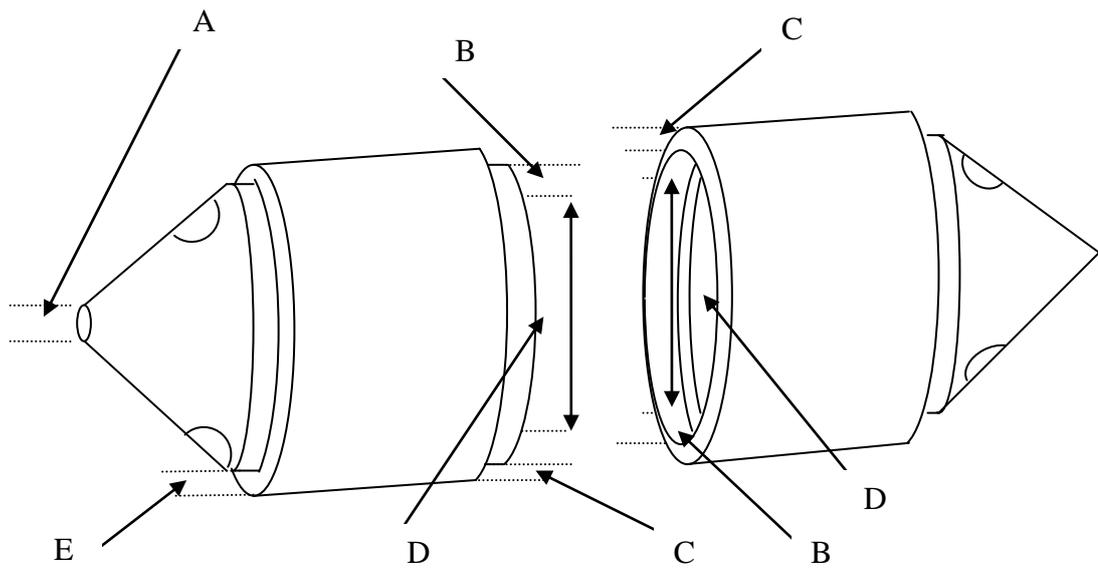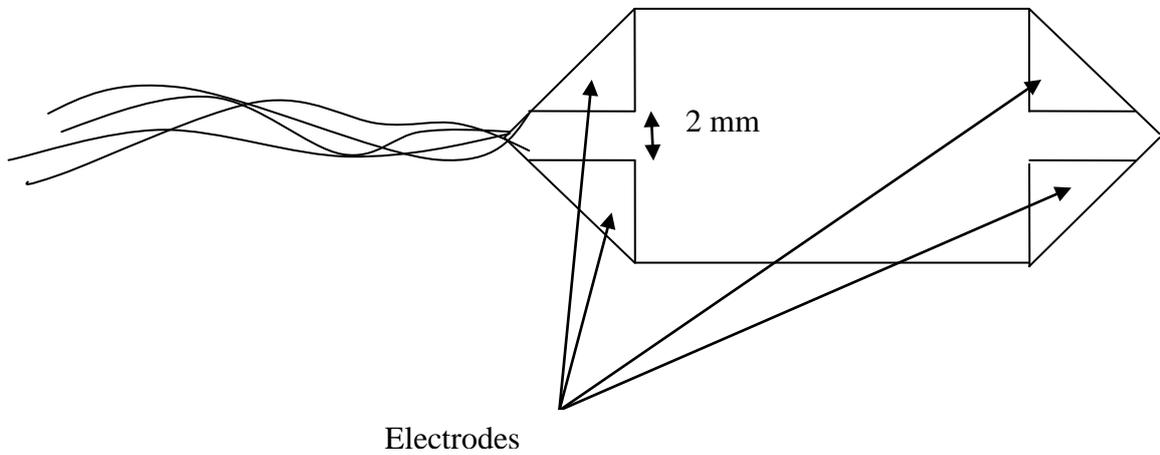
Electrodes

Device diameter (mm)	11	15	20
A: Wire exit hole	2	2	2
B:	3	3	3
C:	2	2	2
D: Inner diameter	6	10	15
E: Taper depth	1	1	1

Fig. 4.11 Schematic diagrams of large electrode bidirectional device

The electrodes were constructed by using a lid from a cruet set. The lid to the salt cellar was used as it had one hole at the apex of the cone which allowed it to fit over the wires snugly as they left the rear of the device. The lid was conical in shape with a cylindrical base which was tapped so that it could screw onto the salt cellar. Once the tapped portion of the lid was removed the conical section was cut in half from apex to base to produce two large area electrodes. Construction of the body of the large electrode device was the same as that for the small electrode device apart for one small adaptation. As the electrodes could not protrude beyond the outer diameter of the device, the maximum diameter of the tapered section was reduced by a millimetre. The electrodes were then attached to the tapered section with an excess of epoxy resin, which was allowed to pass out through the gap between the electrodes. When set, the excess epoxy resin was filed away leaving the electrodes with the appearance of having been counter sunk into the device with a 2 mm insulated gap between them.

This new design shown in Fig. 4.11, enabled the electrodes of the 11 mm diameter capsule to remain in contact with the lumen of the small intestine, regardless of their orientation. In a pig during laparotomy, this larger electrode design overcame the problems associated with the previous small electrode design allowing the 11 mm device to work continuously as it remained in electrical contact at all times.

All the previous experiments were qualitative, based on visual observations to estimate how successful the stimulation had been. They showed that in principle a bidirectional stimulation device worked effectively.

With this degree of reliability, a more quantitative set of experiments were devised to measure how different parameters affect the speed that the devices travelled along the small intestine during a one minute period.

4.4.5 The One Minute Tests

This section describes the variety of one minute tests that were performed to help in the development of the final design of the bidirectional device. All of the following *in vivo* experiments described were performed in the small intestines of anaesthetised pigs during laparotomy. This procedure involved an incision in the abdomen through which loops of the small intestines were drawn. Once exposed, a small incision in the wall of the small intestine was made to allow the devices to be introduced.

The distance the devices moved during the one minute stimulation period was measured. The measurements were taken between two marker points produced with the aid of an electric diathermy scalpel that was used to mark the wall of the small intestines at the start and finishing positions of the back of the device.

Electrostimulation was applied for one minute and then switched off. It was observed that the devices continued to move for a few seconds after the electrostimulation was switched off. This was an interesting phenomenon and could have been due to the reaction time of the smooth muscle.

4.4.5.1 The Effect of Capsule Diameter on Movement

The three devices were then used to determine quantitatively the effect that the diameter of the capsule had on its *in vivo* movement capabilities. The method used was to activate the stimulator for a one minute period using the stimulation parameters from the initial experiment that produced definite movement (20 V, 15 Hz, and 15 ms). The stimulator used had an output impedance of 1 kΩ implying an output current of approximately 1 mA to each 1 V output.
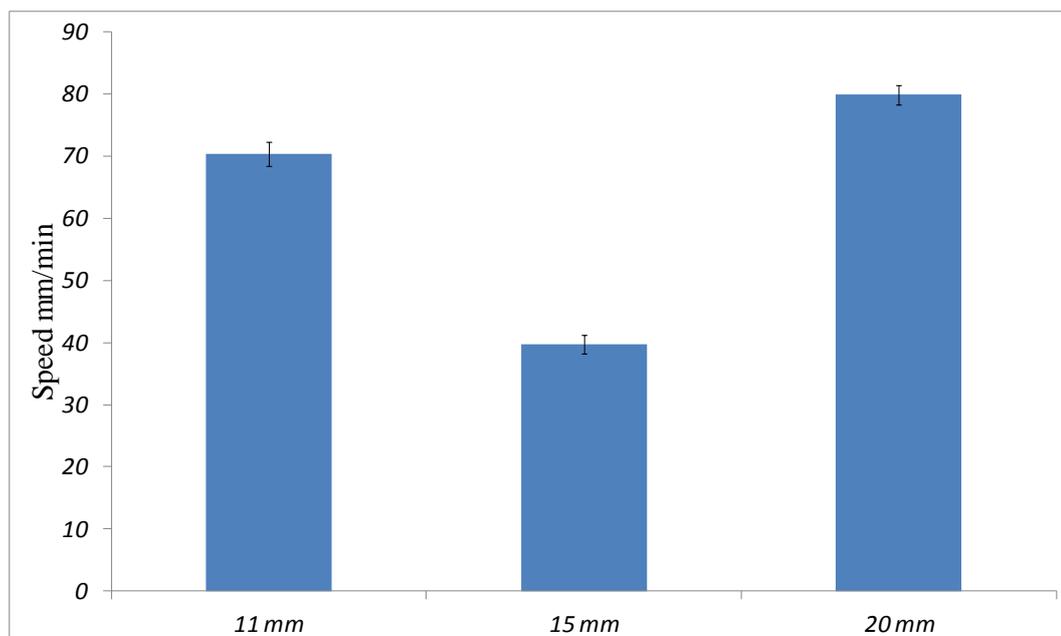
Fig. 4.12 The impact of the capsule diameter on device speed.

The results from this experiment (Fig. 4.12) show that the 11 mm and 20 mm devices moved by comparable distances 70 mm (SD 1.8) (N = 10) and 80 mm (SD 1.6) (N = 10) respectively, while the 15 mm device movement was

40 mm (SD 1.8) (N = 10). Although this was a promising result from the point of view of constructing a device that could be swallowed (i.e. the 11 mm capsule), the result for the 15 mm device was surprising. It was postulated that again the screw electrodes may have been the cause of the problem as they may not have been in full contact with the tissue at all times with the 15 mm device.

With this in mind large area electrodes were fitted to 15 mm and 20 mm devices. These devices were constructed using the same method as the 11 mm device producing counter sunk electrodes covering the whole tapered section with a 2 mm insulating gap between them. The experiment to determine the effect of device diameter was repeated. The results from this revealed that the 15 mm device performed as well as the 20 mm device and just slightly better than the 11 mm device.

 This was a very promising result as it showed that the performance of the 11 mm device with the large area electrodes was comparable to that of the larger diameter devices. This suggests that a device that can be swallowed could be propelled as effectively along the small intestines by electrostimulation as a larger device which fills the whole lumen.

4.4.5.2 11 mm Bidirectional Device Compared with Dummy Video Capsule Endoscope Device

Once it was determined that the 11 mm large electrode device would perform in a satisfactory and reliable way, the focus of the project was transferred to designing a video capsule endoscope that would perform with electrodes attached directly to it. Although the diameter of the video capsule

endoscope was the same, the ends of it were hemispherical and not conical. Therefore, a new device design (Fig. 4.13) was produced using as its framework a dummy copy version of an M2A passive video capsule endoscope that could be swallowed. This dummy version had the same dimensions as the real video capsule endoscope with no electronics inside, and was therefore considered to be a good guide to the genus of a device that could be initially swallowed and then propelled by electrostimulation. The performance of the dummy video capsule endoscope device was compared with that of the bidirectional device to determine how the hemispherical ends would affect movement.

The dummy capsule device was constructed around a replica of an M2A capsule. Although these replicas had been made to give clinicians an idea of the size and weight of a video capsule endoscope, they were an ideal base on which to construct a device to show how a real video capsule endoscope would perform when compared to the 11 mm large electrode bidirectional device.

One pair of semi-hemispherical large area stainless steel electrodes similar in design to those on the bidirectional device were soldered to 2 m long 0.5 mm diameter insulated wires and attached to the rear of a dummy M2A capsule using epoxy resin. Once in place, insulating tape was used to hold the electrodes in a fixed position relative to the device until the epoxy was set. Once set the epoxy was filed to produce a device with counter sunk electrodes.
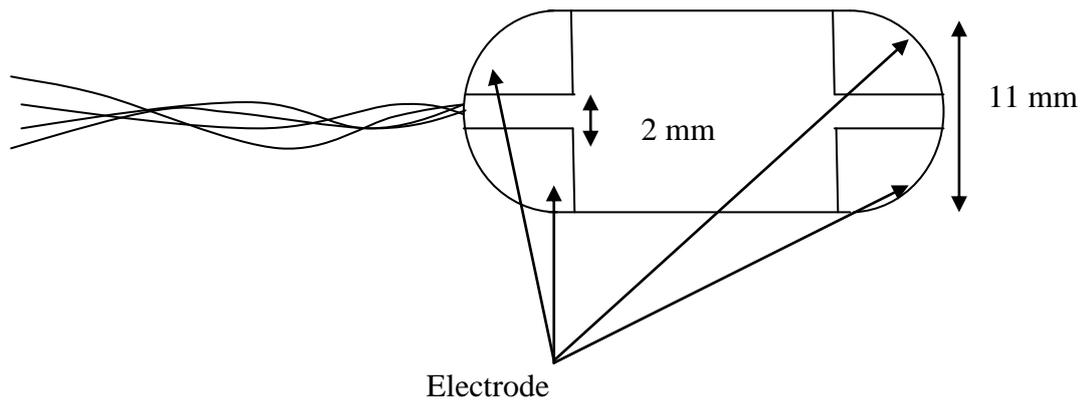
Fig. 4.13 Schematic diagram of the dummy device.

A new set of one minute tests was carried out to determine how the hemispherical ended device would perform relative to the bidirectional device. The dummy copy was fitted with a pair of rounded large area electrodes attached to the rear of the capsule. This was tested against the 11 mm bidirectional device in a pig during laparotomy. Stimulation of 15 Hz, 20 ms with a voltage of 20 V was used as these parameters had been shown to give smooth movement in the original tests.
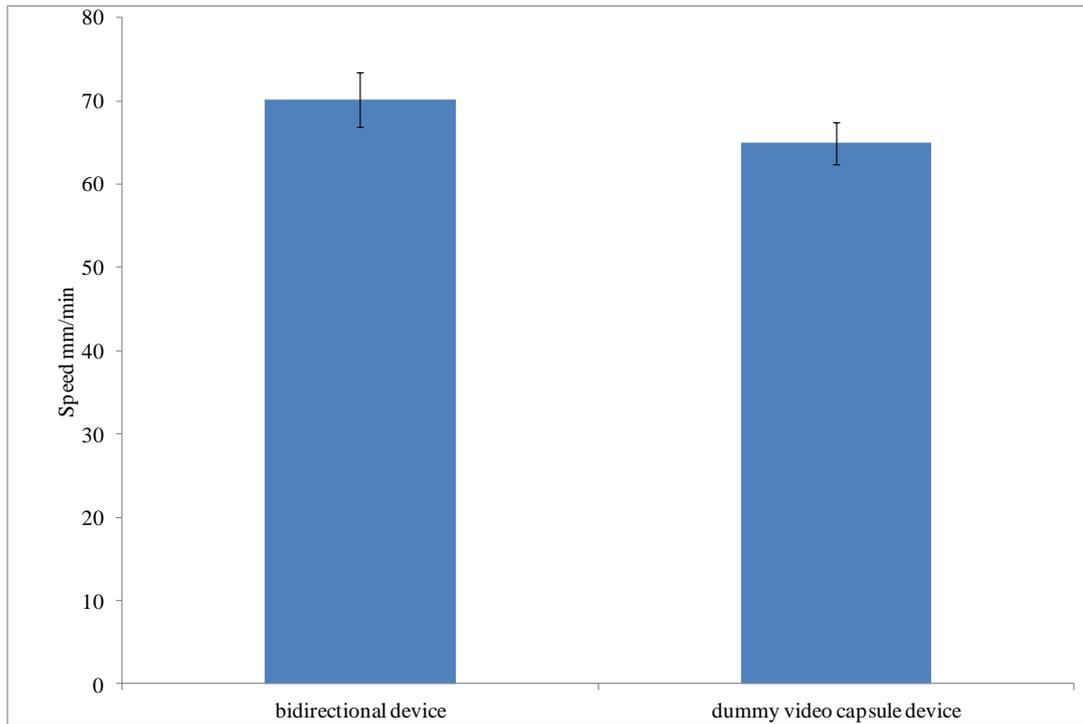
Fig. 4.14 Performance of hemispherical ended device (dummy lozenge)

compared with bidirectional device (lozenge).

The experimental results (Fig. 4.14) showed that there was very little difference between the performances of the two designs. Within one minute the bidirectional device moved 70 mm (SD 3.2) (N = 9) and the dummy capsule device moved 67 mm (SD 1.0) (N = 9). This result was very promising as it would allow electrodes to be placed directly onto functioning video capsule endoscopes. This would allow for their use during later experiments to show real time footage of what the clinician would see during stimulation. With this in mind future designs of the 11 mm device were constructed using dummy copies of the M2A video capsule endoscope device as the framework.

4.4.5.3 Effect Caused by Changes in Frequency on Movement

The revised rounded device was then used to determine if the frequency parameter had any effect on its movement. After placement in the small intestine during laparotomy, the electrodes were activated using the Grass SD9 stimulator for a one minute period at different frequencies. As with the earlier one minute tests, the distance the device travelled for each set of values over one minute was recorded. The voltage and pulse duration values were kept constant, at 20V and 20 ms respectively.
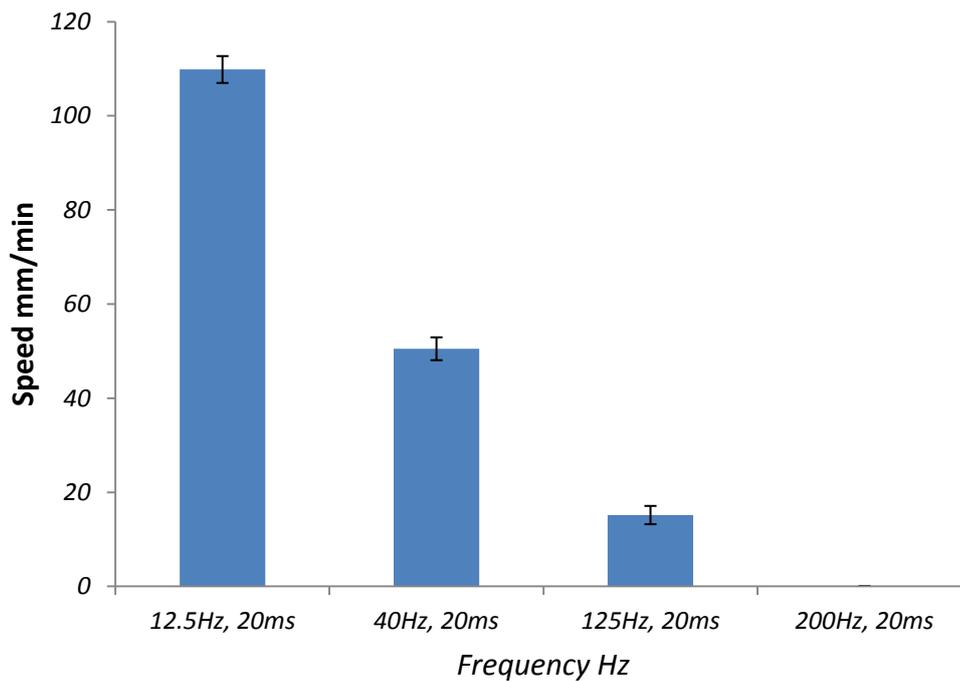
Fig. 4.15 Test of the effect of frequency on duration.

The results shown in Fig. 4.15 reveal that a frequency of 12.5 Hz produced the greatest movement of 110 mm/min (SD 2.9) (N = 6).

Measurements presented earlier have already established that frequencies below 12.5 Hz could not be used because they produce judders in the muscle around the device.

4.4.5.4 Effect Voltage has on Device Movement

Another set of one minute tests were used to determine the effect that different voltage settings had on the devices movement. The method used was to activate the stimulator for a one minute period with different voltages, and record the corresponding distances travelled by the capsule. The other electrical parameters were kept constant (frequency 12.5 Hz, pulse duration 20 ms).
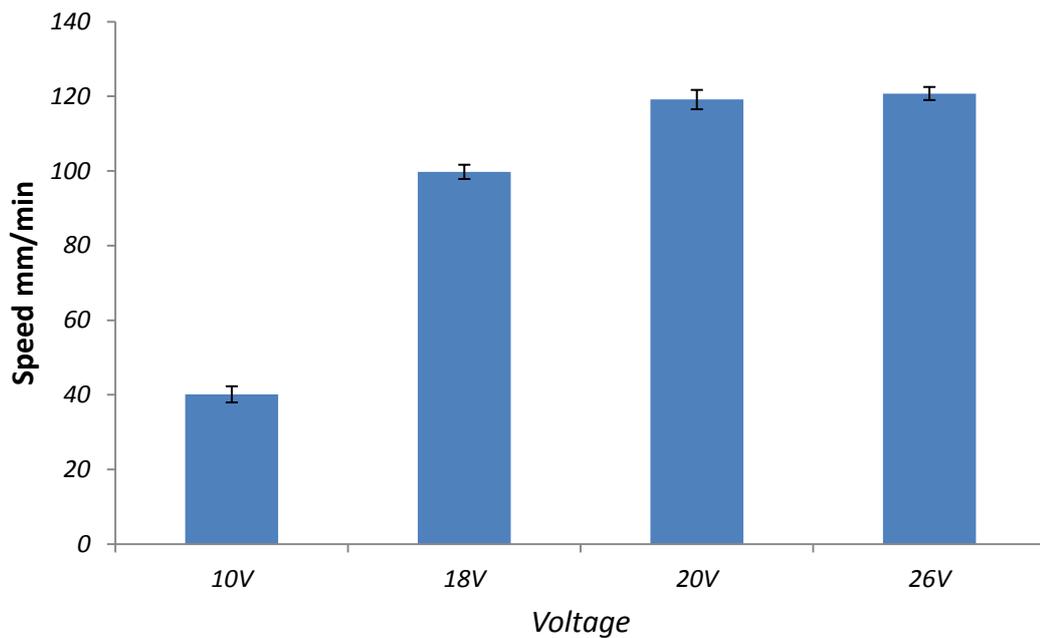
Fig. 4.16 Effects on voltage.

These results (Fig. 4.16) show that the maximum speed with which the capsule moved within the porcine small intestine was 121 mm/min (SD 1.8)

(N = 10), achieved at a voltage of 20 V. The speed did not increase when the voltage was increased to 26 V suggesting that 20 V was sufficient to activate all the local muscle tissue. Thus the optimal stimulation parameters which gave the best movement were 12.5 Hz, 20 ms, and 20 V.

Fig. 4.17 shows the progression of the device along an exposed loop of small intestines. The device is circled in the initial photo and its progress can clearly be seen through the series of photos. The time represented by the series of photos is 23 seconds, during which the device travelled at least its own length (27 mm), suggesting a speed in this video of about 70 mm/min.
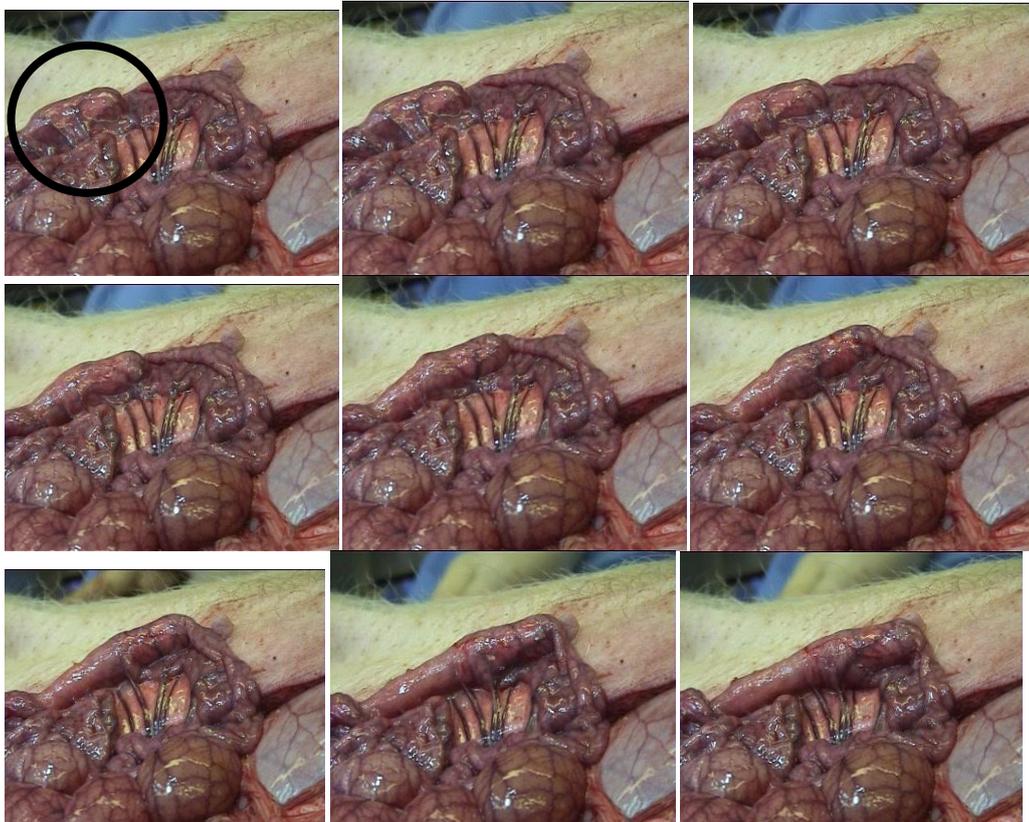
Fig. 4.17 Stills from a 23 second video showing the progression of an 11 mm device being propelled along a loop of exposed small intestine.

4.4.5.5 Double Ended Video Capsule Endoscope Device

The next stage in the design development was to add a pair of electrodes to the front of video capsule endoscope which needed to be slightly different to those at the rear. These electrodes had to be redesigned because the original design, which up until now had been used to determine optimal stimulation parameters, would have obscured the camera's field of view when attached to a real working M2A video capsule endoscope device. The front electrodes were placed further back along the body of the capsule so that they did not obscure the camera's field of view. This led to a gap greater than 2 mm between the electrodes and it was thought that this may once again produce the non contact problem that produced the initial need for the large area electrodes. (Fig. 4.18)

Fig. 4.18 Double Ended video capsule endoscope

The front pair of electrodes was therefore redesigned by the author to encircle the front end of the capsule just behind the lens. As can be seen in

149

Fig. 4.19. The electrodes once again had the same small insulating gap between them as the rear electrodes.

Fig. 4.19 Bidirectional video capsule endoscope

This front end design produced a performance which was comparable to that of the larger area rear design. Using a 12.5 Hz, 20 ms stimulation pulse with a voltage of 20 V within the small intestines the front electrodes pushed the device at 117 mm/min (SD 1.7) (N = 10). The rear electrodes pushed the device forward at 119 mm/min (SD 2.1) (N = 10).

This design was then applied to a functioning M2A video capsule endoscope for testing. With a few modifications to the connecting wires, this design evolved into that employed for the future human experiments. For reasons explained in the next section the wires needed to be replaced with those having a greater strength and covered with additional flexible rubber tubing.

4.4.6 Capsule Construction from Animal to Man

Unlike the earlier tapered devices, which were constructed from perspex, the outer casing of the dummy M2A capsules are constructed from PTFE. This makes them difficult to bond electrodes to. However, epoxy resin was found to bond the stainless steel electrodes and the PTFE casing securely to the devices constructed for the earlier tests. This caused its own set of problems as electrodes connected to wires had a tendency to move during the curing process of the epoxy. This caused the electrodes attached to initial devices to be somewhat out of alignment when the epoxy had set. To overcome this the electrodes and unset wet epoxy were encased in tape which held the electrodes in a fixed position until the epoxy had cured. This produced devices which although not perfect, produced good movement in the small intestine. This design then evolved into a bidirectional device which used the same size electrodes at the front and rear. The front electrodes had to be placed further back along body of the capsule so that they did not obscure the camera's field of view. This produced an unwanted large gap between the front electrodes, which was shown in section 4.4.3 to cause intermittent contractions due to the orientation of the electrodes relative to the lumen of the intestine. To compensate for this, the front electrodes were redesigned to wrap around the body of the capsule just behind the lens. This design allowed them to be in constant contact with the lumen at all times, whatever the orientation of the capsule. The positioning of the electrodes did not affect the performance of the device so that the design was adopted for the human test.

The successful construction of bidirectional dummy M2A devices led to the construction of a bidirectional functioning video capsule endoscope. The video capsule endoscope construction process identified two additional concerns. The circuit of a M2A video capsule endoscope is activated by the removal of a magnet which is placed within its packaging. Therefore, the electrodes had to be attached and taped quickly so the capsule could be deactivated as quickly as possible by being returned to the magnetic field. During construction, every effort had to be made to ensure no epoxy resin obscured the view of the camera.

Fig. 4.20 Bidirectional video capsule endoscope

Although the design of the electrodes had been determined, the prototype design was far from acceptable for a human trial as the contruction was not up to a suitable standard. It can be seen in Fig. 4.20 that the wires from the front electrodes had to be incorporated within the body of the device. As it was not possible to pass the wires into the video capsule endoscope, they were taped to the exterior of the capsule using insulating tape. Once the electrodes were correctly positioned, a coating of epoxy resin was applied to the whole

body of the capsule, leaving only the lens free of resin. This was then taped to ensure the electrodes were held in place until the epoxy had set. When set the tape was removed and the resin coating was filed back to expose the electrodes. At the end of a human trial the device will have to be retrieved from the subject's small bowel by pulling it out through the mouth, and therefore the wires need to be sufficiently strong. Therefore for the final design, (Fig. 4.21) the wires used were nylon coated steel fishing line. For an added extra safety precaution the wires were encased in silicone rubber tubing to prevent damage to the volenteer's gastrointestinal tract during the withdral of the device.
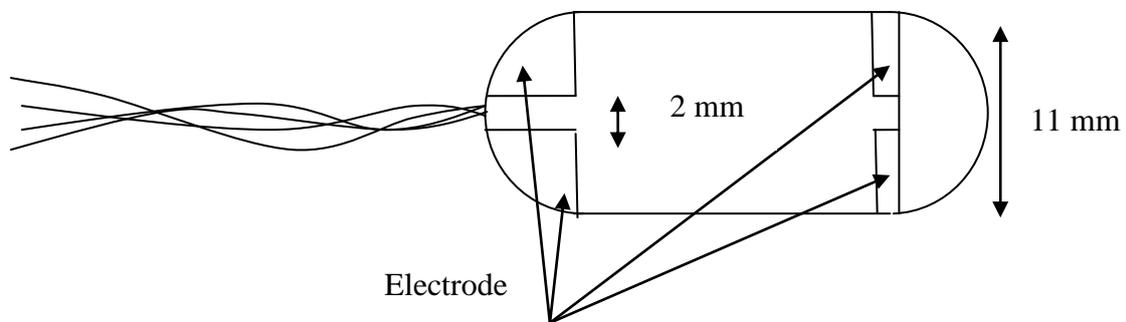
Fig. 4.21 Schematic diagram of bidirectional video capsule endoscope for the human test.

A device without a camera was made to be used in a preliminary set of animal tests. These were performed to ensure this design and production method produced a device that would provide an adequet performance during

153

the human tests. Stimulation with a frequency and duration of 12.5 Hz and 20 ms at 20 V was supplied to the electrodes. The device performed much better than expected during these tests, moving with a speed of 300 mm/min (SD 1.8) (N =10) in both directions. When compared to the results from previoius tests (section 4.4.5.4), the device produced over twice the speed using the same stimulation parameters. This was due to better construction methods which enclosed the wires from the front electrodes and ensured better electrode placement. The tissue was examined after the proceedure to look for signs of damage due to electrolysis from excessive charge. None was found. Therefore, two devices of this design with cameras were then constructed for the human tests.

4.5   Human Subject Experiments

To determine exactly how the device would function in humans, the final design development stage of the capsule requires that it be made suitable for use on a human volunteer. Ethics committee approval was granted to Swain to conduct four human experiments. This section begins with a description of the modifications made to produce the final capsule design. It continues with a description of the procedures used during the experiment and ends with an analysis of the results.

4.5.1 Modifications to the Capsule

As discussed previously, the capsule needs to be retrieved by pulling it back out through the subject's mouth via the attached connecting wires. Therefore, the thin electrical wires used for previous devices were replaced by Nylon coated steel fishing wire. The electrical conductivity of the wires did not pose much of a problem. The resistance of the wires was in the region of a few tens of ohms per meter, which was insignificant compared with the output impedance of 1 kΩ of the Grass stimulator.

Fig. 4.22 Video endoscope capsule with attached electrodes.

It was also necessary that the wires were covered with a soft coating so that the device could be retrieved via the mouth without causing any harm to the

subject. With this in mind the wires were covered with flexible medical grade silicone rubber tubing. (Fig. 4.22) Markings were then placed at 200 mm intervals along the outside of the tubing so that the distance the device had travelled through the gastrointestinal tract would be instantly known.

4.5.2 The First Human Subject Experiment

During the experimental investigation it was essential to monitor the possible effects on the subject's pulse rate and to test any muscular sensation felt when intestinal muscular contractions were induced by electrostimulation. The capsule was initially swallowed by the healthy consenting male volunteer and allowed to pass naturally through the oesophagus and stomach into the small intestine. Once in the small intestine the connecting wires of the device were connected to the Grass stimulator. The stimulator was set to the optimal parameters of 12.5 Hz and 20 ms. The effects of a range of voltages starting at 2 V and increased in 2 V increments to 10 V were investigated as a cautious preliminary test to determine the minimum voltage which would produce satisfactory capsule propulsion. The effect of using alternate electrode pairs to induce forward and backward movement in the voltage range 0-7 V was also investigated.

Before starting the experiment the volunteer used an anaesthetic spray to reduce their gag reflex. The spray was administered throughout the duration of the experiment at the request of the volunteer, as and when it became too uncomfortable to continue. The experiment took place partly in the preparation

room and partly in an X-ray suite. Within the preparation room was a computer running the video capsule endoscope's real time viewer. This enabled the transit of the device to be observed in real-time and allow the attending clinician to determine when the capsule had reached the volunteer's small intestine. The volunteer swallowed the device, seven minutes after which the transmitted images from the pill camera showed that the device had entered the stomach. After a further seventeen minutes the device was observed to enter the small intestine of the subject.

The subject was then moved from the preparation room to an X-ray room with a video screening facility so that the progress of the capsule through the intestine could be monitored using X-ray fluoroscopy. When the subject was correctly positioned on the table so that fluoroscopy could take place, the connecting wires of the capsule were connected via a switching-box to the Grass stimulator.

The switching-box had been built to facilitate an instant method of selecting the electrode pair which delivers the stimulation at any given time. This was a simple device which included a pair of input terminals and two pairs of output terminals. An integral double-throw switch allowed the signal from the input terminals to pass through either of the output terminal pairs. The output signal of the Grass stimulator was connected to the input terminals of the switching-box. The front and rear electrode were connected as pairs to the output terminals on the device. This allowed the direction of induced movement of the capsule to be selected at the flick of a switch.

Once all the equipment was set up correctly it was tested on the subject. The pulse of the subject was monitored using a pulse oximeter, and verified

using palpation. This was required to detect any adverse effects the stimulation

had on the subject's pulse. The results are summarised in Table 4.3.

Pulse rate of the subject	Direction of intended movement	Time	Grass voltage	Observations
Stable at 75	Forward	09:53	2 V	No internal muscular sensation. No movement
Stable at 75	Forward	09:55	4 V	No internal muscular sensation. No movement
Drops 75-69	Forward	09:55	6 V	No internal muscular sensation. No movement
Drops 75-67	Forward	10:01	6 V	No internal muscular sensation. No movement
Fluctuates 75-56-66	Forward	10:04	0-8 V	No internal muscular sensation. Device felt to move at mouth
Drops 68-55	Forward	10:05	0-8 V	No internal muscular sensation
Fluctuates 68-55-63-43	Forward	10:10	0-10 V	No internal muscular sensation. Movement observed 10V gave many extra systoles

Table 4.3. Initial human test results.

Immediately the reduction of heart rate was observed the test was

stopped. And as soon as the stimulation was stopped, the heart rate of the

volunteer returned to normal. The volunteer reported no adverse sensations

during the test and wished to carry on with the experiment. It was postulated that the reduction in heart rate had been produced by an inadvertent stimulation of the vagus nerve, the extremity of which can reach as far as the top of the small intestine. After this set of tests the subject was returned to the preparation room. Further tests were then performed so that pictures of the intestine taken by the capsule camera could be seen in real time on a monitor screen. The device was observed to move forward and backwards a few times, all at 0-7 V, with the subject in a sitting position. Again, a frequency of 12.5 Hz with signal pulse duration of 20 ms was used. The results are summarised in Table 4.4.

Stable at 68	Forward	10:17	0-7 V	No internal muscular sensation. Movement observed
Drops 69-67	Backwards	10:20	0-7 V	No internal muscular sensation. Movement observed
Raises 63-66	Forward	10:23	0-7 V	No internal muscular sensation. Movement observed
Drops 66-50	Backwards	10:25	0-7 V	No internal muscular sensation. Movement observed

Table 4.4 Initial bidirectional human test results

When the switch on the switching-box was set to the forward movement position, the real time viewer appeared to show forward movement. When set to the backwards position, the device appeared to move backwards a little, then forwards, and then back again, i.e. no discernible net movement was observed. The subject gagged during these tests from the wire pulling in his throat. At 7 V

there appeared to be induced movement, but the results were ambiguous, because there was still a marked movement of the intestine even after the electrode voltage was switched off. This may have been caused by continual peristaltic activity.

The subject was then taken to another X-ray room, as the original X-ray room was occupied. This X-ray room also had video screening. The results of these tests are summarised in the Table 4.5.

Pulse of the subject	Direction of intended movement	Time	Grass voltage	Frequency	Duration	Observations
67-75-67	Forward	11:13	0-7 V	12.5 Hz	20 ms	No internal muscular sensation. Movement observed
67-70-69	Forward	11:14	0-9 V	12.5 Hz	10 ms	No internal muscular sensation. No movement observed
66-74-68	Forward	11:18	0-9 V	12.5 Hz	20 ms	No internal muscular sensation. Movement observed
66-74-68	Backwards	11:21	0-9 V	12.5 Hz	20 ms	No internal muscular sensation Slight movement observed
72-78-72	Forward	11:56	0-7 V	12.5 Hz	20 ms	No internal muscular sensation. Movement observed
78-74	Forward	11:58	0-10 V	12.5 Hz	20 ms.	No internal muscular sensation. Movement observed
70	Backwards	12:01	0-10 V	12.5 Hz	20 ms	No internal muscular sensation. Slight movement observed

Table 4.5 Bidirectional human test results.

The capsule was then pulled back to the 800 mm distance mark so the device was in the small intestine approximately 300 mm from the pylorus. It was tested at 0-10 V in the forward direction. Intestinal contractions were observed with X-ray imaging. Rhythmic contractions were observed before and after the voltage signal was switched on. At this point the subject wished to terminate the testing session, as the discomfort caused by movement of the wires on the back of his throat had become unbearable.

4.5.3 The Second Human Subject Experiment

The second experiment was performed in much the same way as the first. The same subject volunteered to take part in this new experiment under the same conditions and using a video capsule endoscope device constructed to the same specifications as before. The difference in the two experiments was the way in which the second one was monitored.

Due to the observed reduction in heart rate of the subject during the first trial when the electrostimulation was applied, an anaesthetist was now present in case fibrillation of the subject's heart was unintentionally induced. A number of different methods of monitoring the progress of the capsule were used.

The X-ray video monitor and the capsule real time camera video viewer were only used separately during different portions the first experiment. However, this time they were both monitored simultaneously. In addition, the signal output current was measured and recorded using a computer oscilloscope. There were also three video cameras present. One of these was placed in a

position to view the entire room. A second was focused onto the monitor showing the real time images from the capsule, and the third was focused on the monitor of the computer oscilloscope that was showing the signal output current.

The outputs from the three cameras together with the output from the X-ray video-monitoring device were connected to an adapter device that enabled the four distinct images to be simultaneously shown in separate quarter segments of a video screen. This multi-image video picture was then transferred to a video recorder in order to obtain a comprehensive record of the entire procedure.

As with the first test, the subject swallowed the capsule, which was allowed to pass naturally through the oesophagus and stomach into the small intestine. With the presence of the real time viewer, the progress of the capsule could be continually monitored and timed. The capsule was observed to enter the small intestine about 30 minutes after it had been swallowed.

When the capsule was observed to be inside the small intestine of the subject the wires from the two electrode pairs were connected to the switching-box, which was then in turn connected to the Grass stimulator. The stimulator was set to 20 ms 12.5 Hz. The signal voltage was initially set at 2 V and then increased in steps of 1 V, so that each step could be individually tested.

It was essential to monitor the possible effects on the subject's pulse rate and to test any muscular sensation felt when intestinal muscular contractions were induced by electrostimulation. The front pair of electrodes was the first to be connected. There was no observed effect on the subject's heart rate produced by the device up to a signal voltage of 15 V.

As there had been no detectable response to a range of signal voltages supplied to the front pair of electrodes, the rear pair of electrodes were switched on to observe any effects that might occur. However, the 15 V setting was still switched on and the subject felt a sharp pain causing him to sit up and bring his legs up. The stimulator was turned off immediately. After ensuring the subject was unharmed and willing to resume testing, the signal voltage was reduced to 4 V and the experimentation was then continued.

The signal voltage was then increased as before in 1 V steps until movement was observed on the X-ray monitoring screen at a signal voltage of 5 V. The signal voltage was then increased to 8 V, 10 V and 12 V. There were no observable adverse effects produced by any these signal voltages. Movement of the capsule was observed at all signal voltages above 5 V. The greatest movement observed at a signal voltage of 10 V. Fig. 4.23 shows a set of stills taken from a video indicating the forward movement of the device recorded with the four way video system described earlier. Unfortunately due to technical difficulties the camera videoing the room malfunctioned. The three remaining video feeds were: the image from the video capsule endoscope (top left), the X-ray image (bottom left) and the computer based oscilloscope in (top right). The device can be seen to move in the X-ray image, while the stimulation is being applied. The video feed from the capsule shows what a clinician would see while the device is being propelled.
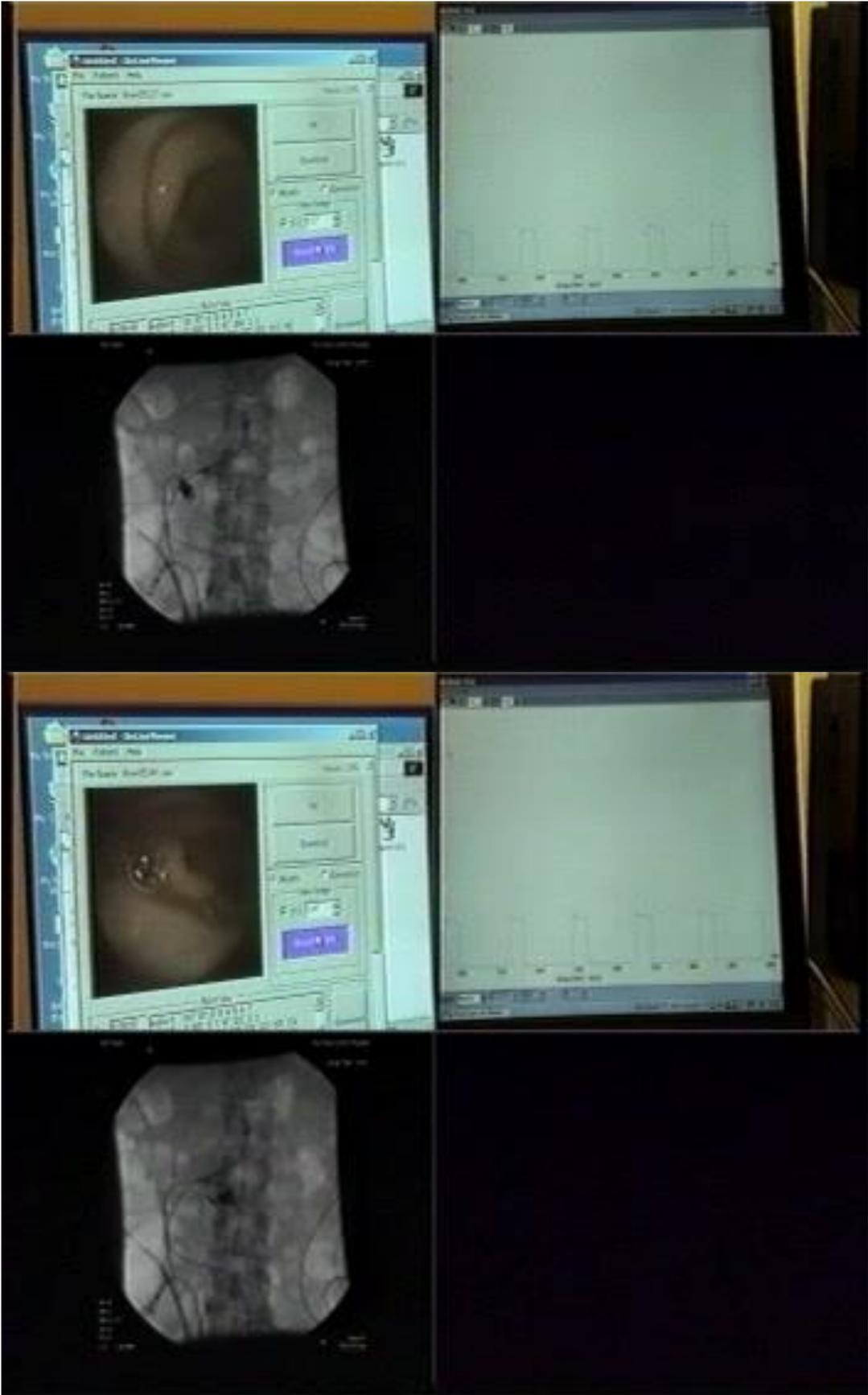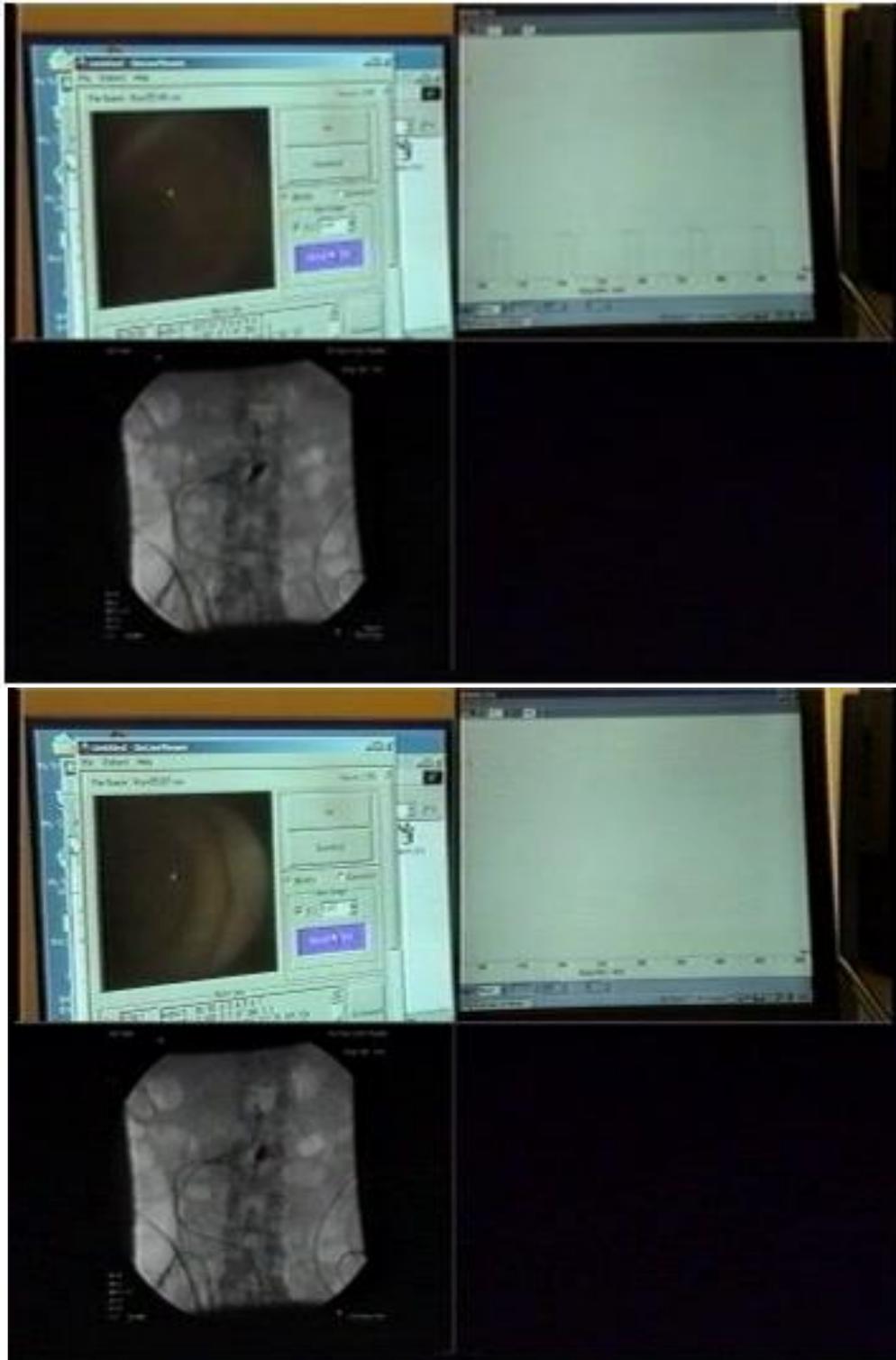
Fig. 4.23 Stills from video showing forward propulsion along the small intestine of device in human subject. Each slide shows view from device camera, stimulation parameters and X-ray showing relative position of the device in the small intestine.

Following this, the effects of direction change were investigated. A signal voltage of 10 V was initially applied across the front pair of electrodes. This propelled the capsule against the natural flow of the small intestine. The switching-box was then used to apply the signal voltage to the rear pair of electrodes. This caused the capsule to move with the natural flow of the small intestine.

Fig. 4.24 shows a selection of stills from the X-ray video of the change of direction experiment. Initially, the device is facing away from the observer when front electrodes are activated. Circled in slide 1, the device reverses against the natural peristaltic flow towards the reader and has turned around a small intestinal loop by slide 3. It can be seen to continue to reverse along the small intestine until slide 9 at which point stimulation was switched from the front electrodes to the rear electrodes producing instant direction change. The device can be seen in slides 10 – 12 to move in the opposite direction along the small intestine.

1

2

3

4
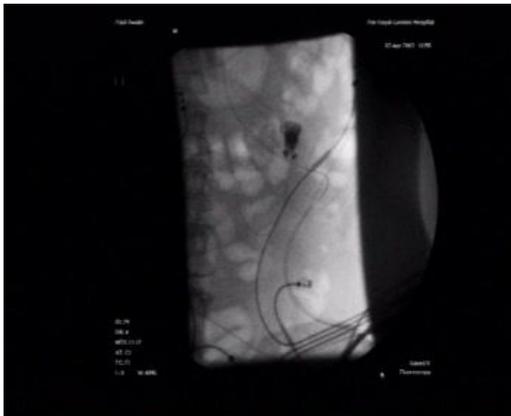
5

6
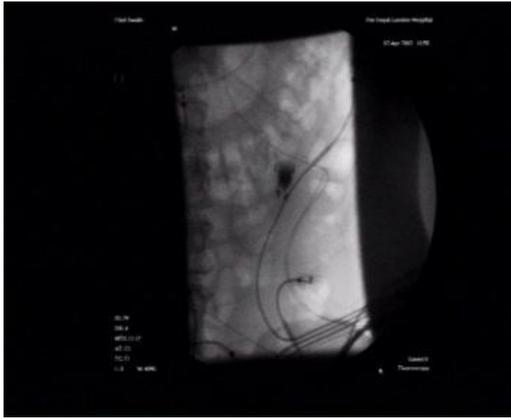
7

8

9

10

11
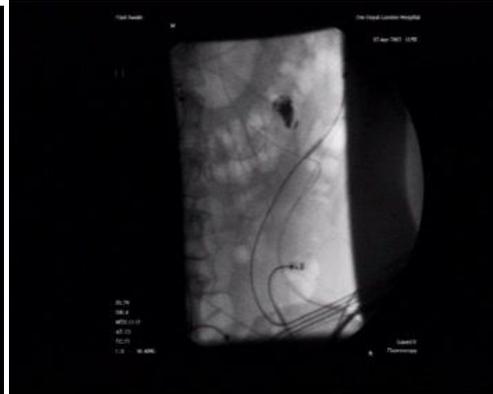
12

Fig. 4.24 Stills from X-ray video of bidirectional human test showing that the propelled device achieved controlled forwards and backwards motion inside the small intestine.

The current supplied by the stimulator during these tests was recorded. A supply voltage of 5 V supplied a current of 2.5 mA, 8 V supplied a current of 3.7 mA, 10 V supplied a current of 4.9 mA, 12 V supplied a voltage of 9.0 mA, and 15 V supplied a current of 12 mA. Good movement was observed at 10 V supplied at a current of 4.9 mA with no apparent improvement in performance when higher voltages and currents were used.

4.6   Conclusions

In an effort to find the most practical material for the construction of the device, Delrin, PTFE and Acrylic were considered. The results show that both the coefficients of static and dynamic friction for all the materials is low enough to produce a frictional force which will be negligable. Therefore, when chosing one of the materials, the major considerations were how they would machine and how they would work with adhesive. Acrylic proved to be the best for both of these so it was the material finally chosen.

In the investigation of how the angle of the sloping face would affect the magnitude of the propulsive force produced by the contraction force, it was derived that for Acrylic, a taper angle of 47° would theoretically result in the maximum propulsion force.

The device design underwent a series of radical changes. Starting off as a tear drop shaped single ended taper design with a diameter of 15 mm and small area electrodes at one end, it progressively evolved into a round-ended

device with a diameter of 11 mm that had a pair of larger area electrodes at both ends.

Early changes to the design and construction of the bidirectional device enabled stimulation to induce movement in both directions along the small intestine. The changes in the design of the electrodes, which now covered the whole tapered section apart from a 2 mm insulating gap between them, produced an improvement in the movement performance of the 11 mm device by preventing the loss of electrical contact with the lumen of the small intestines that had occurred with the smaller area electrodes. This design was also incorporated into the two larger diameter devices. Further experiments showed that devices with a diameter of 11 mm performed comparably to 15 mm and 20 mm diameter capsules of similar design. This was a promising result as it showed that a device with a diameter that could be swallowed safely could work as effectively as devices with diameters large enough to fill the lumen cavity of the small intestine to a greater extent.

After the tapered electrodes had proved to be successful in propelling an 11 mm device, the use of rounded electrodes that could be attached to a video capsule endoscope was investigated.

A final change to the forward electrode design, which only slightly affected the movement performance, allowed the capsule to incorporate a working camera. This final design performed well in *in vivo* animal experiments as a precursor to the *in vivo* human experiments. These experiments showed that an electrostimulation device design, similar to the design of a M2A video capsule endoscope which could be swallowed, worked as effectively as the larger diameter bidirectional devices in the pig model.

Although results of the experiments suggested that the design which gave the optimal performance was a bidirectional device with large area electrodes enclosing the tapered sections with taper angles of 47º, the final design chosen was a device with rounded end sections, based on the design of a M2A video capsule endoscope. Although not producing the best performance, the compromise in performance allowed the device to be swallowed and a M2A video capsule endoscope to be used in future experiments.

The final adaptation of the device which was designed for the human model, was more rigorously constructed and incorporated strong wires enclosed in a protective silicon tube to enable the retrieval of the device from the small intestine through the mouth without causing injury to the volunteer.

The final design of the device was successfully tested *in vivo* in an unanaesthetised human volunteer on two separate occasions. Both trials showed that the device worked successfully with speeds approximately 120 mm/min being observed at 10 V, 4.9 mA, with 20 ms pulse duration at l2.5 Hz.

The brief reduction of heart rate that occurred at the beginning of the first human test was not repeated at any other stage of either human test. It was postulated that this effect had been produced by an inadvertent stimulation of the vagus nerve, the extremity of which can reach as far as the top of the small intestine. Sitdikov et al[199] showed that "simultaneous bilateral stimulation of the vagus nerve in intact and sympathectomised rats of various ages significantly reduced heart rate. Lewis et al[200] found that in pigs when stimulating the left cervical vagus nerve, a square wave negative pulse in a 6 second train at 10 Hz, 0.1 ms and 20 V, was sufficient to reduce the heart rate by 20 ± 4 beats per minute. They had similar findings in humans, when stimulating the left vagus

nerve proximal to the origin of the cardiac vagal bunch, with a negative square wave pulse in a 6 second train at 25 Hz, 0.1 ms, and 20 V, an immediate reduction of the heart rate occurred causing a systole. However, with the introduction of glycopyrrolate, a muscarinic antichologenic, they inhibited the effect that vagal nerve stimulation had on heart rate.

The objective of this section of the project was to implement bidirectional propulsion of devices along the small intestine. This study shows that controlled electrostimulation of the mucosal surface of the small intestinal wall can be used for the propulsion and positioning of video endoscope capsules. The experimental results have produced a set of stimulation parameters for both a pig model and a human model, with which a swallowable device can be propelled by electrostimulation along the small intestine. The device underwent a series of design changes. Some of these included workable compromises in performance in order to forward the design towards the human model. It can be seen that a brief reduction of heart rate occurred at the beginning of the first human test and it was postulated that this effect had been produced by stimulation of the vagus nerve. This suggests that it may be inappropriate to use this stimulation device in the eosophagus or the proximal small intestine. In the device's present form, wires are required to deliver the signal to the electrodes and to provide a means of extraction after the procedure. This device could be used for clinical investigations in its present form. However, to make this a more practical device, the wires must be removed. Therefore, in the next chapter a proposed solution is investigated.

5. The Remote Controlled Device

5.1 Objectives and Strategies

To build a miniature stimulator and a radio control circuit that fit inside a device with similar dimensions to a video capsule endoscope. The dimensional constraints of a swallowable device impress strict limitations on the design specification. The electrostimulator will need to have dimensions small enough to fit inside an 11 mm diameter device.

Although initially a workable circuit could be designed and tested using ordinary electronic components, the final design will need to be made from miniaturized components and powered by miniature batteries that would run the device safely for many hours inside the gastrointestinal tract.

With these constraints it will be necessary to construct a miniature electrostimulator that will require a low current so that it can be powered for hours by a miniature 3 V battery supply. The miniature elctrostimulator will have to produce the optimal stimulation parameters of 12.5 Hz, 20 V and 20 ms used in the pig model as provided by the Grass SD9 stimulator.

5.2 Introduction

During the experiments described in the previous chapter a Grass SD9 medical electrostimulator was used to induce intestinal contractions to produce movement of the bidirectional device. Although the Grass stimulator produced effective results with the wired devices, a practical piece of medical equipment would require such devices to be completely self contained. This implies that

the next practical step is a device containing its own internal miniaturised electrostimulator, power supply and radio receiver.

In order to design and construct a remote controlled device which emulates the Grass SD9's stimulation parameters, a sound knowledge of its function is essential. Therefore, section 5.3 provides a description of the fundamental properties of the Grass SD9.

The following section continues with a description of the development and testing of the initial design of the internal stimulator for a radio-controlled device. It includes a description of the prototype circuit designed for the miniaturised stimulator and details of how this stimulator performed in comparison with the Grass stimulator. Improvements which were introduced to enhance the original design are then discussed, including the necessity for the addition of an internal voltage converter to produce the required output signal voltage from a 3 volt supply.

Section 5.5 describes the design and construction of the circuits of the miniaturised stimulator to be incorporated into the radio-controlled device. Within this is a description of the tests designed to compare the performance of the radio-controlled device against that of the Grass stimulator in an anaesthetised animal.

Section 5.6 introduces the concept of a wireless control system for the radio-controlled device to give the user full directional control along the intestine. This includes a discussion about the design constraints of a wireless system to control the miniaturised stimulator, a description of the design and construction of the circuit and finally testing of the circuit. This section

concludes with a description of the design and construction of a fully controllable bidirectionally propelled device.

Sections 5.7 and 5.8 describe the *in vivo* tests of the wireless radio-controlled device. This includes comparison tests using the Grass SD9 with wired devices. The final section presents a short summary of the work described in the chapter and the conclusions that have been drawn from it.

5.3 The Commercial Stimulator

The Grass SD9 electrostimulator produces a square shaped pulse and can be used for a large variety of applications. It provides a wide range of parameters in terms of voltage, frequency, and pulse duration. It also allows the operator to perform refractory measurements with its twin pulse circuit and delay features. A built-in isolation circuit is included, which allows data recording with the stimulator at the preparation site with minimal intervention. This is made possible because the output voltage, which is polarity selectable, is not referenced to ground

The SD9 stimulator produces a square wave stimulation signal, which can have a three decade output voltage range from 0.1-100 V, a three decade frequency range from 0.2-200 Hz, and a four decade range of duration from 0.02-200 ms. It has a maximum output impedance of 1000 Ω, a peak output current of 50 mA, with a maximum power output of 2.5 W (peak).

The delay function, with a four decade range from 0.02-200 ms, allows the separation of the pre-stimulation and the stimulation pulses through the

synchronous outputs. This means that the SD9 stimulator can produce three different types of output stimulation pulses: single, repetitive or twin.

The SD9 stimulator has both monophasic and biphasic outputs, and has a maximum mains power requirement of 30 W, with an average power requirement of 5 W. It has an accuracy of ± 5% for all the parameters except for the voltage, which has an accuracy of ± 10%.

5.4   Initial Design of Electrostimulator

It can be seen from the above description that the Grass SD9 is a very versatile item of equipment that can be used to create a number of different types of electrostimulation pulses. Therefore, to create a stimulator which performs as well the Grass SD9 did during the experiments described in the previous chapter, one must first examine which functions of the device were used.

Throughout the experiments, the Grass SD9 was used to produce a continuous set of monophasic square wave stimulation pulses. Useful parameter ranges were voltage: 0-50 V, frequency: 10-100 Hz and pulse width: 1-50 ms. Therefore, the replacement stimulator needs to be able to supply a similar range of parameters.

The author initially designed a square wave electrostimulator based on a simple astable oscillator circuit as described in Appendix C.   This circuit consisted of a comparator with a only a few discrete external components. The comparator circuit chosen was the LM331V. However, as size was not initially

a consideration, one quarter of an LM339 Quad comparator was used. This chip consists of four independent precision voltage comparators that each have identical characteristics to the LM331V. The comparator was chosen because it has a wide supply voltage range 2–36 V, and a very low supply current drain of 0.8 mA, which is independent of the voltage. This gave the author great versatility for future design changes to the circuit. A major design concern for a stimulator that is to be used within a capsule would be its power requirements.
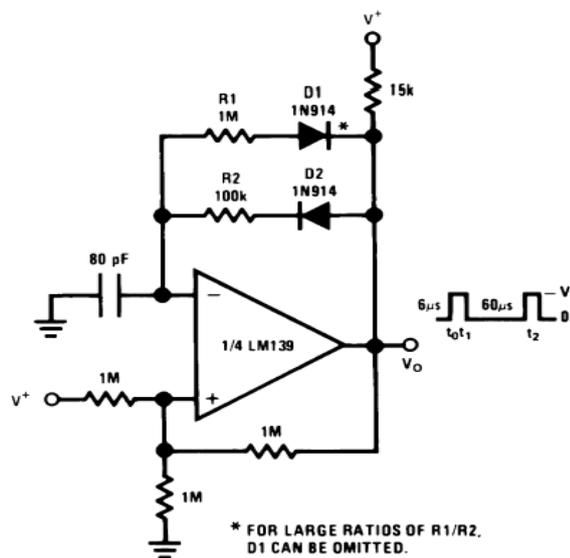
Fig. 5.1. Adjustable astable oscillator circuit.

The dimensional constraints of a swallowable device imposed strict limitations on the design specifications. The electrostimmulator would need to have dimensions small enough to fit inside a capsule with a maximum diameter of 11 mm similar to the PillCam. Although initially a workable circuit could be constructed and tested using ordinary electronic components, the final design would need to be constructed from miniaturized components and powered by

177

miniature batteries that would run the device safely for many hours inside the gastrointestinal tract. With these constraints it was decided to construct an electrostimulator circuit that would require a low current and could be powered for hours by a miniature 3 V battery supply. Therefore, it was decided to limit the power supply of the stimulator circuit to 3 V.

5.4.1 Square Wave Stimulator Construction and Initial Animal Test

The initial construction of the square wave stimulator used veroboard so that the principle of operation could be easily tested in an animal. The board was populated using discrete components with the values discussed at the end of Appendix C, to produce the circuit shown in Fig. 5.1. The stimulator therefore produced a square wave with a voltage the same as the power supply voltage with a frequency of 15 Hz and 10 ms pulse length.

In the preliminary experiment described in Chapter 3, it was shown that the bidirectional device achieved movement at 20 V with frequencies of 15 Hz. Contraction, but no movement, was observed at 10 V and 15 V at a frequency of 15 Hz. The tapered device also achieved movement at 20V with frequencies of 15 Hz and contraction, but no movement, was observed at the 10 V and 15 V.

These two devices were also used in an initial square wave generator comparison test. The devices were fed through an over tube into the oesophagus of a pig with the help of a following endoscope. The electrodes were attached to the square wave generator instead of the Grass stimulator. Initially, a 3 V supply (two AA batteries) was attached to the wave generator. As expected, the devices

showed no contractions in the oesophagus with either device. However, when the 3 V supply was replaced with a 9 V battery contractions were observed.

From this preliminary result it was concluded that this square wave stimulator generator required a supply of at least a 9 V supply to produce a contraction. However, the initial experiments described in Chapter 3, showed that an output voltage of at least 20 V was required to produce movement with these devices. With the stipulation that the supply voltage could be no more than 3 V, a stimulator would need to be designed that could produce an output signal of at least 20 V.

This could be achieved by the incorporation of a DC-DC voltage converter or charge pump circuit. After investigating a number of alternatives, the LT1615 was the only voltage converter that could produce a voltage increase of up to 36 V from a 3 V supply in a package size appropriate to the dimensions of the circuit. Therefore, the LT1615 was chosen because its characteristics encompassed the design specification.

5.4.2 The Addition of the Voltage Converter Circuit: The LT1615

The LT1615 is a micropower DC-DC step up voltage converter that can produce an output voltage of up to a maximum of 36 V from a 1.2 V to 15 V supply voltage. It has an extremely low quiescent current of 20 μA when active and only 0.5 μA in shutdown mode. The operation of the LT1615 can be best understood by referring to a diagram of its internal circuitry. (Fig. 5.2)
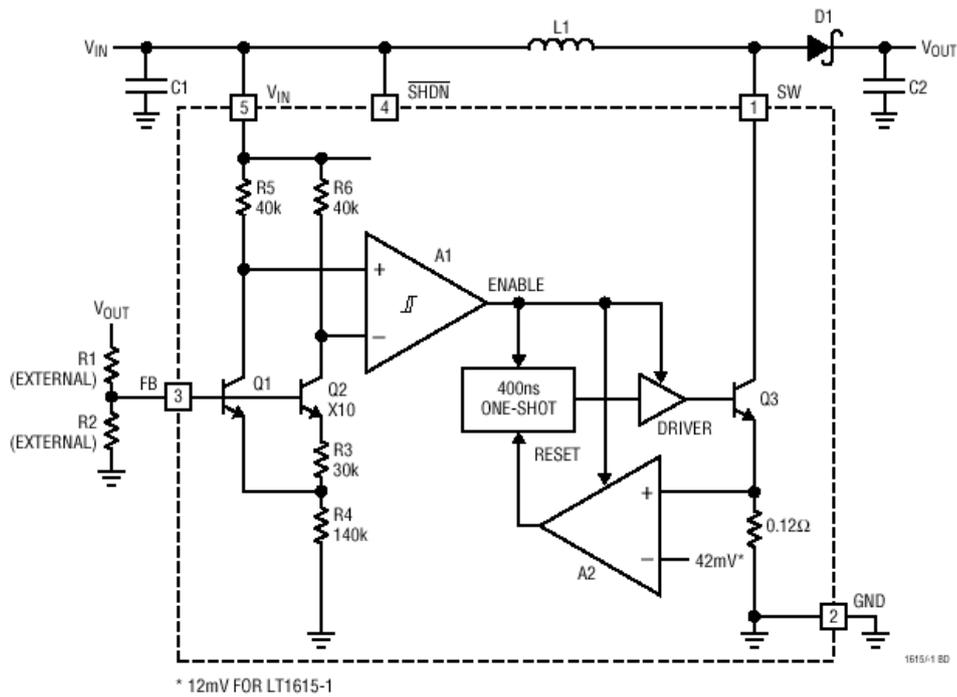
Fig. 5.2. Voltage converter internal circuit of the LT1615

Q1 and Q2 together with resistors R3 and R4 form a band-gap reference, which is used to regulate the output voltage. When the voltage at the FB pin is slightly above 1.23 V, comparator A1 disables most of the internal circuitry. Output current is then provided by capacitor C2, which slowly discharges until the voltage at the FB pin drops below the lower hysteresis point of A1 (typical hysteresis voltage at the FB pin is 8 mV).

At this low voltage state the comparator A1 then enables the internal circuitry once again, turning on the power switch Q3, and the current in inductor L1 begins ramping up. Once the Q3 switch current reaches 350 mA, the comparator A2 resets the one-shot, which then turns off the Q3 switch for 400 ns.

The inductor L1 then delivers current to the output through diode D1. As the inductor current ramps down, switch Q3 then turns on again and the inductor current ramps back up to 350 mA, at which point the comparator A2 resets the one-shot, again allowing L1 to deliver current to the output. This switching action continues until the required output voltage is achieved (until the FB pin reaches 1.23 V), then the comparator A1 turns off the internal circuitry and the complete cycle repeats.

The LT1615 contains additional circuitry to provide protection during start-up and under short-circuit conditions. When the FB pin voltage is less than approximately 600 mV, the switch off time is increased to 1.5 ms and the current limit is reduced to around 250 mA (70% of its normal value). This reduces the average inductor current and helps minimise the power dissipation in the LT1615 power switch and in the external inductor and diode.

It was recognised that with the shutdown facility, which has a maximum activation/deactivation time of 1.5 μs, the DC-DC converter could easily be used to produce a square wave signal of the appropriate parameters and voltage. With this terminal connected to the output of the astable oscillator, it was found possible to produce the required high voltage square wave from an initial 3 V supply.

5.4.3 Initial Animal Test

The stimulator circuit was tested to see how it performed against the Grass SD9 stimulator. After a set of bench tests, in which they performed

comparably, they were used to control a capsule in the intestine of a pig at laparotomy. Using a bidirectional device, each stimulator was used in turn. As Fig. 5.3 and Fig. 5.4 show, both the stimulators caused the device to move along the intestine. The Grass SD9 caused the device to move at a slightly greater speed than the prototype stimulator, 100 mm/min (SD 2.4) (N = 3) and 96 mm/min (SD 1.8) (N = 3) respectively. This difference was acceptable, so a miniature stimulator was designed and constructed.
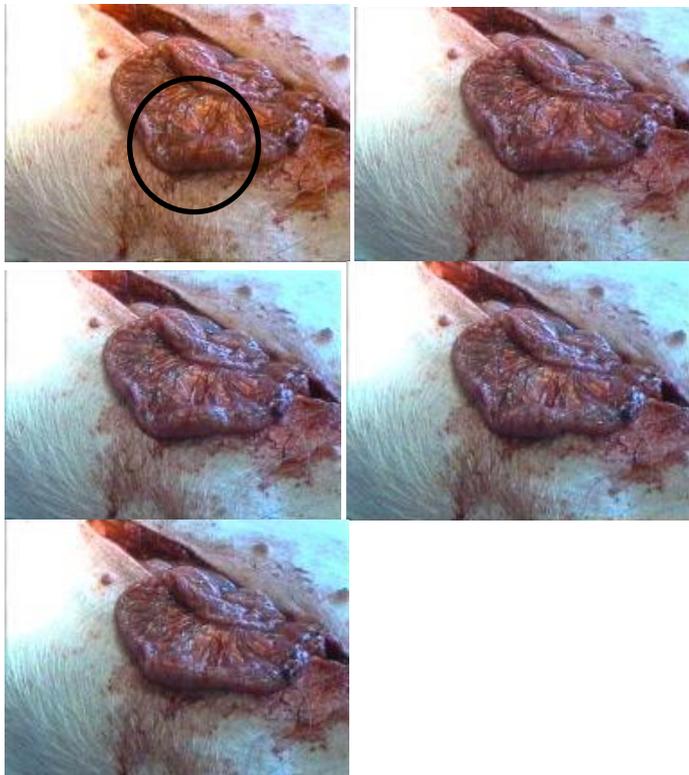
Fig. 5.3. Grass Stimulator propelled device.
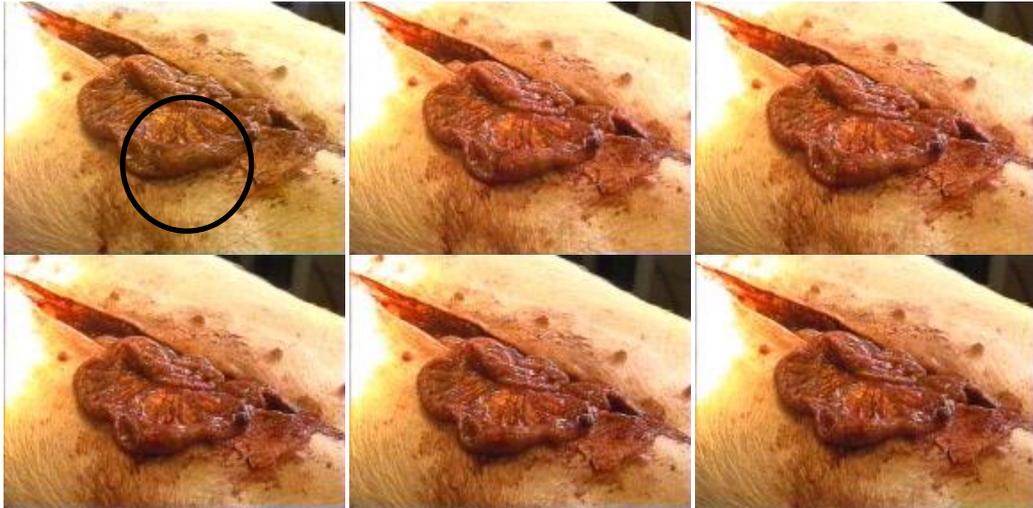
Fig. 5.4. Internal stimulator propelled device.

5.5 Unidirectional Device

The results presented in the previous section showed that the square wave stimulator produced propulsion of the devices which was comparable to the grass stimulator. Therefore, a miniature circuit was designed to fit inside an 11 mm device.

5.5.1 Miniature Signal Generator

The high voltage output generator was constructed by combining the simple astable oscillator circuit with the charge pump circuit. The LT1615 DC-DC converter was only available in a surface mount 5-lead SOT-23

package. With this in mind, and to minimise the overall size, the entire circuit was built from surface mount components only.

The author designed circuit boards using Easy PC, a printed circuit board (PCB) design package produced by Number One Systems (Gloustershire, UK). A template of the PCB design was printed on transparent acetate with a normal PC printer. The template was fixed to the photosensitive side of a single sided PCB which was then exposed to UV radiation. The board was then developed, etched and rinsed. The small size of the boards and thickness of the tracks made the etching process quite difficult. Once the boards were successfully constructed, they were populated and tested.

After producing a square wave signal similar to that produced by the Grass stimulator, the PCB was redesigned to reduce its size still further. The first change was the use of double sided PCB. The production method was the same as for single sided PCB except the board had a circuit to be etched on both sides. With the scale of the boards being produced, the template placement was as important as the etching process. In the final design the dimensions of the template for both sides of the PCB were 6.5 mm by 6.8 mm. (Fig. 5.5)
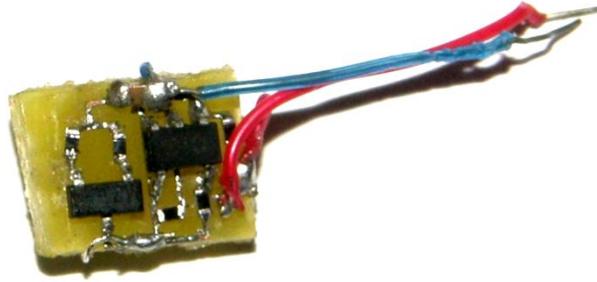
Fig. 5.5. Photographs of the miniature stimulation circuits.

5.5.1.1 Miniaturised Astable Oscillator Circuit

A miniaturised version of the square wave generator described in Appendix C was constructed, with R_1 and R_2 as fixed resistors instead of potentiometers, due to the lack of space. The stimulator was required to produce a frequency of 12.5 Hz, with pulse duration of 20 ms in line with the findings of the one-minute tests described in Chapter 4.

These resistor values were calculated in a similar manner to those chosen for the original square wave generator, with an upper limit once again placed on

the value for R_2 of 1 MΩ. Using this to obtain the values for t_2 of 60 ms, required a value of 43 nF for the capacitor C_1. With the closest value for a commercially available capacitor being 47 nF, the calculated value for t_2 was acceptable at approximately 65.2 ms.

The value for R_1 was then calculated using the same method as used for the original square wave generator. Using the value for C_1, the calculated value for R_1 was approximately 307 kΩ. With the closest preferred value for a resistor being 330 kΩ, the calculated value for t_1 was acceptable at approximately 21.5 ms.

The astable oscillator produced an output signal with a frequency of approximately 11.5 Hz and pulse duration of approximately 21.5 ms. With both parameter values within 8% of the desired figures, the circuit was then constructed with components having the above values.

5.5.1.2 Miniaturised DC-DC Voltage Converter Circuit

The DC-DC converter section of the square wave generator was constructed using an LT1615. The values of the external components of the circuit were selected to produce the maximum circuit output voltage. The capacitors within the circuit have the effect of reducing the output ripple voltage. The values chosen for capacitors C_2 and C_3 were 4.7 μF and 1 μF respectively, which were found adequate to minimise the output ripple voltage. The inductor within the circuit controls the current limit but has the added effect

of increasing the output ripple voltage. A 22 μH inductor was chosen as this value produced only a small increase in the output ripple voltage. The resistors in the circuit control the peak output voltage, which was calculated using the equation:

$$V_{out} = 1.23\left(\frac{R_1}{R_2} + 1\right) \qquad [5.1]$$

With this in mind, the values chosen for the resistors R_1 and R_2 were 2 MΩ and 70 kΩ respectively. This produced an acceptable output voltage with a value of approximately 35 V.

The two separate circuits were connected so that they had a common ground and both used the same supply voltage. The output terminal of the signal generator was connected to the shut down pin of the DC-DC voltage converter circuit. The output from the composite device was first taken from the ground and from the positive output of the DC-DC voltage converter section. This was found to produce a square wave signal between 3 V and 35 V. To avoid the 3 V DC voltage the output was therefore taken from the supply rail and the positive output of the DC-DC voltage converter, which produced a 0-32 V square wave signal.

5.5.2 Wireless Device Construction

Once the author had determined the components, both sides of the PCB were populated and the complete stimulator circuit was then installed inside a 11 mm unidirectional device with the circuit output connected to the large area electrodes of the device. The design of the device (Fig. 5.6) was similar to that of the large electrode bidirectional devices described in Chapter 4. Unlike the bidirectional devices the device had only one pair of electrodes at the rear and a rounded front end. Constructed in much the same way the device consisted of two halves, one with a tapered end and the other rounded which when brought together produced a hollow device. The circuit boards and the batteries were housed within the hollow cavity of the device. The circuit boards were placed in the cavity of the rear of the device allowing the wires for the electrodes to protrude through the holes on the tapered section. The electrodes were then soldered to the wires and bonded to the tapered section of the device with epoxy resin. Power for the stimulator was provided by two internal 1.5 V button cell batteries, which were connected to the circuit by wires attached to two small metal contacts and housed in the front half of the device.

B:	1 mm
C:	1 mm
D: Inner diameter	9 mm
E: Taper depth	1 mm
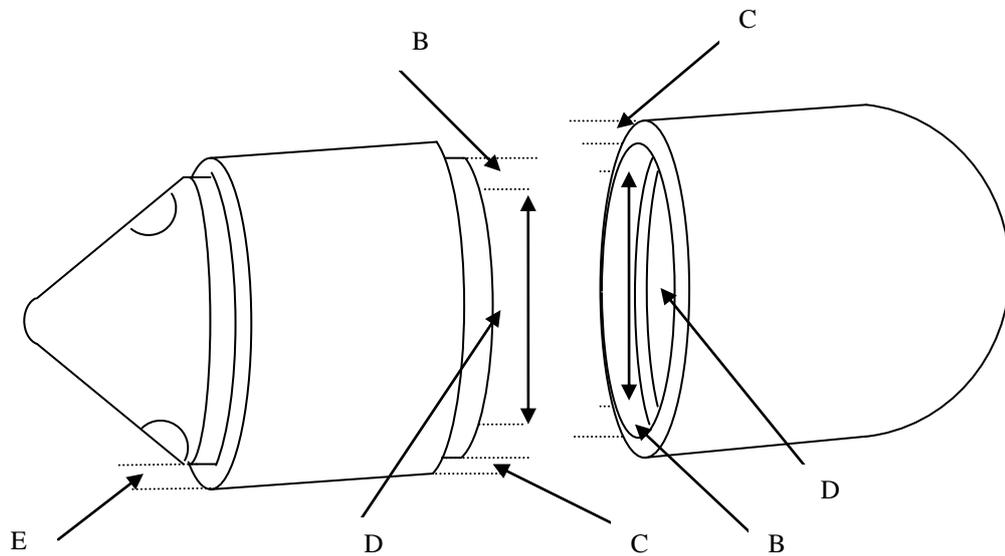
Fig. 5.6. Schematic diagram of the wireless unidirectional device.

5.5.2.1 Wireless Device Testing

The batteries were connected to activate the stimulator and placed inside the wireless device and it was then closed. The first test was in the small intestine of a pig during laparotomy. The wireless device was compared with a wired version connected to the Grass SD9 stimulator. The Grass stimulator was set to produce the same stimulation parameters as the miniature stimulator. The performance of the two devices was compared. The device attached to the

Grass stimulator at 12.5 Hz, 20 ms at a 20 V was tested first and showed a movement speed of 118 mm/min (SD = 18, N = 6). The wireless device was then tested. The device produced a strong contraction with movement of 62 mm/min (SD = 1.6, N = 6).

Thereafter, the device was thoroughly bench tested and compared with the Grass stimulator. The voltage, frequency, and pulse duration of both devices were the same. However, when a larger load was applied corresponding to that of the maximum output impedance of the Grass stimulator, the resulting output of the Grass simulator was double that of the miniature stimulator, suggesting that the latter could only deliver a quarter of the power of the Grass stimulator.

5.5.3 Adjustments to the Miniature Circuit

The miniature circuit did not perform as well as was hoped during the animal experiment. When tested on the bench afterwards it became apparent that the miniature stimulator only produced a quarter of the power of the Grass stimulator under the same load conditions. The power required to propel the device in the intestines of an anaesthetised pig could be quite simply achieved with the introduction of a second voltage converter circuit running in parallel to double the current output of the signal generator.

However, the results show that the device could travel the six metre length of the small intestine in about 100 minutes. This is faster than the average transit time of natural peristalsis, which takes 232 minutes within a range of

72-392 minutes.[1] The results from Chapter 4 suggest that the power required to propel the device in the intestines of a human without anaesthetic using the Grass stimulator is only about a quarter of that required for an anaesthetised pig. These results show that the voltage required to propel the device in the unanaesthetised human volunteer was only 10 V with a current of 4.9 mA compared with that of 20 V with a current of 10 mA required for an anaesthetised pig. As halothane has been shown to reduce intestinal motility, it is possible that the miniature device could have given a better performance in an unanaesthetised pig, but as it was almost impossible to monitor the movement of the device in a pig that was not anaesthetised, this conclusion could not be verified.

5.6   Wireless Device Control Unit

The final stage in the construction of the fully controllable radio-controlled device is to design and construct a wireless unit to control the miniature stimulation device. The circuit not only had to be able to operate within the intestines, but also had to be small enough to fit along with batteries and the stimulation circuitry inside the casing of the video endoscope. A prototype control circuit (Fig. 5.7) was based on a Pericom Technology International (Shanghai, China) 27.145 MHz PT8A967B receiver. This option was chosen because of the chip size and the small number of external

components required to complete the circuit, allowing for ease of miniaturization. This device provides two channels, which were used to control the two pairs of stimulation electrodes.

The PT8A976B is a CMOS receiver chip designed for use in a remote controlled toy. The signal received from the transmitter is amplified by a three-stage amplifier, after which the appropriate signal is sampled, checked for faults, and then decoded to control the actions of the device. There is an oscillator circuit within the PT8A976B which requires the addition of an external resistor. Adjusting the value of the external resistor adjusts the oscillator frequency. The PT8A976B requires a power supply voltage within the range of 2.0-5.5 V.

The radio-control circuit boards were designed using the same software package (Easy PC) that was used for the stimulator circuit. The 8 mm by 13 mm double sided boards were produced in the same way as the original single sided stimulator circuit boards.
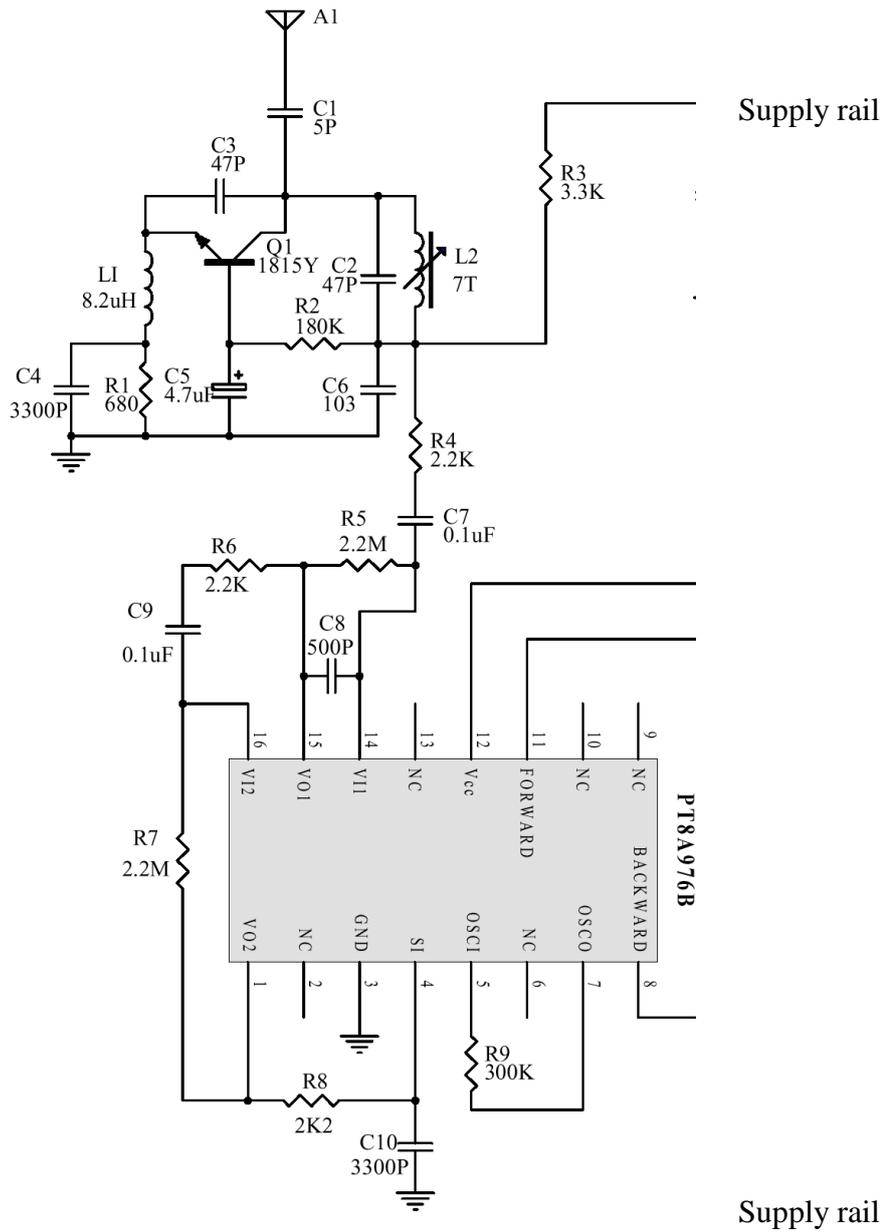
Fig. 5.7. Receiver circuit for the remote device control.
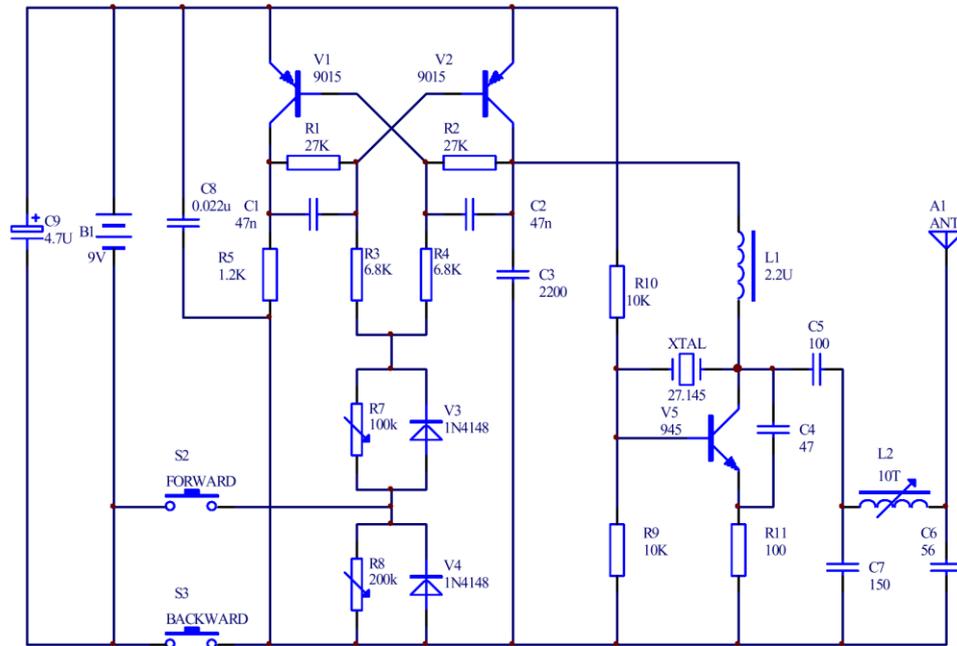
Fig. 5.8. Transmitter circuit for the device control unit.

The transmitter circuit shown in Fig 5.8 uses frequency modulation and transmits at 27.145 MHz. It is coded using pulse width modulation. The transmitter and receiver circuits are matched by adjusting L_2, a 10 turn variable inductor in the transmitter.

To determine whether or not the device would work within the intestines, an experiment with the prototype circuit was devised on veroboard. The test involved placing the receiver circuit which activated LED's within a water proof, transparent container, which was placed in a vessel of saline solution to simulate blood and body tissue. There was at least 300 mm of saline between the receiver and the transmitter. This was used to simulate the effectiveness of the receiver circuit when contained within the body.

194
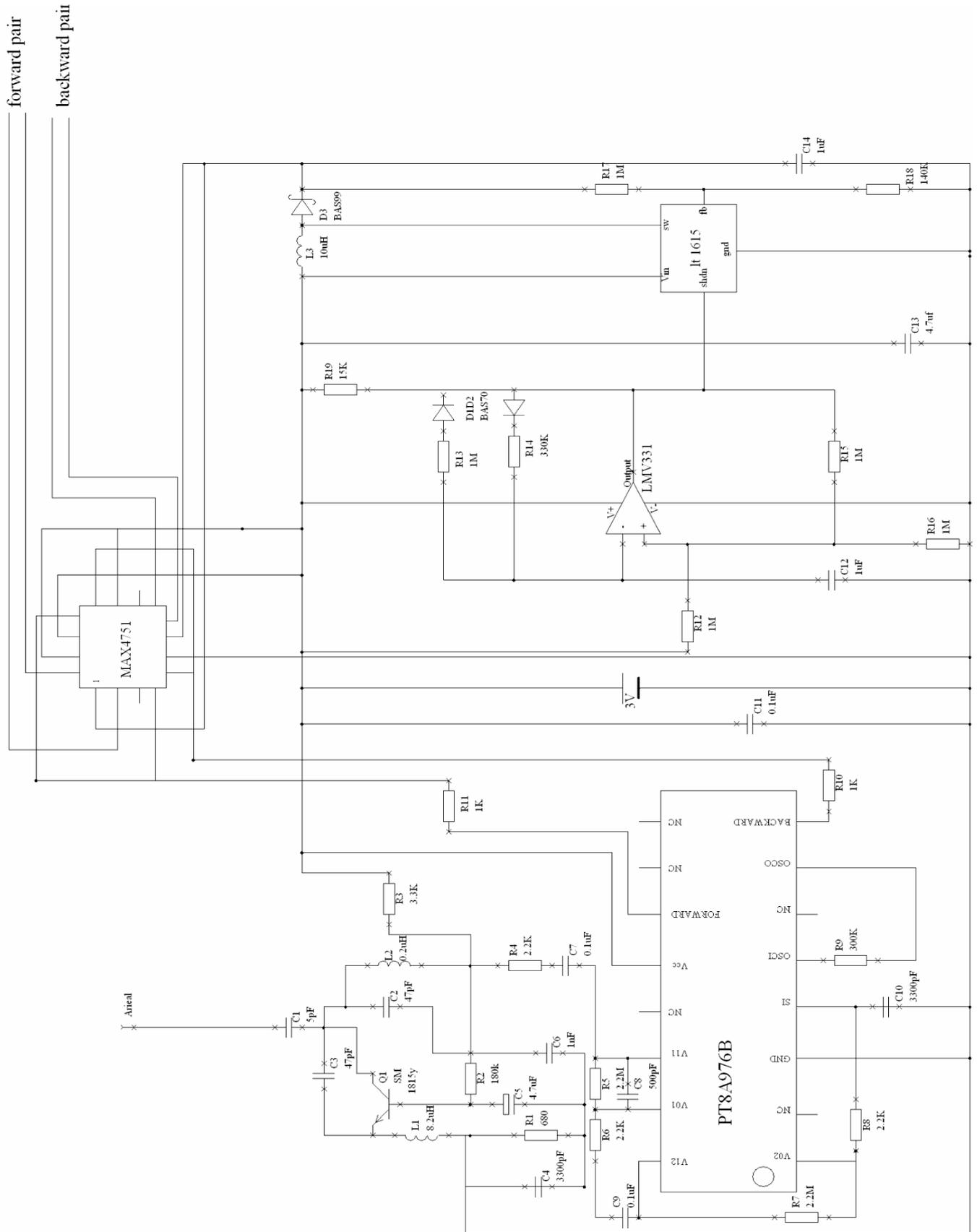
Fig. 5.9. Complete radio control stimulator circuit

195

Once the circuit was shown to remotely activate a small LED whilst submerged within the saline, the author designed and constructed a prototype of a miniaturised version of the circuit which was then evaluated. The PCB was designed and constructed using the same method as described in section 5.4.1. The board was populated (Fig. 5.10) and tested using saline solution in the method described in the previous section. Once it had been established that the circuit worked successfully, the author realised that realistically due to the complicated nature of the design, the combining of the control circuit and the stimulation circuit (Fig. 5.9) at these dimensions, and its ultimate role in human medicine, that the device would require professional manufacture.
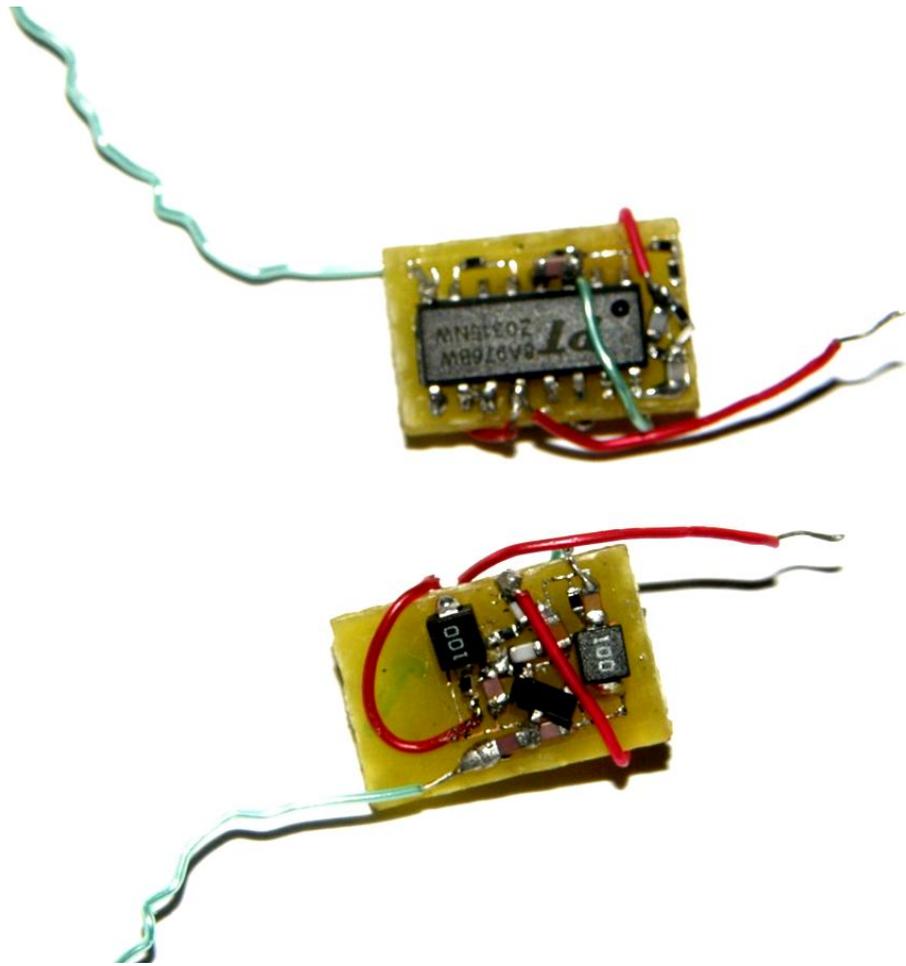
Fig. 5.10 Photographs of the miniature radio receiver circuits

The author produced a design of the circuit which would be incorporated into the professionally manufactured device. This circuit design includes the addition of a switching component which would allow a user to remotely activate stimulation at the front or rear electrodes. This circuit design was incorporated into a design brief which included the authors PCB designs templates and component lists for each board.

The design brief was initially sent to DCA Design International, (Warwick), who after learning that the devices were to be used for human trials

required a full liability waiver to protect them should a patient be harmed as the result of device failure. A risk assessment document was prepared for this company but an agreement with UCL on liability was not forthcoming. Therefore, the construction was passed to another company Paragon Medsystems Inc (San Diego, USA), who agreed to construct devices for both animal and human trials. Their initial attempt to construct the PCB did not succeed due to the small dimensions of the tracks, so they had to remake the boards. Taking advantage of this, a request for coloured LEDs to be added to the circuit was made. Each colour was used to indicate which set of electrodes were being supplied by the signal generator; that is, one colour flashed at the rate of the stimulation to indicate that the stimulation signal was being applied to the front pair of electrodes and the other to supply to the back set of electrodes. A third LED flashed when the device was activated. A request for the addition of a switch to activate the device before use was also made. As these components were not an integral part of the stimulation circuit, the addition was left to Paragon. They chose a light sensitive switch which allows the circuit to be activated or deactivated with a photographic flash gun. The LED's were located at one end of the device so that the flashes could be seen with a following endoscope, thus allowing the operational state of the device to be easily determined.

The wireless device produced by Paragon could only provide a stimulator with parameters of 15 Hz at 10 ms at 30 V. Although these were not the optimal parameters as described in Chapter 4, it was anticipated that the increase in voltage would compensate for the change in frequency and duration and therefore the parameters would be sufficient to produce device movement.

5.7   *In Vivo* Animal Tests of the Remote Control Device

Because of the closure of the animal house at the Royal London Hospital a set of experiments was undertaken at the Royal Veterinary College animal house in Camden. The remote control device was initially tested in the oesophagus of an anesthetised pig. A different anaesthetic regime was used. Pigs were anaesthetised with a prep of 3 ml of atropine and 16 ml of ketomine, with 1 ml of ketomine delivered intravenously. They were then rendered unconscious with 4% halothane, and anaesthetised with 2% halothane.

As the device was wireless a piece of cotton thread was attached to it so that it could be drawn back out of the pig at the end of the test. The device was placed into the oesophagus through an overtube with a following endoscope in an orientation such that the activation LED's could be seen. Once in place, the overtube was removed and the endoscope was withdrawn slightly so the device could be observed without interference.

Using the remote control the electrodes farthest from the endoscope were activated and an LED began to flash to indicate activation. The device was observed to move at a rate of approximately 30 mm/min towards the endoscope. The device was deactivated and the endoscope was used to reposition it. The other pair of the electrodes was then activated and contractions were observed between the device and the endoscope. When the device was deactivated the contractions subsided and the device was observed to have moved away from the endoscope at the same rate.

Although in this qualitative test the device worked, it did not perform as well as expected. Therefore a dummy wired version was connected to the grass stimulator to determine how it would perform using the same stimulation parameters. It performed comparably to the remote control device, moving slowly during stimulation. The optimal stimulation parameters identified in Chapter 3 (12.5 Hz, 20 ms at 20 V) were then tested to see if performance was comparable (i.e. approximately 30 mm/min). The device once again moved more slowly than expected. The voltage was increased and it was found that 30 V was required to produce movement of about 60 mm/min, about half that observed in earlier tests described in Chapter 4.

The radio-control device was also tested in the small intestine of an anesthetized pig during laparotomy. In a manner similar to the tests described in Chapter 4, the speed of the wireless device was measured by activating it for one minute and measuring the distance travelled. Once in place the device was activated and movement at a speed of 19 mm/min (SD) was observed. Like the oesophagus test, the device did not perform as expected due to the anaesthetic. Again a comparison was made with the dummy wired device with the grass SD9 stimulator. Using stimulation parameters of 12.5 Hz, 20 ms at 20 V the wired device moved with a speed of 23 mm/min (SD). The voltage was increased to 30 V and the wired device was observed to move at 45 mm/min (SD).

5.8   *In Vivo* Human Test of the Remote Control Device

After the author had completed practical studies for this thesis, the remote controlled device was tested on a human volunteer. Swain et al. report the use of the radio-controlled device attached by a cord to a video capsule endoscope. It was reported that the device worked well in both animal and human trials. The device was used to pull or push a PillCam at will which imaged in real-time the direction and effect of the electrostimulation signal. The capsule-tug combination proved easy to swallow by a human volunteer. The device was observed functioning in the oesophagus, stomach and duodenum using both conventional endoscopes and the attached wireless capsule endoscope. [220]

5.9   Conclusion

An initial design of a stimulator circuit was developed to produce a square wave electrostimulation signal from a 3 V supply. This produced an output voltage of up to 32 V, and required sufficiently few external components for the circuit to be small enough to be accommodated in a device that could be swallowed.

Although the performance of the stimulator circuit did not match that of the Grass stimulator, it still provided propulsion for the device which would allow it to travel the length of the small intestine in 100 minutes. The results

from the human trials reported in Chapter 4 showed that a high output voltage of 32 V is not required for the final design of the device as only 10 V was required.

The radio-controlled device did not perform as well as the Grass stimulator or its non-controllable wireless counterpart in the small intestines. This could be as a result of two things. First, the power that is required for the radio-control circuit could be limiting the power available for the stimulator circuit. Although this was tested for, it could become more apparent as the batteries are used for a long time. Secondly, and perhaps more importantly, the anaesthetic halothane which was used during these tests is known to reduce intestinal motility.[216] The initial wireless device was tested at a different animal house where the anaesthetic procedures were different. This could explain why the Grass stimulator did not perform as well under halothane as it did in the tests described in Chapter 4, as nitrous oxide and not halothane was used in the first set of experiments. This is also supported by the report of Swain et al[220] who reported the device performed well in an unanaesthetised human volunteer.

Although the radio-controlled device did not perform as well as hoped, it is a device that could be swallowed and move with or against the natural flow of the small intestine. The possible effects of the anaesthetic could explain the lack of speed. However, the device, performing as it did would be able to travel the whole length of the small intestine in either direction within 100 minutes.

The device was successfully tested within a human volunteer and performed well in the oesophagus, and intestines. Although not as rapid as had been hoped, the remote device has been shown to effectively move with or

against the natural peristaltic flow. This would therefore give an attending clinician real time remote control of a video capsule endoscope within the small intestine. This makes it the first non-invasive method of controlled video observation of the small intestine.

6. Other Possible Applications of Electrostimulation

6.1 Introduction

Although the major focus of this thesis was to investigate the use of electrostimulation to propel devices such as video capsule endoscopes along the small intestines, this chapter will discuss other possible applications of electrostimulation. It will describe initial investigations into other applications where electrostimulation is applied to the mucosal wall of the gastrointestinal tract.

As discussed in earlier chapters, electrostimulation can be used effectively to propel small devices along the small intestine by inducing contractions. Although effective here, the question arises; how well would these small devices perform in the large intestine? Therefore, the first section of this chapter investigates the different problems which are encountered when trying to propel small devices along the large intestine. Included are descriptions of initial tests of the propulsion of devices within the large intestine, and the design modifications and electrostimulation parameters required to produce movement. Following this is a discussion of how devices to be used in the large intestine could be developed further into a useful clinical system.

Propulsion of capsules is not the only use for the contractions induced by the electrostimulation of the mucosal surface. The second section of this chapter investigates the use of contractions to introduce tissue into a chamber of a device from which a biopsy sample could be taken. Included are descriptions of the initial design and construction of a device with a chamber into which

contracting tissue could enter, testing of the device to determine stimulation parameters required to introduce tissue into the chamber, and a discussion of the possible method for taking a biopsy from the tissue within the chamber. Following this will be a discussion of how such a device can be developed further.

6.2   Large Intestine Device

As the small intestine becomes the large intestine at the ileo-caecal junction, the diameter of the lumen increases from 25 mm to 30 mm. From here the diameter decreases slightly until it reaches the colon where it increases again to a maximum diameter of 65 mm. The greater diameter of the large intestines poses a few potential problems if a small diameter device is used. Contact of both electrodes is required to induce a contraction, but because of the differences in diameter contact may be lost. Due to the differences in their diameters, when contraction does occur, there may not be enough force applied to the correct part of the device to cause it to move in the required direction. Therefore, dimensional modifications to the design of a small intestine device are required to produce an effective large intestine device.

To evaluate a device in the large intestine, a set of simple tests was devised early on in the project. Following measurements using the small intestines of a pig, a small loop of the large intestine was exposed to allow testing of the bidirectional devices in the large intestines. The large intestine of a pig is not one of the nicest environments to work in. Pigs cannot be prepared before this type of experiment as they will not be starved. If a pig goes without

food for too long it starts to eat anything vaguely edible including flooring. Therefore these experiments were undertaken in unevacuated bowel.

Three bidirectional devices with diameters of 11 mm, 15 mm and 20 mm described in Chapter 4 were used. Following clearance of the required part of the large intestine, each of the devices was introduced. Using a frequency of 12.5 Hz, 20 ms shown in Chapter 4 to produce good movement, at a range of voltages, the performance of the devices was observed.

Starting at 10 V the 11 mm device produced a slight contraction of the large intestine. Increasing the voltage to 15 V caused stronger contractions but no movement. 20 V produced strong contraction but due to the large difference in the diameters of the device and the large intestine, the 11 mm device appeared to become completely enclosed by the lumen preventing it from moving.

Similarly the 15 mm device produced a slight contraction at 10 V and stronger contractions at 15 V. At 20 V slow movement was observed but the large intestine was still contracting along the body of the device as well as the tapered section as was desired.

As the 20 mm device filled more of the lumen of the large intestine, less of it was enclosed by the contractions. This meant that it performed better than its smaller counterparts. Strong contraction was observed at 10 V and slow movement was observed at 15 V and more convincing movement was observed at 20 V.

In the previous experiments conducted in the small intestine, reported in Chapter 4, there was a better match between the diameters of the devices and the lumen. Whereas in the small intestine, the contractions only occurred around the

tapered section of the device, in the large intestine, the contractions occurred over more of the device's surface area preventing it from moving. Therefore it is hard to draw a comparison between the sets of results. However, at 20 V the 20 mm devices moved convincingly in both the small and large intestines.

The results of these large intestine tests suggest that if a device is to be effectively propelled along the large intestine it requires a diameter of at least 20 mm. This diameter is nearly double the maximum 11 mm diameter allowed for a device which has to be swallowed. Therefore, the construction of a device with a fixed diameter, which could be swallowed and propelled along the whole of the gastrointestinal tract using electrostimulation, is not a feasible proposition.

However, one can imagine a device with a diameter that could be altered remotely. Such a device would therefore be able to be swallowed and controlled within the large intestines. Due to the restricted internal volume of the device, the concept of a mechanically controllable variable diameter would appear to be impractical. During discussion with Given Imaging Ltd (Israel), it became apparent that there is interest in a device that could be administered anally to examine the large intestine only. This therefore removed the requirement for the large intestine device to be able to pass through the pylorus.

The earlier large intestine tests showed the device, which was designed to operate solely in the large intestine, required a larger diameter than the small intestine device due to the bigger lumen of the large intestine. As with the smaller device this large device was able to travel with or against the direction of natural flow of the large intestine. Therefore, a possible use for this device could be in emergency colonoscopies, where it could be used to travel up and

down the large intestine allowing the attending physician to examine more closely areas of concern. If the rate of propulsion of the larger device is comparable to that of the smaller device, it would be able to travel 3 m return journey of the entire length of the large intestine in about 25 minutes. This time is comparable with conventional colonoscopy, a procedure that can take between 30 and 60 minutes to complete. However, this device would not pose any risk of perforation and would be deemed more comfortable by the patient.

6.2.1 Design and Construction of Large Intestine Device

The minimum diameter of the large intestine is where it meets the small intestine, which can be as small as 25 mm. Therefore, the large intestine device (Fig. 6.1) should have a diameter of no more than 25 mm. As with the small intestine devices, the large intestine device had a taper angle of 47°. Therefore the large intestine device needed to be longer to incorporate the larger taper sections and the cylindrical portions of the device.

Fig. 6.1. 25 mm large intestine devices

The device would therefore have two tapered sections, one at each end, which would each be 12.5 mm in length. The central section of the device would be a 50 mm long cylinder with a diameter of 25 mm. Each of the tapered section requires a pair of electrodes. Fig. 6.2 shows a schematic of the design of the large intestine device. The diagram shows the electrodes which were placed on the tapered section of the capsule. It also shows the 2.5 m wires which were used to connect the electrodes to the electrostimulator that passed through the rear section of the capsule. The initial design of the large intestine device was then constructed from Perspex, with the four large area electrodes constructed from stainless steel.
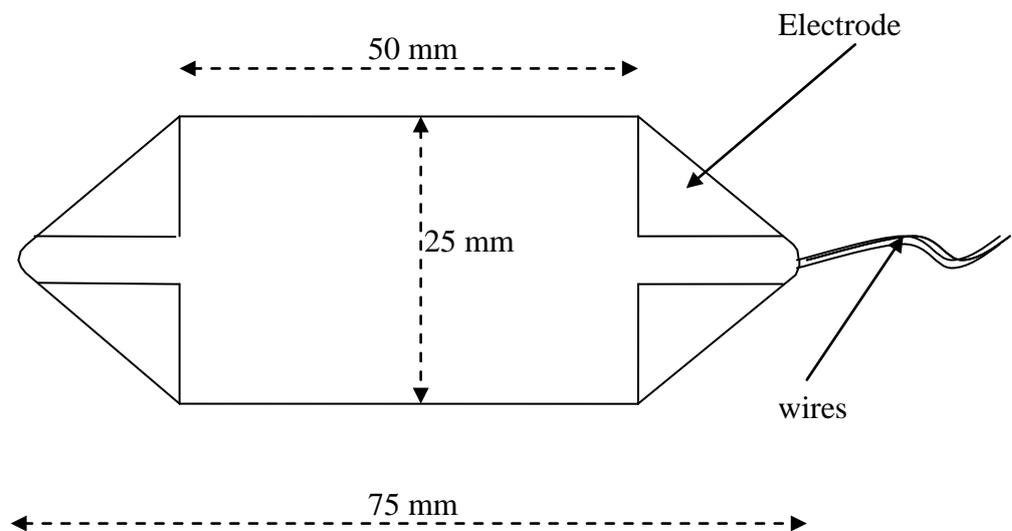
Fig. 6.2. Schematic drawing of the large intestine device.

To determine the usefulness of the large intestine device, 25 mm and 20 mm devices were tested in the large intestines of an anesthetised pig. This

test, similar to the one minute tests described in Chapter 3, measured the speed that the device moved. Using the Grass SD9 stimulator, the devices were activated for one minute and the distances they travelled along the large intestine were recorded.

A loop of large intestine was exposed at laparotomy and a small incision was made in it through which the content was removed. Each device was placed in turn into the large intestine. Visually, the 20 mm device appeared to perform as it had in the previous test. It moved at a speed of 61 mm/min (SD 1.7) (N = 3). The larger 25 mm device performed better, and moved at a speed of 97 mm/min (SD 1.7) (N = 3).

6.2.2 Conclusion

Conventional colonoscopy requires a great amount of skill and can be quite a dangerous procedure. It is highly challenging for a clinician to do this while trying to observe the lumen of the intestine at the same time. Colonoscopy is also a daunting prospect for some patients.

In contrast however, the large intestine device described in this chapter could use induced contractions of the intestinal walls to propel a camera along the large intestine in real time. This would allow the attending physician to concentrate solely on diagnosis, not having to worry about the risk of perforating the intestine. The device would provide a method of introducing a video capsule endoscope directly into the large intestine which is a less daunting

prospect than colonoscopy for the patient. At the speeds achieved experimentally using a 25 mm device, a video capsule endoscope could complete the 3 m return journey of the large intestine within 35 minutes. This is comparable to the time for a normal colonoscopy (30-60 minutes), and removes the high level of skill, risk and discomfort associated with that procedure.

Colorectal cancer is the second leading cause of death in North America. However, colonoscopy is usually reserved for patients with positive results from screening tests or a higher than average risk of colorectal cancer, in favour of an occult blood test or sigmoidoscopy. This proposed device could offer a risk free alternative, as a viable screening procedure for colorectal cancer. It would give the attending physician direct visualisation of the large intestine during the initial screening process, reducing the overall diagnostic time, and speed up the initiation of the therapeutic process.

6.3 Biopsy Capsule

Until now this thesis has primarily focussed on the propulsion of devices along different portions of the gastrointestinal tract by means of electrostimulation induced contraction. This section investigates the question: can electrostimulation cause the intestinal wall to contract sufficiently to produce movement of a small device, and can it also be used to contract the intestinal tract in such a way as to introduce a small amount of gut wall through an aperture on a device? One proposed use for these induced contractions is a

biopsy capsule, which uses electrostimulation to introduce sample tissue into a chamber from which a biopsy can be taken.

One of the most important aspects of a biopsy device for use in the gastrointestinal tract is that it only takes a sample from the intended region. Therefore, a biopsy capsule casing was designed which could incorporate a biopsy tool within a chamber. This would eliminate interaction between the biopsy tool and the lumen of the intestinal tract during transit. The design had to also allow the tissue from an area of interest to be introduced through an aperture into the biopsy chamber.

Devices such as the Crosby capsule use suction produced by an external source to introduce tissue into their biopsy capsule.[217] This is not possible in a wireless device, so another method would have to be found. As electrostimulation of the lumen of the intestinal tract has already been shown to produce a contraction, the casing of a biopsy capsule was designed with two electrodes placed around an aperture as shown in Fig. 6.4.

However, the wall of the intestinal tract is very thin. This means that only a small thickness of tissue can pass into the chamber before there is a risk of perforation during biopsy. Therefore, a major consideration of this section is to determine a set of stimulation parameters that introduce a safe thickness of lumen into the chamber. Once the tissue is inside the chamber, there are a number of different methods by which a biopsy could be taken. A discussion of these and other uses of such a device will be included in this section.

6.3.1 Initial Design of the Aperture

Based on the small intestine device, an aperture was cut out of the side wall of a device. Electrodes were placed about the biopsy aperture, each of which had a wire attached for connection to an electrostimulator during testing. Fig. 6.3 shows a schematic drawing of the design of the biopsy capsule.
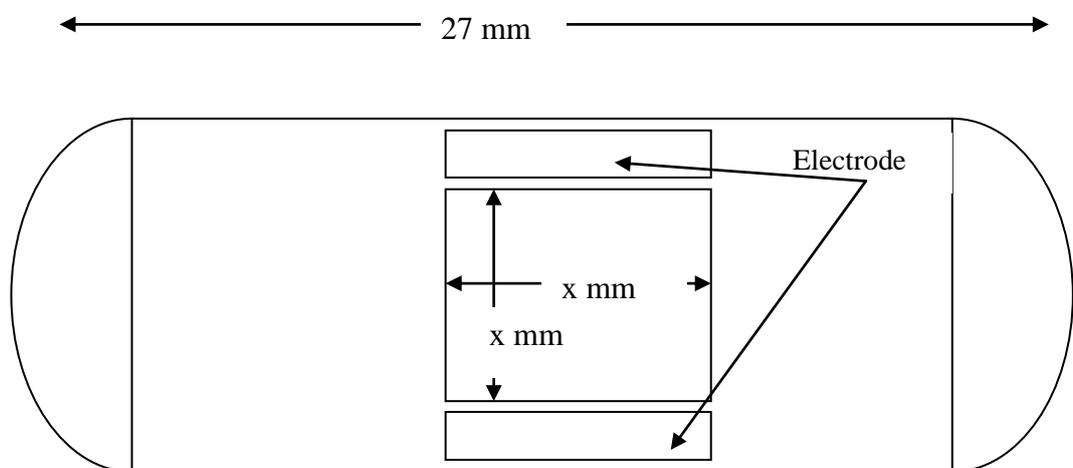
Fig. 6.3. Schematic diagram of the biopsy device.

An experiment was devised to determine whether or not tissue will be introduced into the aperture when stimulated. Two capsules with different sized apertures were used to investigated the effect of the dimensions of the aperture on the effectiveness of the stimulation to introduce the tissue.
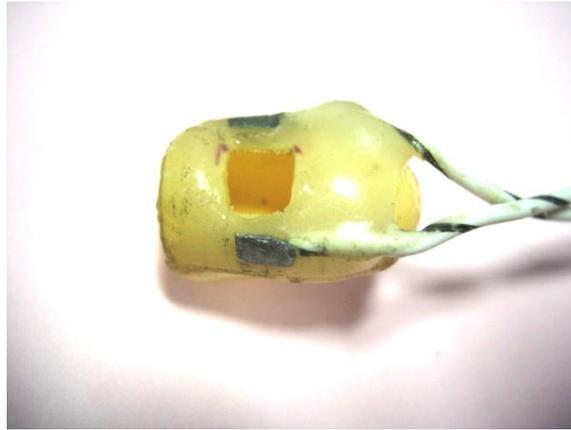
Fig. 6.4 Biopsy capsule casing showing electrodes and aperture

6.3.2 Stimulation Experiment to Introduce Lumen into an Aperture

Two 11 mm video capsule endoscope shaped capsules were used in this experiment. Each had a square aperture along its side wall, one measured 5 mm by 5 mm, and the other 7 mm by 7 mm. Around each aperture was mounted a pair of electrodes. These were used to induce a contraction of the small intestine. One end of each biopsy capsule was left open so that a conventional endoscope could be attached and used to observe the internal portion of the aperture and determine how much lumen entered during stimulation.

A pig was anaesthetised with a preperation of 3 ml of atropine and 16 ml of ketomine, with 1 ml of ketomine delivered intravenously. It was then masked down with 4% halothane, and anaesthetised with 2% halothane. The procedure was performed in the small bowel of the animal during laparotomy, where once

exposed, two small incisions were made in the walls of a section of the small intestinal wall about 300 mm apart. These allowed the introduction of the biopsy capsule and the conventional endoscope into the small bowel, which were then manoeuvred so the inside of the electrodes were supplied with a stimulation signal produced by a Grass SD9 medical stimulator. The biopsy aperture was observed with an endoscope and the depth of lumen tissue, (y mm) of the small intestine that entered the aperture during stimulation was estimated.

Voltage (V)	Depth of Tissue (y) Entering the Aperture (mm)	
	For 5 x 5 mm aperture ($\pm$ 0.5 mm) (N = 5)	For 7 x 7 mm aperture ($\pm$ 0.5 mm) (N = 5)
15	1	1
20	1	2
25	1	2
30	1	2
35	1	2
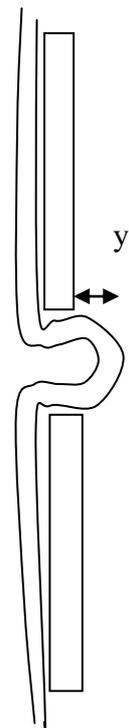
Table 6.1. Depth of tissue (y) entering the aperture during stimulation

Stimulation signals of 12.5 Hz, 20 ms over a range of voltages from 15-35 V were tested in different portions of the small intestines. The results summarised in Table 6.1, show that on application of the stimulation signal

tissue steadily entered the 5 mm aperture, and continued to do so until 1 mm of tissue was visible for all voltages in the range. However, the 7 mm device was too large because at voltages of 20 V and above more that 1mm of lumen tissue entered the aperture. 1 mm would be sufficient to take a biopsy safely without perforating the wall of the small intestine.

6.3.3 Conclusion

Electrostimulation of the intestines was used to introduce the intestinal wall into an aperture of a biopsy chamber. Once in the chamber a biopsy could be taken with a simple abrasive surface, needle or blade.

The first and by far the simplest of these would be an abrasive surface or brush, which would line the walls and base of the chamber. As the tissue was stimulated, the intestinal wall would enter the chamber and cells would be removed due to friction. This type of device would be use to take a sample of surface cells for analysis.

An alternative method would use a needle to perform a puncture biopsy. This could be done by positioning a hollow needle in the centre of the floor of the chamber pointing toward the aperture. Upon stimulation, the tissue would enter the biopsy chamber were the needle punctures the tissue, collecting a sample.

A third and most complicated alternative would be to use a cutting blade similar to that found in a Crosby capsule. A Crosby capsule is a metallic capsule which uses suction to introduce the lumen of the intestine into a chamber. Inside

the chamber is a small sprung blade, which is released by a cord allowing a biopsy to be taken. Therefore, once the tissue had entered the chamber, the blade would have to be released electronically, possibly using a fusible link.

The biopsy chamber is only effective if in the correct position. The positioning of device in the intestine is possible using electrostimulation but the orientation of the chamber relative to the sample area cannot be achieved this way. One solution would be to have multiple apertures around the device to allow samples of a complete circular section of the intestine to be taken.

There would be obvious difficulties in the accurate placement of the biopsy chamber over the area from which the biopsy is to be extracted. The technologies required to allow the capsule the freedom and control of movement to position it correctly are complex. Therefore, the possibility of a biopsy capsule in the near future does not seem feasible.

7. Conclusions

The ultimate aim of this project was to design and build a wireless remote controlled device that could be used to propel small video capsule endoscopes along gastrointestinal tract. Concentrating mainly in the region of the gastrointestinal tract where conventional endoscopy cannot reach without surgery, investigations focussed mainly on the small intestine.

The thesis follows the evolution of the design and construction of what ultimately became a radio-controlled bidirectional device, which could be used to propel a video capsule endoscope with or against the natural peristaltic flow. This would give a clinician the ability to use a video capsule endoscope like a conventional endoscope in the most inaccessible area of the gastrointestinal tract.

The thesis also reports investigations into the development of a bidirectional large intestine device, which when administered anally, could propel a video capsule endoscope the length of the large intestine at a comparable rate to a conventional colonoscope. The advantage being that there is less skill required to operate this device and it would seem to be less daunting to the patient.

Finally the thesis briefly describes initial investigations into the use of electrostimulation to introduce tissue into a biopsy chamber.

7.1 Summary of Achievements

Presented here is a summary of the milestones reached during the investigations of this thesis.

7.1.1 Wired Device

Early changes to the design of the small intestine device enabled electrical stimulation to induce movement in both directions along the small intestine. Once this concept of a bidirectional device had been proven to work, design changes led to the construction of a bidirectional wired M2A video capsule endoscope.

Initially tested *in vivo* in the intestine of pigs, the design of the bidirectional M2A went through a number of changes culminating in a device which, not only performed well *in vivo* in pigs, but also performed well *in vivo* in humans. This was the first bidirectional electrostimulation propelled video capsule endoscope used in man. These tests were performed in a fully conscious human volunteer who reported no pain during normal operation of the device.

7.1.2 Radio-Controlled Device

Early designs of a stimulator for a wireless device performed well. After a number of design modifications and the addition of a radio-control circuit a video capsule endoscope sized bidirectional radio-controlled device was tested *in vivo* in a pig. Although the device did not perform as well as the wired device, it would still be able to travel along the small intestine in 100 minutes. The device was tested in man and performed well in the small intestine of a human volunteer.

7.1.3 Large Intestine Device

Dimensional changes in design of the bidirectional device produced a device that could be successfully used in the large intestines. This device was tested in the large intestines of pigs travelling at speeds that would enable it to complete the 3 metre return journey along human large intestines in about 35 minutes. This is comparable with colonoscopy procedures.

7.1.4 Biopsy Device

Experiments using the biopsy device showed electrostimulation could be applied to successfully introduce lumen tissue into an aperture from which a biopsy sample could be taken. The use of electrostimulation in this way could

allow non-invasive devices such as a video capsule endoscope to obtain biopsy samples. This would allow biopsies to be taken from the small intestines without the need for enteroscopy. However, difficulties involved in the accurate positioning of the aperture are very complex and may not be possible in the near future.

7.2   Potential Applications

Electrostimulation of the intestinal wall has been shown to induce enough contractile force to propel small devices along the gastrointestinal tract. The bidirectional wired devices described in Chapter 4 were fundamentally designed to obtain stimulation parameters for the wireless devices described in Chapter 5. Although the wired devices showed good movement both with and against the natural peristaltic flow within the oesophagus and the small intestine, they do not seem to have any potential applications. The main reason for this is the trailing wire, which when passing through the throat causes activation of the gag reflex. This would cause the subject great and continual discomfort for the duration of the procedure.

However, anally administered devices such as the wired large intestine devices described in Chapter 6 do not share the impractical problem of invoking the gag reflex with a trailing wire. Therefore, such a device could be easily adapted into a practical device to carry a video capsule endoscope along the large intestine. Although still wired, this device seems less daunting than a 1.6 metre colonoscope. With comparable performance to conventional

colonoscopy and requiring less skill to navigate, this device could be useful for potential large participation colorectal screening programs.

The wireless remote control device could be incorporated into or used to propel video capsule endoscopes along the small intestines. Swain et al, have shown this in a test of the radio-controlled device in a human volunteer.[220] This type of device would be the first and only video capsule endoscope which can be swallowed and have its progression fully controlled by the attending clinician. The bidirectional propulsion system would allow the clinician to use the device as a conventional endoscope within the whole small intestine without the need for surgical enteroscopy.

7.3 Future Work

Future improvements to the device would be to produce a stimulator that delivers safer charge injection to reduce potential tissue damage and electrode corrosion by investigating and selecting the optimal square balance biphasic waveform. The electrodes could be improved by inter-linking the electrode edges like the fingers of clasped hands to reduce stray currents

A biopsy capsule could enhance the diagnostic capabilities of video capsule endoscopes by giving them the ability to take a sample biopsy from areas which the clinician has concerns about. Such a device would require a method to rotate the capsule to orientate the aperture.

Since completion of the practical work described in this thesis, the radio-controlled bidirectional device has been tested in a human volunteer. The device

while propelling a video capsule endoscope was reported to function in both directions.[220] This is a promising start to the continuation of the author's work.

Appendix A: Abstracts of the Author's Work Presented at Conference.

The abstracts presented in this appendix report the author's work, which was presented at three American Society for Gastrointestinal Endoscopy's 'Digestive Disease Week' meetings.

A1. Digestive Disease Week 2002, May 19 - 22, 2002; San Francisco, California[218]

A2. Digestive Disease Week 2003, May 18 - 21, 2003; Orlando; Florida[219]

A3. Digestive Disease Week 2005, May 14 - 19, 2005; Chicago, Illinois[220]

A1: Remote Propulsion of Wireless Capsule Endoscopes

Paul C. Swain, Alexander Mosse, Paul Burke, Annette Fritscher-Ravens, Shlomo Lewkovicz, Yehudi Kraizer, Tim Mills, London, UK; Yoqeneam, Israel

Introduction: Wireless capsule endoscopy depends on peristalsis for propulsion. Peristalsis is variable and sometimes too fast and sometimes annoyingly slow. Pathology is sometimes seen on a single frame. Methods for moving capsule endoscopes remotely might allow increased control and image manipulation by varying the speed of the capsules which might allow sufficient control to direct biopsy or therapy remotely: Methods: Electro-stimulation devices were used in combination with wireless capsule endoscopes (modified M2A) to improve remote imaging of the gastrointestinal tract. The shape of the propulsion device was an ovoid with bipolar electrodes set at the back and front. When stimulated with currents of 3 to 10 milliamps, a contraction was elicited in the circular muscle, which exerted a force on the tapered ovoid, which propelled it forwards or backwards. By stimulating the electrodes on the back or the front of the device the wireless capsule could be propelled forward or backward remotely. An M2A capsule was incorporated in some devices and was tugged by others. A miniature circuit was designed and constructed, which allowed the necessary currents to be achieved by using a 3-volt battery. The devices were tested in pigs both at closed endoscopy and open laparotomy. Fluoroscopy, conventional endoscopy, visual observation at surgery, and wireless capsule imaging were used to monitor the movement of the devices. Results: In studies in the esophagus it was possible to propel a capsule endoscope down and then upwards repeatedly. With peristalsis the capsule acquires 1 or 2 images of the oesophagus before entering the oesophagus. With electrostimulation the

acquisition of hundreds of oesophageal images became possible and the capsule could be moved in either direction at a rate of 2 cm/sec. Fluoroscopy showed movements particularly well in the esophagus. In the small intestine of anaesthetized pigs, the devices moved capsules, which were either incorporated into an ovoid or were tugged by separate ovoids. These devices were also successful in the colon. Beads sewn into the intestine were used as imaging targets. Wireless capsule imaging was effective in recording movement of these devices. It was possible to advance until a bead was seen and the capsule passed to object and then move backward with the device until the bead came into view again. Conclusion: Remote controlled movement of wireless capsule endoscopes is feasible in the esophagus, small intestine and colon. Bidirectional movement allowed external manipulation of image.

A2: Development and Testing of an Electrically Propelled Capsule Endoscope in Man

Annette Fritscher-Ravens, Paul Burke, Tim Mills, C. Alexander Mosse,
Maria Mylonaki, C. Paul Swain; London, UK

Introduction: Electrostimulation can cause propulsion of ovoid objects in the lumen of the gastrointestinal tract. Aim: To develop and test in man a new type of endoscope with a propulsion system driven by electrostlmulation.
Methods: Ovoid capsule endoscopes were modified. Four electrodes arranged in bipolar pairs were attached to the front and rear portions of the capsule. By careful attachment and subsequent polishing, it was possible to obtain unimpaired video images from tbe modified capsule endoscope without altering its geometry (11 X 27 mm). Several of these devices were constructed with wires to the front and back electrodes, which allowed an electrical stimulus to be applied to drive the capsule backwards or forwards from an external Grass stimulator which had been rendered electrically safe for use in man. Separate devices were constructed to include the circuitry necessary to drive similar devices without wires or external connectors, all these devices were tested in studies in the pig esophagus and small intestine prior to the use of identical devices in man. Ethical committee permission was given for testing these devices in a human volunteer.
Results: Independent and wired devices were successfully tested in porcine experiments. It was shown that both wired and unwired devices could drive wireless capsule endoscopes backwards and forwards in the small intestine at equal rates. The same devices did not move when electrostimulation was not switched on in these anaesthetized animals.
In an experiment in a human volunteer an electrostimulation capsule was swallowed. It reached the small intestine in 25 minutes. Electrostimulation was tested over a range of settings as the device travelled through the small intestine. The current used in these experiments was never enough to elicit conscious awareness or pain. At the settings used, the device was able to initiate contraction and accelerate the passage of the ovoid. The movements were

analyzed using x-ray screening and capsule image analysis. At high settings, a possible vagal stimulation effect may have been detected. The device was easily introduced and worked well in stimulating propulsive and retropulsive movement. It was easy to remove under screening from the middle of the small intestine. It did not hurt. Conclusion: A new propulsion system for capsule-type endoscopy and enteroscopy was successfully tested for the first time in man.

A3: Radio-controlled Movement of a Robot Endoscope in the Human Gastrointestinal Tract

Paul Swain, Tim Mills, Brian Kelleher, Loren Schmitz, Sandy Mosse, Paul Burke, Keitch Ikeda, Annette Fritcher-Ravens.

Background: Remote controlled movement of wireless capsule endoscope might improve diagnosis by allowing controlled examination of gastrointestinal pathology and is a pre-requisite for precise therapeutic intervention with capsule endoscopy. Aim: To develop a radio-controlled electrostimulation capsule (RESC) to propel and alter the direction of movement of a wireless capsule endoscope and to test it in man. Methods: A radio-controlled electrostimulation capsule measuring 11×33 mm was constructed. It featured paired bipolar electrodes inset at both ends of the capsule arranged to deliver sufficient current to cause circular muscular contraction in the gut to propel the capsule forwards and backwards. Small circuits inside the capsule were designed to receive commands and deliver pulses to move the capsule in the anesthetized pig and unanesthetized human gastrointestinal tract. 2 miniature batteries powered the device. Yellow, green and red LEDs indicated forwards or backwards electrostimulation and a strobe effect coincided with the electrostimulation frequency. An internal photodiode trigger was used to switch the device on and off. The RESC was attached to an identically sized wireless capsule endoscope by a short cable with the endoscope dome-window viewing the RESC. A command radio-control module allowed independent testing of the LEDs could switch the electrostimulation from forwards to backwards and deliver single test pulses to tissue. A go button commanded forwards or backwards motion. A loop aerial over the abdomen delivered radio command signals. Real-time image analysis software was used to acquire capsule images using the Given-Imaging Pill-Cam. Results: The RESC worked well in animal and human trials. A "tongue-test" was developed to check the LED's and physical effect of the electrostimulation prior to swallowing. The RESC was used as a tug or engine to pull or push a Pill-Cam at will. The direction and effect of the electrostimulation signal was imaged in real-time using the wireless capsule endoscope. The combination double sausage capsule-tug combination proved easy to swallow by a human volunteer. The RESC was observed functioning in the esophagus, stomach and duodenum using both conventional endoscopes and the attached wireless capsule endoscope. Conclusion: An autonomous radiocontrolled robotic capsular endoscope with forwards and reverse movement function was tested successfully in the porcine and human gastrointestinal tract.

Appendix B: Anatomy of the Gastrointestinal Tract

A more in depth discussion of the anatomy of the oesophagus, stomach, small intestine and large intestine, as outlined in Chapter 2.[22,23,24]

B1: The Oesophagus

The oesophagus is a 23 cm long muscular tube that extends from the pharynx to the stomach. It is generally vertical in orientation with a few curves along its path. It passes down through the neck along a central path in front of the trachea.

At the bottom of the neck it projects to the left with the thyroid gland and the thoracic duct. It then enters the thorax a little to the left of the median line, and passes behind the aortic arch. It then descends through the posterior mediastinum passing along the right side of the aorta almost to the Diaphragm where it then passes a little to the left of the front of the artery. Finally it enters the abdomen where it terminates at the cardiac orifice of the stomach. The oesophagus is the narrowest part of the alimentary canal, being most constricted at its commencement, and at the point where it passes through the Diaphragm

The oesophagus consists of three coats; the external muscular coat, the areolar coat, and the internal mucous coat.

The muscular coat has two layers of smooth muscle. The external layer of muscle is known as longitudinal muscle because the fibres are orientated along the length of the oesophagus. The internal layer of muscle is known as circular muscle because the fibres are orientated around the circumference of the oesophagus.

The areolar coat loosely connects the external muscular coat to the internal mucous coat.

The mucous coat is relatively thick and has a reddish colour above and pale below. It forms longitudinal folds, which disappear with distension of the oesophageal tube. On the inner surface there are minute papillae and it is completely covered with a thick layer of stratified pavement epithelium. Between the mucous membrane and the areolar coat lies a layer of longitudinally arranged non-striped muscle fibres, known as the muscularis mucousa. At the top of the oesophagus only a few bundles, if any, are apparent, whereas towards the bottom of the oesophagus there is a considerable layer.

B2: The Stomach

The stomach is situated between the oesophagus and the small intestine. As well as being the principal organ of the digestive system, it is also the most dilated part of the gastrointestinal tract. The larger end, known as the fundus, is directed upwards and the smaller end faces to the right of the body. It is positioned in the left hypochondriac and epigastric regions, placed mainly behind the wall of the abdomen and under the Diaphragm.

The size of the stomach varies considerably from person to person. Along its greatest length, when slightly distended the stomach measures 25-30 cm, and at its widest part, has a diameter of 10-12 cm. The distance between the two orifices of the stomach, the cardiac orifice at the terminus of the oesophagus and the pyloric orifice at the commencement of the small intestine, is 7-15 cm.

Between the anterior and posterior walls the stomach measures about 8 cm, and it has a capacity of about 3-4.5 litres. At the pyloric valve the orifice is reduced to about 1.5 cm in diameter.

The stomach wall is composed of four coats; the serous, muscular, areolar, and mucous.

The serous coat, derived from the peritoneum, covers most of the surface of the stomach except for the greater and lesser curvature regions, at the attachment points to the greater and lesser omenta, and near the cardiac orifice on the posterior surface.

The muscular coat, which lies directly beneath the serous coat, has three fibre layers; longitudinal, circular, and oblique.

The longitudinal fibres are continuous with the fibres of the oesophagus. Covering the stomach sparsely, they are distributed most distinctively along the curvatures, especially the lesser, with a thin distribution over the surfaces. At the pyloric orifice, they once again become more densely distributed and are continuous with the fibres of the small intestine.

The circular fibres are situated beneath the longitudinal fibres in a uniformly distributed layer covering the entire stomach. Most abundant at the pylorus, they collect together to form a circular ring, which together with a fold of mucous membrane over its surface forms the pyloric valve.

The oblique fibres are mainly situated in the cardiac region of the stomach. Found on both surfaces the fibres form a thick uniform layer around the cardiac orifice.

The areolar coat connects loosely the external muscular coat to the internal mucous coat.

The mucous membrane is thick with a smooth soft and velvety surface. It is thin in the cardiac region and thicker in the pyloric region. During the contracted state a number of longitudinal folds are formed, with greatest intensity at the lesser end of the stomach, and along the greatest curvature. These folds disappear when the stomach becomes distended.

B3: The Small Intestine

The small intestine extends on average 6 m from the pylorus to the ileo-caecal valve. Gradually diminishing in size from commencement to termination, the small intestine is contained in the central and lower portions of the abdominal cavity, surrounded by the large intestine. A portion of it passes below the brim of the pelvis to lie in front of the rectum. The small intestine is divided into three sections.

The duodenum is about 25 cm in length, making it the shortest and also the widest part of the small intestine. It is roughly U-shaped with its two extremities being positioned at about the same height. The position of the pylorus is dependent on how distended the stomach is. This then alters the position of the right proximal end of the duodenum, while the other end remains fixed. Whatever position it is in it reaches the underside of the liver, where it curves sharply and descends along the right side of the vertebral column to the fourth lumbar vertebra. Curving again it passes across the spine, where it then begins to ascend along the left side of the vertebral column to the second lumbar vertebra terminating at the commencement of the jejunum. Here it turns abruptly forming the duodeno-jejunal angle.

The jejunum and ileum make up the remainder of the small intestine in the ratio of two to three. There is no distinguishable interchange between these two parts, but gradual changes occur along their length, such that there are marked differences observed at either end. The jejunum is thicker, more vascular, and wider than the ileum with a diameter of approximately 4 cm. The

ileum on the other hand is less thick, vascular, or wide, with a diameter of about 3 cm. It follows a path with a large number of coils and convolutions in it. The jejunum mostly occupies the umbilical and left iliac regions whereas the ileum occupies mainly the umbilical, hypogastric, right iliac, and pelvic regions, and terminates in the right iliac fossa.

Occasionally, connected to the lower part of the ileum about 1 m from its terminus, there may be found a blind diverticulum. It is connected at one end to the lumen of the intestine and the other end can be connected to either the

abdomen wall, some other part of the intestine or nothing at all. This is known as Meckel's diverticulum, and is the remains of the duct for communication between the umbilical vesicle and the alimentary canal during early foetal life.

The wall of the small intestine, like the stomach, consists of four coats; the serous, muscular, areolar, and mucous.

Derived from the peritoneum the serous coat almost completely surrounds the first ascending portion of the duodenum at the pyloric end. This reduces to just covering the front of the duodenum along the rest of the first ascending portion and the second descending portion except where it is carried off by the transverse colon.

The third portion of the duodenum lies completely behind the peritoneum. The rest of the small intestine is once again surrounded by the peritoneum.

The muscular coat consists of two layers. The longitudinal (external) layer is comprised of longitudinal fibres that are thinly scattered over the surface of the intestines, more distinctively along its free border. The circular (internal) layer is comprised of circular fibres that surround the entire cylinder of the small intestine.

The thickness of the muscular coat is greater at the top the small intestine, reducing towards its termination.

The areolar coat loosely connects the muscular coat and the mucous coat.

The mucous membrane is thick and highly vascular at the pyloric end of the small intestine becoming paler and thinner toward its termination

B4: The Large Intestine

The large intestine extends from the termination of the ileum to the anus. It has a length of about 1.5 m, which is roughly a fifth of the length of the entire intestinal tract. It is at its largest at the commencement of the caecum, gradually reducing in size, until at the rectum a dilation of considerable size occurs just above the anus. It is larger and more firmly fixed than the small intestine. In its course the large intestine describes an arch which surrounds the small intestine. The large intestine is formed from three sections, the caecum, colon and rectum.

The caecum is a large blind pouch, which is situated below the ileo-caecal valve and forms the commencement of the large intestine. With its blind end facing downwards and its open end facing upwards into the colon, the caecum is positioned immediately behind the abdominal wall, situated in the right iliac fossa above the outer half of the Poupart's ligament.

The ileo-caecal valve is formed from two segments, the colic, (upper), and the cecal, (lower). The upper, following a convex path nearly horizontal in direction, connects the point of junction of the ileum and the colon, whereas the lower, which is more concave and longer, connects to the point of junction of the ileum and caecum.

The colon consists of four parts. These are the ascending, transverse, descending, and the sigmoid flexure.

Although continuous from the caecum, the ascending colon is slightly smaller in size. From its commencement at the ileo-caecal valve the ascending colon passes up to the base of the right lobe of the liver, on the right of the gall

bladder. Here lodged in the impressio colica, it bends abruptly inwards to the left to form the hepatic flexure.

The longest part of the large intestines, the transverse colon, passes from right to left across the abdomen into the left hypochondriac region. Here it curves beneath the lower end of the spleen forming the splenic flexure.

Passing downward through the left hypochondriac, the descending colon continues its downward path through the lumbar regions along the outer border of the left kidney. On reaching the lower end of the kidney, it turns inwards towards the Psoas muscle, along which it descends to the crest of the ileum where it terminates in the sigmoid flexure.

As the narrowest part of the colon, the sigmoid flexure is situated in the

left iliac fossa. Commencing at the termination of the descending colon, it

initially curves forwards, downwards, and inwards for about 5 cm, where it then forms a loop, which varies in length and position and terminates in the rectum at the brim of the true pelvis opposite the left sarco-iliac symphysis.

As the terminal part of the large intestine, the rectum extends from the sigmoid flexure to the anus. From the point of commencement the first part of the rectum passes downwards, backwards, and to the right to the level of the third sacral vertebrate. The second part of the rectum curves forwards and continues downwards to about 3 cm in front of the coccyx. From here the third part of rectum, also known as the anal canal, passes downwards and backwards to its termination at the anus.

The large intestine is composed of four coats; the serous, muscular, areolar, and mucous.

The serous coat is again formed from the peritoneum. The caecum is completely covered, except in a few cases where the upper posterior surface is uncovered. The ascending and descending colon are coated only on the front and sides with variable amounts of the posterior surface remaining uncovered. The transverse colon is completely covered except in the areas corresponding to the attachment of the great omentum and transverse mesocolon. The sigmoid flexure is completely covered apart from the area of connection with the sigmoid mesocolon. Similarly the upper part of the rectum is also completely covered except for the area of connection to the mesorectum. The middle section of the rectum has only covering on its anterior surface with a light covering on the sides towards the top. The third section of the rectum is devoid of any serous covering.

The muscular coat, as in the small intestine, consists of two layers of fibres. The outer longitudinal fibres do not form a uniform layer over the entire large intestine. In the caecum and colon the fibres are especially collected into three flat longitudinal bands, each about 1 cm in width. These bands, nearly one half shorter than the other coats of the large intestine, produce the characteristic sacculi. In the sigmoid flexure the fibres become more scattered. Towards the bottom of the sigmoid flexure and continuing on to the rectum, the fibres spread out to form a layer of complete cover, which is slightly thicker on the anterior and posterior surfaces.

Two bands of plain muscular tissue (retro-coccygeal muscles) arise from the second and third coccygeal vertebrae and blend with the longitudinal fibres on the posterior surface of the final part of the rectum.

The circular fibres form a thin layer over the caecum and colon. In the rectum they are more thickly layered, especially at the lower end where the fibres become the internal anal sphincter.

The areolar coat connects the muscular and mucous layers closely together.

In the caecum and colon, the mucous membrane is pale and smooth with no villi and it follows the folds of the sacculi. In the rectum it is much thicker, darker, and more vascular.

Appendix C: LM339 as an Astable Oscillator

Within this appendix is included a description of the operating parameters of the LM339 comparator when it is to be used as an astable oscillator. Included are circuit diagrams and equations the author found useful when designing the square wave generator described in Chapter 5.

The LM339 comparator can be used as the basis of an astable oscillator, that is as a square wave signal generator. It forms the core of the simple RC frequency circuit shown in Fig.C.1. Components R_4 and C_1 determine the frequency of the output while the resistors R_1, R_2 and R_3 are used to form a hysteresis loop. The frequency maximum is limited by the large signal propagation delay of the comparator together with the capacitive loading through the output, which also reduces the output slew rate.

Taking the voltage at the positive input as V_{A1}

$$V_{A1} = \frac{+V_{CC}R_2}{R_2 + (R_1 \parallel R_3)} \qquad [C.1]$$

When $R_1 = R_2 = R_3$

then

$$V_{A1} = \frac{2V_{CC}}{3} \qquad [C.2]$$

When the circuit is activated C_1 charges up through R_4 until it is charged to a potential value equal to V_{A1}. This causes the comparator output to switch to low. With the output voltage $V_0 =$ GND the value of V_A is reduced by the hysteresis network to:

$$V_{A2} = \frac{+V_{CC}}{3} \qquad\qquad [C.4]$$

With the above resistor values C_1 now discharges towards ground through R_4. This causes the output to return to its original high state when the voltage across C_1 has discharged to the V_{A2} value.
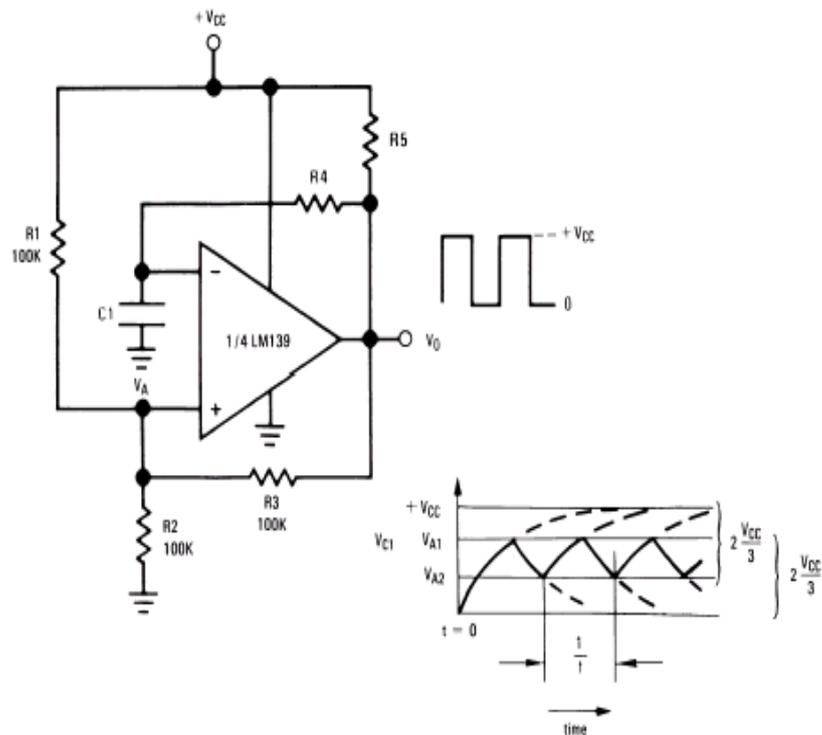
Fig C.1. Astable oscillator circuit.

248

By providing separate charge and discharge paths for the capacitor C_1 the circuit can be modified to produce an adjustable duty cycle pulse generator as shown in Fig. C.2. This is achieved by replacing R_4 with two variable resistor/diode pathways; R_1, D_1 and R_2, D_2. One path, (R_1, D_1), charges the capacitor and sets the pulse width duration i.e. the time from t_0 to t_1. The other path, (R_2, D_2), discharges the capacitor and sets the time between the pulses, i.e. from t_1 to t_2.
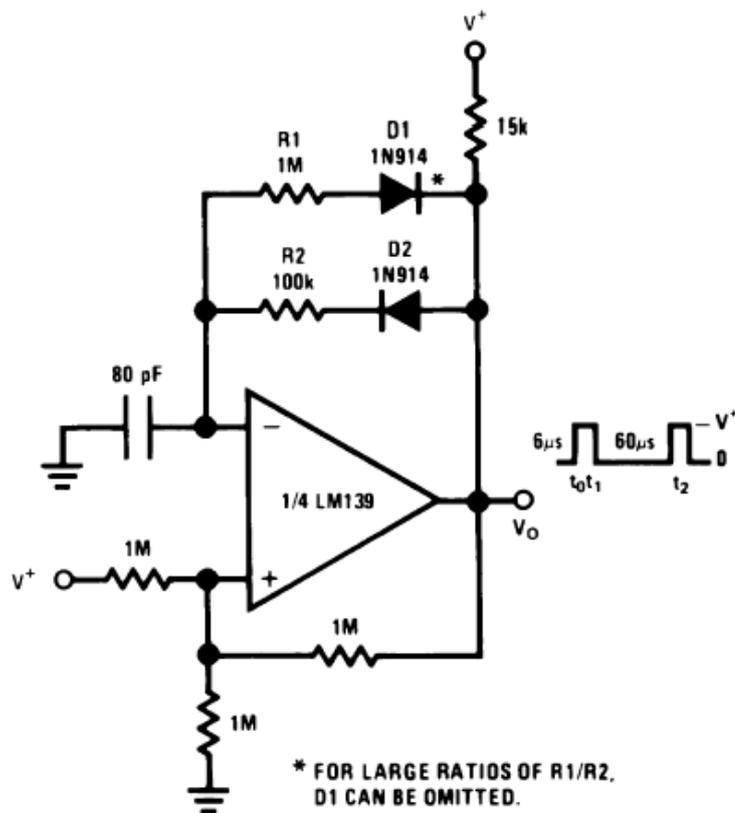
Fig. C.2. Adjustable astable oscillator cicuit.

The pulse duration width and the time between pulses can be calculated from:

$$V_1 = V_{MAX} e^{-t_2/R_5 C_1} \quad (\text{falltime}) \qquad [C.4]$$

Where

$$V_{MAX} = \frac{2V_{CC}}{3} \qquad [C.5]$$

and

$$V_1 = \frac{V_{MAX}}{2} = \frac{V_{CC}}{3} \qquad [C.6]$$

The value for t_1 is obtained from:

$$\frac{1}{2} = e^{-t_1/R_4 C_1} \qquad [C.7]$$

The value for t_2 is obtained from:

$$\frac{1}{2} = e^{-t_2/R_5 C_1} \qquad [C.8]$$

This is an over simplified representation since a slight adjustment to the V_{max} value is required due to a diode voltage drop reducing the value to:

$$V_{MAX} = \frac{2}{3}(V_{CC} - V_{BE}) \qquad\qquad [C.9]$$

Therefore,

$$\frac{1}{2(1-V_{BE})} = e^{-t_2/R_2C_1} \qquad\qquad [C.10]$$

and

$$\frac{1}{2(1-V_{BE})} = e^{-t_1/R_1C_1} \qquad\qquad [C.11]$$

A pulse generator used to drive the current through the tissue is required to produce a square wave pulse within the frequency range 10-100 Hz, with a duration range of 10–20 ms. To produce a device with an adjustable range of parameters, variable resistors VR_1 and VR_2 were included in the circuit. The optimum values of these components as well as that of the capacitor C_1 were calculated using the following equations obtained by rearranging the earlier equations:

$$t_1 = \ln(R_1C_1) \qquad\qquad [C.12]$$

and

$$t_2 = \ln(R_2C_1) \qquad\qquad [C.13]$$

In order to produce the required range of frequency and duration parameters for the stimulation, the t_0-t_1 and t_1-t_2 values need to have a range of values of 10–20 ms and 10–100 ms respectively. In order to produce the maximum value of 100 ms for t_2, a value of 72 nF for the capacitor C_1 is required, when the potentiometer VR_2 is set to its maximum of 1 MΩ. The closest available value was 82 nF, which allows a maximum value for t_2 of approximately 114 ms.

To find the maximum value of VR_1, the calculated value for C_1 was used with the required maximum value for t_1. This gave a maximum value for the potentiometer VR_1 of 176 kΩ. The closest available value to this is a 250 kΩ potentiometer, which gives a maximum value of approximately 28 ms for t_1.

The values for the other resistors in the circuit were 1 MΩ except for the step up resistor, which has a value of 15 kΩ. Ordinary silicon signal diodes were used.

Appendix D: Charge Density on the Electrode

A crude model of the charge density was used to determine the order of magnitude of the maximum charge density on the electrode for four the different electrode types used for different devices during the project. The charge density per cycle was calculated by $\frac{pulse\ width\ x\ current\ supplied}{electrode\ area}$

Stimulation Parameters and Radius			Electrode Type			
			Charge Density (A/cm²)			
pulse duration (ms)	current (mA)	radius (mm)	screw	cone	hemi	lens
20	5	4.5	0.00015719	0.0002223	0.00015719	0.000354
20	5	5.5	0.000105226	0.000148813	0.000105226	0.000289
20	5	6.5	7.53396E-05	0.000106546	7.53396E-05	0.000245
20	5	7.5	5.65884E-05	8.00281E-05	5.65884E-05	0.000212
20	5	8.5	4.40567E-05	6.23056E-05	4.40567E-05	0.000187
20	10	4.5	0.00031438	0.000444601	0.00031438	0.000707
20	10	5.5	0.000210453	0.000297625	0.000210453	0.000579
20	10	6.5	0.000150679	0.000213093	0.000150679	0.00049
20	10	7.5	0.000113177	0.000160056	0.000113177	0.000424
20	10	8.5	8.81135E-05	0.000124611	8.81135E-05	0.000374
20	15	4.5	0.00047157	0.000666901	0.00047157	0.001061
20	15	5.5	0.000315679	0.000446438	0.000315679	0.000868
20	15	6.5	0.000226019	0.000319639	0.000226019	0.000735
20	15	7.5	0.000169765	0.000240084	0.000169765	0.000637
20	15	8.5	0.00013217	0.000186917	0.00013217	0.000562
20	20	4.5	0.00062876	0.000889201	0.00062876	0.001415
20	20	5.5	0.000420906	0.00059525	0.000420906	0.001157
20	20	6.5	0.000301358	0.000426185	0.000301358	0.000979
20	20	7.5	0.000226354	0.000320112	0.000226354	0.000849
20	20	8.5	0.000176227	0.000249223	0.000176227	0.000749
10	10	2	0.000795775	0.001125395	0.000795775	0.000796
20	15	1	0.009549297	0.013504745	0.009549297	0.004775
10	20	4.5	0.00031438	0.000444601	0.00031438	0.000707
10	20	5.5	0.000210453	0.000297625	0.000210453	0.000579

Table D.1. Charge density on the electrode.

References

1. Screening for colorectal cancer: medical and economic aspects.
   Sanduleanu S, Stockbrugger RW.
   Scand J Gastroenterol suppl. 2003; (239): 73-7.

2. The risks of screening: data from Nottingham randomised controlled trial of faecal occult blood screening for colorectal cancer.Robinson MHE, Hardcastle JD, Moss SM, Amar SS, Chamberlain JO, Armitage NCM, Scholefield JH, Mangham CM.
   Gut 1999; 45:588-592.

3. Costs of screening for colorectal cancer: an Australian programme.
   Gow J.
   Health Econ. 1999; 8: 531-540.

4. Summary of colorectal cancer in adults at average risk: a summary of the evidence of the U.S. preventative task force.
   Pignone M, Rich M, Teutsch SM, Berg AO, Lohr KN.
   Ann Intern Med. 2002; 137: 132-141.

5. A randomised study of screening for colorectal cancer using faecal occult blood testing: results after 13 years and seven biennial screening rounds.
   Jorgensen OD, Kronborg O, Fenger C.
   Gut 2002; 50: 29-32.

6. Randomised controlled trial of faecal occult blood screening for colorectal cancer.
   Hardcastle JD, Chamberlain JO, Robinson MHE, Moss SM, Amar SS, Balfour TW, James PD, Mangham CM.
   Lancet 1996; 348: 1472-77.

7. Effect of faecal occult blood screening on mortality from colorectal cancer: results from a randomised controlled test.
   Scholefield JH, Moss SM, Sufi F, Mangham CM, Hardcastle JD,
   Gut 2002; 50: 840-844.

8. Protective effect of faecal occult blood test screening for colorectal cancer: worst prognosis for screening refusers.
   Niv Y, Lev-El M, Fraser G, Abuksis G, Tamir A.
   Gut 2002; 50:33-37.

9. Colorectal cancer screening.
   Almeida FFN, Araujo SEA, Santos FPdS, Franco CJCdS, Santos VR, Nahas SC, Habr-Gama A. rev. hosp.
   Clin. Fac. Med. S. Paulo. 2000; 55(1): 35-42.

10. Screening for colorectal cancer using the faecal occult blood test: a critical literature review.
    Craven O.
    European Journal of Oncology nursing 2001; 5(4): 234-243.

11. Randomised study of screening for colorectal cancer with faecal occult blood test.
    Kronborg O, Fenger K, Olsen J, Jorgensen OD, Sondergaard O.
    Lancet 1996; 348: 1467-71.

12. Promoting early detection tests for colorectal carcinoma and adenomatous polyps.
Levin B, Smith RA, Feldmen GE, Colditz GA, Nadel M, Rothenberger DA, Schroy PS, Vernon SW, Wender R.
Cancer 2002; 95 (8): 1618-1628.

13. A new variable stiffness colonoscope makes colonoscopy easier: a randomised controlled trial.
Brooker JC, Saunders BP, Shah SG, Williams CB.
Gut 2000; 46: 801-805.

14. A snapshot of colonoscopy practice in England: stimulus for improvement.
Palmer K, Morris AI.
Gut 2004; 53: 163-165.

15. Wireless capsule endoscopy.
Iddan G, Meron G, Glukhovsky A, Swain CP.
Nature 2000; 405: 417.

16. Wireless endoscopy.
Gong F, Mills TN, Swain CP.
Gastrointest Endosc 2000; 51: 725-729

17. Wireless capsule diagnostic endoscopy for recurrent small-bowel bleeding.
Appleyard M, Glukhovsky A, Swain CP,
N Engl J Med 2001; 34: 232-233.

18. A randomized trial comparing wireless capsule endoscopy with push enteroscopy for the detection of small-bowel lesions Appleyard M, Fireman Z, Glukhovsky A, Jacob H, Shreiver R, Kadirkamanathan S, Lavy A, Lewkowicz S, Scapa E, Shofti R, Swain CP, Zaretsky A.Gastroenterology 2000; 119: 1431-1438.

19. Wireless capsule endoscopy: a comparison with push enteroscopy in patients with gastroscopy and colonoscopy negative gastrointestinal bleeding.
Myloniki M, Fritcher-Ravens A, Swain CP. Gut 2003; 52: 1122-1126.

20. Wireless capsule video endoscopy: Three years of experience.
Eliakim R. World J Gastroenerol 2004; 10(9): 1238-1239.

21. Wireless capsule endoscopic detection of Meckel's Diverticulum after nondiagnostic surgery. Myloniki M, MacLean D, Fritcher-Ravens A, Swain CP.
Endoscopy. 2002;34:1018–1020.

22. Anatomy, Descriptive and Surgical, Henry Gray, F.R.S. Chancellor Press, Fifteenth Addition, 1985, reprinted 1987

23. The CIBA Collection of Medical Illustrations. Volume 3. Part 1. Frank H. Netter, M.D. CIBA © 1959, Third Printing 1971.

24. The CIBA Collection of Medical Illustrations. Volume 3. Part 2. Frank H. Netter, M.D. CIBA © 1962, Third Printing 1973.

25. Clinical Radiology and Endoscopy of the Colon. W.A.J Reeders and Gerd Rosenbusch. Jaques. Thieme Medical Pub, 1994

26. Quantitative analysis of peristalsis in the guinea-pig small intestine using spatio-temporal maps G. W. Hennig, M. Costa, B. N. Chen and S. J. H. Brookes Journal of Physiology (1999), 517.2, pp.575-590 575

27. Baehr PH, McDonald GB. Esophageal infections: risk factors, presentation, diagnosis, and treatment. Gastroenterology, 1994; 106: 509.

28. Kaye MD. Postprandial gastroesophageal reflux in healthy people. Gut, 1977; 18: 709.

29. Fisher RS, Roberts GS, Grabowski q, Cohen S. Altered lower esophageal sphincter function during early pregnancy. Gastroenterology, 1978; 74: 1233.

30. Locke GR, Talley NJ, Fett SL, Zinsmeister AR, Melton LJ. Prevalence and clinical spectrum of gastroesophageal reflux: a population-based study in Olmsted County, Minnesota. Gastroenterology, 1997; 112: 1448.

31. Dent J, Holloway RH, Toouli J, Dodds WJ. Mechanisms of lower oesophageal sphincter incompetence in patients with symptomatic gastrooesophageal reflux. Gut, 1988; 29: 1020.

32. Kasapidis P, Xynos E, Mantides A. et al. Differences in manometry and 24-H ambulatory pH-metry between patients with and without endoscopic or histological esophagitis in gastroesophageal reflux disease. Am J Gastroenterol. 1993;881893-189

33. Gastro-oesophageal reflux—Pathogenesis and clinical implications T. R. Weihrauch European Journal of Pediatrics Volume 144, Number 3 (1985), 215-218

34. Bontempo I, Piretta L, Corazziari E, Michetti F, Anzini F, Torsoli A. Effects of intraluminal acidification on oesophageal motor activity. Gut. 1994;35884- 890

35. Salivary gland scintigraphy in gastro-esophageal reflux disease Y. Urita, K. Domon, T. Yanagisawa, S. Ishihara, M. Hoshina, T. Akimoto, H. Kato, N. Hara, Y. Honda and Y. Nagai, *et al.* Inflammopharmacology Volume 15, Number 4 (2007), 141-145

36. Mechanisms of Gastroesophageal Reflux and Gastroesophageal Reflux Disease Vandenplas, Yvan; Hassall, Eric Journal of Pediatric Gastroenterology & Nutrition: August 2002 - Volume 35 - Issue 2 - pp 119-136

37. The Endoscopic Assessment of Esophagitis: A Progress Report on Observer Agreement David Armstrong, John R. Bennett, Andre L. Blum, John Dent, Timothy De Dombal, Jean–Paul Galmiche, Lars Lundell, Mariana Margulies, Joel E. Richter, Stuart J. Spechler, Guido N. J. Tytgat, and Lene Wallin Gastroenterology 1996;111:85–92

38. Amy E. Noffsinger (*2009*) Update on Esophagitis: Controversial and Underdiagnosed Causes. Archives of Pathology & Laboratory Medicine: July 2009, Vol. 133, No. 7, pp. 1087-1095.

39. Eosinophils in the Esophagus—Peptic or Allergic Eosinophilic Esophagitis? Case Series of Three Patients with Esophageal Eosinophilia Peter Ngo MD, Glenn T Furuta MD, Donald A Antonioli MD and Victor L Fox MD *The American Journal of Gastroenterology* (2006) **101**, 1666–1670

40. Severity of Basal Cell Hyperplasia Differs in Reflux Versus Eosinophilic Esophagitis Steiner, Steven J. MD; Kernek, Kevin M. MD; Fitzgerald, Joseph F. MD Journal of Pediatric Gastroenterology & Nutrition: May 2006 - Volume 42 - Issue 5 - pp 506-509

41. The normal human esophageal mucosa: a histological reappraisal. Weinstein WM, Bogoch ER, Bowes KL Gastroenterology [1975, 68(1):40-44]

42. Norman Barrett, "Doyen of Esophageal Surgery" Reginald V. N. Lord, Fracs Annals Of Surgery Vol. 229, No. 3, 428-439, 1999 March.

43. Grande L, Lacima G, Ros E. et al. Dysphagia and esophageal motor dysfunction in gastroesophageal reflux are corrected by fundoplication. J Clin Gastroenterol. 1991;1311- 16

44. Wild CP, Hardie LJ. Reflux, Barrett's oesophagus and adenocarcinoma: burning questions. Nat Rev Cancer 2003; 3: 676–684.

45. Spechler SJ. Clinical practice. Barrett's Esophagus. N Engl J Med 2002; 346: 836–842.

46. Chronic Inflammation: A Common and Important Factor in the Pathogenesis of Neoplasia Dr. David Schottenfeld MD, MSc, Dr. Jennifer Beebe-Dimmer PhD, MPH CA Cancer J Clin 2006;56:69–83

47. Dysplasia as a predictive marker for invasive carcinoma in Barrett esophagus: A follow-up study based on 138 cases from a diagnostic variability study Elizabeth Montgomery, MD, John R Goldblum, MD, Joel K Greenson, MD, Marian M Haber, MD, Laura W Lamps, MD, Gregory Y Lauwers, MD, Audrey J Lazenby, MD, David N Lewin, MD, Marie E Robert, MD, Kay Washington, MD, PhD, Marianna L Zahurak, MS, John Hart, MDHuman Pathology Volume 32, Issue 4, April 2001, Pages 379–388

48. Barrett's esophagus, dysplasia, and adenocarcinoma Rodger C. Haggitt, MD Human Pathology Volume 25, Issue 10, October 1994, Pages 982–993

49. Distribution of dysplasia and early invasive carcinoma in Barrett's esophagus Joseph E. McArdle, MD, Klaus J. Lewin, MD, Gayle Randall, MD, Wilfred Weinstein, MD Human Pathology Volume 23, Issue 5, May 1992, Pages 479–482

50. Spechler SJ, Robbins AH, Rubins HB et al. Adenocarcinoma and Barrett's esophagus: an overrated risk? Gastroenterology, 1984; 87: 927.

51. CameronAJ, Ott BJ, Payne WS. The incidence of adenocarcinoma in columnar-lined (Barrett's) esophagus. N Engl' Med, 1985; 313: 857.

52. van der VeenAH, Dees J, BlankensteijnJD, van Blankenstein M. Adenocarcinoma in Barrett's oesophagus: an overrated risk. Gut, 1989;30:14.

53. Miros M, Kerlin P, Walker N. Only patients with dysplasia progress to adenocarcinoma in Barrett's oesophagus. Gut, 1991; 32: 144l.

54. Drewitz DJ, Sampliner RE, Garewal HS. The incidence of adenocarcinoma in Barrett's esophagus: a prospective study of 170 patients followed 4.8 years. Am J Gastroenterol. 1997 Feb;92(2):212-5

55. Tytgat GNJ, Hameeteman W, Onstenk R, Schotborg R. The spectrum of columnar-lined esophagus-Barrett's esophagus. Endoscopy, 1989;21: 177.

56. Gonzalez-Crussi IF, lung OS. Esophageal moniliasis as a cause of death.AmJ Surg, 1965; 109: 634.

57. Weiss J, Epstein BS. Esophageal moniliasis. Am J Roentgenol, 1962;88:718.

58. Huchzermeyer H, Paul F, Seifert E et al. Endoscopic results in five patients with Crohn's disease of the esophagus. Endoscopy, 1976; 8:75.

59. Degryse HRM, De Schepper AMAP. Aphthoid esophageal ulcers in Crohn's disease of ileum and colon. Gastrointest Radiol, 1984; 9: 197.

60. Freedman PG, Dieterich DT, Balthazar EJ. Crohn's disease of the esophagus: case report an review of the literature. Am 1 Gastroenterol, 1984; 79: 835.

61. Geboes K, Janssens J, Rutgeerts P, Vantrappen C. Crohn's disease of the esophagus. 1 Clin Gastroenterol, 1986; 8: 31.

62. Lenaerts C, Roy CC, Vaillancourt M et al. High incidence of upper gastrointestinal tract involvement in children with Crohn disease. Pediatrics, 1989; 83: 777.

63. Parnell SAC, Peppercorn MA, Antonioli DA, Cohen MA, Joffe N. Squamous cell papilloma of the esophagus. Report of a case after peptic esophagitis and repeated bougienage with review of the literature. Gastroenterology, 1978; 74: 910.

64. Staples DC, Knodell RG, Johnson LP. Inflammatory pseudotumor of the esophagus. A complication of gastroesophageal reflux. Gastrointest Endosc, 1978; 24: 175.

65. Rabin MS, Bremner CG, Botha JR. The reflux gastroesophageal polyp. Am J Gastroenterol, 1980; 73: 451.

66. Parkin OM, Laara E, Muir CS. Estimates of the world-wide frequency of sixteen major cancers in 1980. Int J Cancer, 1988; 41: 184.

67. Minielly JA, Harrison EG Jr, Fontana RS, Payne WS. Verrucous squamous cell carcinoma of the esophagus. Cancer, 1967; 20:2078.

68. Parkinson AT, Haidak GL, Mclnemey RP. Verrucous squamous cell carcinoma of the esophagus following lye stricture. Chest, 1970;57:489.

69. Agha FP, Weatherbee L, Sams JS. Verrucous carcinoma of the esophagus. Am J Gastroenterol, 1984; 79: 844.

70. McKay JS, Day DW. Herpes simplex oesophagitis.Histopathology, 1983;7:409.

71. Brayko CM, Kozarek RA, Sanowski RA, Lanard BJ. Type 1 herpes simplex esophagitis with concomitant esophageal moniliasis. J Clin Gastroenterol, 1982; 4: 351.

72. Deshmukh M, Shah R, McCallum RW. Experience with herpesesophagitis in otherwise healthy patients. Am J Gastroenterol, 1984; 79: 173.

73. McBane RD, Gross JB Jr. Herpes esophagitis: clinical syndrome,endoscopic appearance, and diagnosis in 23 patients. Gastrointest Endosc,1991;37:600.

74. EI-Serag HB, Johnston DE. Mycobacterium avium complex esophagitis. Am 1 Gastroenterol, 1997; 92: 1561.

75. ChangAD, Drachenberg Cl, James SP. Bacillary angiomatosis associated with extensive esophageal polyposis: a new mucocutaneous manifestation of acquired immunodeficiency disease (AIDS). Am 1 Gastroenterol, 1996; 91: 2220.

76. Kiviranta UK. Corrosion carcinoma of the oesophagus: 381 cases of corrosion and 9 cases of corrosion carcinoma. Acta Otolaryngol, 1952; 42: 89.

77. Appelqvist P, Salmo M. Lye corrosion carcinoma of the esophagus. A review of 63 cases. Cancer, 1980; 45: 2655.

78. KikendallJW, FriedmanAC, Oyewole MA et al. Pill-induced esophageal injury. Case reports and review of the medical literature. Dig Dis Sci, 1983; 28: 174.

79. Goin Jc, Sterin-Borda L, Bilder CR et al. Functional implications of circulating muscarinic cholinergic receptor autoantibodies in chagasic patients with achalasia. Gastroenterology, 1999; 117: 798.

80. Kazlow PG, Shah K, Benkov KG, Dische R, LeLeiko NS. Esophageal cryptosporidiosis in a child with acquired immune deficiency syndrome. Gastroenterology, 1986; 91: 1301.

81. Butler C, Madden JW, Davis WM. Morphologic aspects of experimental lye strictures. I. Pathogenesis and pathophysio logic correlations. 1 Surg Res, 1974; 17: 232.

82. Burgess HM, BaggenstossAH, Moersch HJ, Clagett OT. Cancer of the esophagus: a clinicopathologic study. Surg Clin N Am, 1951;31: 965.

83. Scanlon EF, Morton OR, Walker JM, Watson WL. The case against segmental resection for esophageal carcinoma. Surg Gynecol Obstet, 1955; 101:290.

84. Takubo K, Takai A, Takayama S,Sasajima K, Yamashita K,Fujita K. Intraductal spread of esophageal squamous cell carcinoma.Cancer, 1987;59: 1751.

85. Watson WL. Carcinoma of the esophagus. Surg Gynecol Obstet,1933; 56: 884.

86. Mandard AM, Chasle J, Mamay J et al. Autopsy findings in 111 cases of esophageal cancer. Cancer, 1981; 48: 329.

87. Bosch A, Frias Z, Caldwell WL, Jaeschke WH Autopsy findings in carcinoma of the esophagus. Acta Radiol Oncol, 1979; 18: 103.

88. Anderson LL, Lad TE. Autopsy findings in squamous-cell carcinoma. Cancer, 1982; 50: 1587.

89. Chan KW, Chan EYT, Chan CW. Carcinoma of the esophagus: an autopsy study of 231 cases. Pathology, 1986; 18: 400.

90. Toreson WE. Secondary carcinoma of the esophagus as a cause of dysphagia. Arch Pathol, 1944; 38: 82.

91. Hale RI, Merchant W, Hasleton PS. Polypoidal intra oesophageal thyroid carcinoma: a rare cause of dysphagia. Histopathology, 1990; 17: 475.

92. Polk HC Jr, Camp FA, Walker AW. Dysphagia and oesophageal stenosis: manifestations of metastatic mammary cancer. Cancer,1967; 20: 2002.

93. Varanasi RV, SaltzmanJR, Krims P, CrimaldiA, Colby J. Breast carcinoma metastatic to the esophagus: clinicopathological and management features of four cases, and literature review. Am J Gastroenterol, 1995;90: 1495.

94. Gowing NFC. In: Tanner NC, Smithers DW, eds. Tumours of the Oesophagus. Edinburgh: Churchill Livingstone, 1961.

95. Gross P, Freedman LJ. Obstructing secondary carcinoma of the esophagus. Arch Pathol, 1942; 33: 361.

96. Gore RM, Sparberg M. Metastatic carcinoma of the prostate to the esophagus. Am J Gastroenterol, 1982; 77: 358.

97. Nussbaum M, Grossman M. Metastases to the esophagus causing gastrointestinal bleeding. Am J Gastroenterol, 1976; 66: 467.

98. Zarian L P, Berliner L, Redmond P. Metastatic endometrial carcinoma to the esophagus. Am J Gastroenterol, 1983; 78: 9.

99. Kolodziejczyk P, Yao T, Oya M et al. Long-term follow-up study of patients with gastric adenomas with malignant transformation .Cancer, 1994;74:2896.

100. Ming SC. The classification and significance of gastric polyps. In: Yardley JH, Morson BC, Abell MR, eds. The Gastrointestinal Tract. Baltimore: Williams & Wilkins, 1977: 149.

101. Parkin DM, Uiara E, Muir CS. Estimates of the worldwide frequency of 16 major cancers in 1980. Int J Cancer, 1988; 41: 184.

102. Pisani F, Parkin DM, Bray F, Ferlay J. Estimates of the worldwide mortality from 25 cancers in 1990. Int J Cancer, 1999; 83: 18.

103. Stout AP. Pathology of carcinoma of the stomach. Arch Surg, 1943;46:807.

104. Maruyama K, Gunven P, Okabayashi Ket al. Lymph node metastases of gastric cancer. Ann Surg, 1989; 210: 596.

105. Crohn BB, Ginzberg L, Oppenheimer GD. Regional ileitis: a pathological and clinical entity. JAMA, 1932; 99: 1323.

106. Dalziel TK. Chronic interstitial enteritis. Br Med J, 1913; ii: 1068.

107. Fielding JF, Toye DK, Beton DC, Cooke WT. Crohn's disease of the stomach and duodenum. Gut, 1970; 11: 100l.

108. Basu MK, Asquith P, Thompson RA, Cooke WT. Proceedings: Oral lesions in patients with Crohn's disease. Gut, 1974; 15:346.

109. Huchzermeyer H, Paul F, Seifert E, Frohlich H, Rasmussen CW. Endoscopic results in five patients with Crohn's disease of the esophagus. Endoscopy, 1977; 8: 75.

110. Rankin GB, Watts HD, Melnyk CS, Kelley MLJr. National Cooperative Crohn's Disease Study: extraintestinal manifestations and perianal complications. Gastroenterology, 1979; 77: 914.

111. GreensteinAJ, Sachar DB, Smith H, Janowitz HD,Aufses AH Jr. Patterns of neoplasia in Crohn's disease and ulcerative colitis. Cancer, 1980; 46: 403.

112. Chen CC, Neugut AI, Rotterdam H. Risk factors for adenocarcinomas and malignant carcinoids of the small intestine: preliminary findings. Cancer Epidemiol Biomarkers Prev, 1994; Apr-May; 3(3): 205-7

113. Barclay RN, Schapira DV. Malignant tumors of the small intestine. Cancer, 1983;51 (5): 878.

114. Weiss NS, Yang CP. Incidence of histologic types of cancer of the small intestine. J Natl Cancer Inst, 1987; 78 (4): 653.

115. DiSario JA, Burt RW, Vargas H, McWhorter WP. Small bowel cancer: epidemiological and clinical characteristics from a population-based registry. Am J Gastroenterol, 1994; 89 (5): 699.

116. Matsuo 5, Eto T, Tsunoda T, Kanematsu T, Shinozaki T. Small bowel tumors: an analysis of tumor-like lesions, benign and malignant neoplasms. Ellr J SlIrg Oncol, 1994; 20 (1): 47.

117. Williams AR, Balasooriya BAW, Day DW. Polyps and cancer of the large bowel: a necropsy study in Liverpool. Gut, 1982; 23: 835.

118. Jass JR, Young PJ, Robinson EM. Predictors of presence, multiplicity, size and dysplasia of colorectal adenomas. A necropsy study in New Zealand. Gut, 1992; 33: 1508.

119. Clark JC, Collan Y, Eide TJ et al. Prevalence of polyps in an autopsy series from areas with varying incidence of large-bowel cancer. Int J Cancer, 1985;36: 179.

120. Bernstein MA, Feczko PJ, Halpert RD, Simms SM, Ackerman LV. Distribution of colonic polyps: increased incidence of proximal lesions in older patients. Radiology, 1985; 155: 35.

121. Röntgen, W. C. "Sitzungsberichte der physikalisch-medizinischen Gesell-schaft zu Würzburg." *Sonderdruck vom* 28 (1895).

122. Becher W. Zur Anwendung des roentgenischen Verfahrens in der Medizin. Dtsch Med Wochenschr 1896;22:202

123. Reeders, Jacques WAJ, Ad J. Bakker, and Gerd Rosenbusch. "9 Contemporary radiological examination of the lower gastrointestinal tract."*Baillière's clinical gastroenterology* 8.4 (1994): 701-727.

124. Rieder H., - Contribution à la topographie du tube gastro-intestinal chez l'homme vivant et recherches concernant la durée de la digestion. Fortehr. Röntgenstr., Fév 1905.

125. Radiologic History Exhibit Brief History of Gastrointestinal Radiology[1] Ronald L. Eisenberg, MD Alexander R. Margulis, MD RadioGraphics 1991; 1 1:12 1-132.

126. Fischer AW. *Frühdiagnose des Dickdarmkrebses, insbesondere seine Differentialdiagnose gegen Tuberkulose mit Hilfe der kombinierten Luft- und Bariumfüllung des Dickdarms. Deutsch Ges f. innere Med* 1923; 35:86-87

127. Bouwers, A., 1927. Uber den Temperaturverlauf an der Anode .einer Rontgenr . ohre. Zeitschr. f. techhn. Physik 8, 271–277.

128. Andren L, Frieberg S, Welin S. Roentgen diagnosis of small polyps in the colon and rectum. *Acta radiol.* 1955 Mar;43(3):201–208.

129. Selink JL. Radiologic examination of the small intestine by duodenal intubation. Acta Radiol 1974;15:318.

130. Hamelin L, Hurtubise M: Remote control technique in double contrast study of the colon.*Am J Roentgenol 119*:382–392, 1973

131. Miller RE, Chernish SM, Skucas J, Rosenak BD, Rodda BE. Hypotonic roentgenography with glucagon. *Am J Roentgenol* 1974; 121: 264–274

132. Bozzini P. Lichtleiter, eine Enfindung zur Auschschauung innere Theiler und Krankheiten. Journal der Practischen Arzneykunde und Wunderartzney kunst 1806; 24:107–24.

133. Killian G. Zur Geschichte der Oesophago und Gastroskopie.Deutsche Zietschrift fur Chirirgie 1900; 59:499–512.

134. Mikulicz-Radecki J (1881) Über Gastroskopie und Ösophagoskopie. Wiener Med Presse 22:1405–1408, 1437–1443, 1473–1475, 1505–1507, 1537–1541, 1573–1577, 1629–1631.

135. The History of Endoscopy, Especially of Gastroscopy Sachio Takasu (Kanto-Teishin Hospital) Gastroenterological Endoscopy; ISSN:0387-1207; Vol.21; No.10; Page.1159-1177; (1979)

136. [Rudolf Schindler (1888--1968)--"father" of gastroscopy].Schäfer PK, Sauerbruch T. Z Gastroenterol. 2004 Jun;42(6):550-6.

137. A Flexible Fibrescope, using Static Scanning H. H. Hopkins & N. S. Kapany *Nature* 173, 39 - 41 (02 January 1954)

138. Hirschowitz B, Peters CW, Curtis LE. Preliminary report on a long fibres cope for examination of stomach and duodenum. Mich Med Bull 1957; 23:178–80.

139. Oshiba S, Watanabe A: Endoscopy of colon. Gastroenterol Enclose (Tokyo) 1965,7: 400-402, 159-170, 183-186

140. Clinical radiology and endoscopy of colon, Jacques W. A. J. Reeders, Gerd Rosenbusch, illustrated, Georg Thieme Verlag, 1994

141. Introduction M. A. Meyers (Ed-in-Chief) Abdom Imaging 27:231;2002

142. CT colonography: an overview. C. D. Johnson. Abdom Imaging 27:232-234;2002.

143. CT colonography: examination prerequisites. J. Lee. Abdom Imaging 27:244-252;2002.

144. Challenges for computer-aided diagnosis for CT colonography. R. M. Summers. Abdom Imaging 27:268-274;2002.

145. CT colonography: pitfalls and interpretation. H. M. Fenlon. Abdom Imaging 27:284-291;2002.

146. Reader strategies for CT colonography. E. G. McFarland. Abdom Imaging 27:275-283;2002.

147. Optimization of multidetector array acquisition parameters for CT colonography. C. H. McCollough. Abdom Imaging 27:253-259;2002.

148. Future directions in CT colonography. J. G. Fletcher. Abdom Imaging 27:301-308;2002.

149. MR colonography: status and perspective. W. Luboldt, M. M. Morrin. Abdom Imaging 27:400-409;2002.

150. Diagnostic performance of virtual colonoscopy. A. H. Dachman. Abdom Imaging 27:260-267;2002.

151. Oral contrast agents in MRI of the gastrointestinal tract. A. Giovagnoni, A. Fabbri, F. Maccioni. Abdom Imaging 27:367-375;2002.

152. Fletcher JG, Johnson CD, Welch TJ, et al. Optimization of CT colonography technique: prospective trial in 180 patients. Radiology216:704-711;2000.

153. Rex DK, Vining D, Kopecky KK. An initial experience with screening for colon polyps using spiral CT with and without CT colography (virtual colonoscopy). Gastrointest Endosc 50:309-313;1999.

154. Clinical radiology and endoscopy of colon, Jacques W. A. J. Reeders, Gerd Rosenbusch, illustrated, Georg Thieme Verlag, 1994

155. Gong F, Swain P, Mills T. Wireless endoscopy. Gastrointest Endosc. 2000;51:725-9

156. Jerome D. Wanye (ed). The development of the swallowable video capsule (M2A). Gastrointest Endosc 2000 52(1)

157. Iddan G, Meron G, Glukhovsky A, Swain P. Wireless capsule endoscopy. Nature 2000;405:417.

158. www.givenimaging.com/en-us/Innovative-Solutions/Capsule-Endoscopy/Pillcam-SB/HCP-Resources/Pages/What-Your-Patient-Can-Expect.aspx

159. Small bowel capsule endoscopy in 2007: Indications, risks and limitations Emanuele Rondonotti, Federica Villa, Chris JJ Mulder, Maarten AJM Jacobs, Roberto de Franchis *World J Gastroenterol* 2007 December 14; 13(46): 6140-6149

160. Agile patency system eliminates risk of capsule retention in patients with known intestinal strictures who undergo capsule endoscopy. Gastrointestinal Endoscopy Volume 67, Issue 6, May 2008, Pages 902–90

161. www.givenimaging.com/en-int/Innovative-Solutions/Capsule-Endoscopy/PillCam-Patency/Pages/default.aspx (2012)

162. www.givenimaging.com/en-us/Innovative-Solutions/Capsule-Endoscopy/Pages/default.aspx (2012)

163. Five years' experience with capsule endoscopy in a single center Taylan Kav, Yusuf Bayraktar *World J Gastroenterol* 2009 April 28; 15(16): 1934-1942

164. European Society of Gastrointestinal Endoscopy (ESnjmcvc\GE): Recommendations (2009) on clinical use of video capsule endoscopy to investigate small-bowel, esophageal and colonic diseases S. D. Ladas1, K. Triantafyllou1, C. Spada2, M. E. Riccioni2, J.-F. Rey3, Y. Niv4, M. Delvaux5, R. de Franchis6, G. Costamagna2and the ESGE Clinical Guidelines Committee Endoscopy 2010; 42: 220–227

165. Small Bowel Capsule Endoscopy: A Systematic Review *Sumeeta Mazzarolo, MD, and Patrick Brady, MD Southern Medical Journal* • Volume 100, Number 3, March 2007, 274-280

166. Encyclopaedia Britannica 2000 CD-ROM edition.

167. Gastrointestinal Motility, David grundy. 1985, MTP Press Limited.

168. Functional Electrical Stimulation. Rushton DN.Physiol Meas. 1997 Nov;18(4):241-75.

169. Nashold B S, Friedman H, Glenn J F, Grimes J H, Barry W F and Avery R 1972 Electromicturition in paraplegia *Arch. Surg.* 104 195–202

170. Bradley W E, Wittmers L E, Chou S N and French S A 1962 Use of a radio transmitter receiver unit for the treatment of neurogenic bladder. A preliminary report *J. Neurosurg.* 19 782–6

171. Brindley G S, Polkey C E, Rushton D N and Cardozo L D 1986 Sacral anterior root stimulators for bladder control
in paraplegia: the first 50 cases *J. Neurol. Neurosurg. Psychiatry* 49 1104–14

172. Kantrowitz, A.: Electronic Physiologic Aids. A Report of the Maimonides Hospital of Brooklyn, N.Y. 1963

173. Kralj A, Bajd T, Turk R, Krajnik J and Benko H 1983 Gait restoration in paraplegic patients: a feasibilitydemonstration using multichannel surface electrode FES *J. Rehab. Res. Dev.* 20 3–19

174. Kralj A and Bajd T 1989 *Functional Electrical Stimulation: Standing and Walking after Spinal Injury* (Boca Raton,FL: Chemical Rubber Company)

175. Holsheimer J, Bulstra G, Verloop A J and Hermens H 1993 Implantable dual channel peroneal nerve stimulator
Proc. Ljubljana FES Conf. (Ljubljana, 1993) ed R Jaeger and T Bajd (Kocevje: Slovenian Society of Medical
and Biological Eng.) pp 42–4

176. Djourno A and Eyries C 1957 Proth`ese auditive par excitation ´electrique `a distance du nerf sensoriel `a l'aide d'unbobinage inclus `a demeure *Presse M´ed.* 65 1417–23

177. Gastric Neurostimulation For Gastroparesis: Time To Pick Up The Pace. Selected Summaries. Henry J. Binder, M.D.Gastroenterology 2003;125:979-986.

178. Treatment of Gastroparesis with Electrical Stimulation. Zhiyue Un, Jameson Forster, Irene Sarosiek, And Richard W. Mccallum, Md. Review Article. Digestive Diseases and Sciences, Vol. 48, No. 5 (May 2003), pp. 837-848 (© 2003)

179. Gastric Electrical Stimulation At Proximal Stomach Induces Gastric Relaxation In Dogs. I. H. Xing, P. Brody,F J. Brodsky,F B. Larive,T J. Ponskyf & E. Soffer. Newogastroenteml Motil (2003) 15, 15-23

180. Electric Activity of the Colon in Subjects With Constipation Due to Total Colonic Inertia An Electrophysiologic Study. Ahmed Shafik, MD, PhD; Ali A. Shafik, MD; Olfat El-Sibai, MD, PhD; Randa M. Mostafa, MD, PhD. Arch Surg. 2003;138:1007-1011

181. Colonic pacing in patients with constipation due to colonic inertia Ahmed Shafik, Ali A.Shafik, Olfat EI-Sibai, Ismail Ahmed Med Sci Monit, 2003; 9(5): CR243-248

182. Rectal Pacing: Pacing Parameters Required for Rectal Evacuation of Normal and Constipated Subjects. Ahmed Shafik, M.D., Ph.D., and Olfat El-Sibai, M.D., Ph.D. Journal of Surgical Research 88, 181-185 (2000)

183. Colonic Pacing In The Treatment Of Patients With Irritable Bowel Syndrome: Technique And Results. Ahmed Shafik, Olfat El-Sibai, Ali A. ShaHk, Ismail Ahmed Frontiers in Bioseience 8, b l-5, January 1,2003

184. Grundfest-Broniatowski S, Moritz A, Olsen E, Kasick J, Ilyes L, Jacobs G, Nose Y. Electrical control of intestinal reservoirs in a chronic dog model. ASAIO Trans 1988 Jul-Sep;34(3):664-8.

185. Grundfest-Broniatowski S, Moritz A, Ilyes L, Jacobs G, Kasick J, Olsen E, Nose Y. Voluntary control of an ileal pouch by coordinated electrical stimulation. A pilot study in the dog. Dis Colon Rectum 1988 Apr;31(4):261-7.

186. Moritz A, Grundfest-Broniatowski S, Ilyes L, Kasick J, Jacobs G, Nose Y. Contractile response to electrical stimulation of the small intestine in anesthetized and awake dogs. Artif Organs 1989 Dec;13(6):553-7.

187. Moritz A, Grundfest-Broniatowski S, Ilyes L, Kasick J, Jacobs G, Olsen E, Nose Y. Electrical pulse train and single pulse stimulation of the small intestine: acute and chronic studies in the dog. Artif Organs 1989 Apr;13(2):116-22.

188. Mosse CA, Mills TN, Appleyard MN, Kadirkamanathan SS, Swain CP. Electrical stimulation for propelling endoscopes. Gastointest Endosc 2001;54(1):79-83.

189. PhD Thesis of Dr C.A. Mosse

190. Medical physics and biomedical engineering, Brown BH, Smallwood RH, et al, 1999, IOP Publishing Ltd.

191. Helmholtz, H. Studien uber electrische Grenzschichten. *Ann. Phys. Chem.* 7:337-382, 1879.

192. The kinetics of electrode reactions and the electrode material Roger Parsons Surface Science Volume 2, 1964, Pages 418–435

193. Warburg, E. Ueber das Verhalten sogenannter unpolarisbarer Electoden gegen Wechselstrom. *Annalen der Physik und Chemie, vol.* 67 pp, 493-499, 1899.

194. Principles of Applied biomedical instrumentation (3rd), Geddes LA, Baker LE, 1989, Wiley.

195. Neural prostheses fundamental studies, Agnew WF, McCreery DB, (ed) 1990, Prentice Hall.

196. Atrial pacing thresholds measured in anaesthetised patients with the use of an oesophageal stethoscope modified for pacing. Pattison CZ; Atlee JL 3d; Mathews EL; Buljubasic N; Entress JJ. Anaesthesiology, May 1991, 74(5) p854-9.

197. Thresholds for transesophageal atrial pacing. Dick M 2d, Campbell RM, Jenkins JM. Cathet Cardiovasc Diagn 1984; 10(5):507-13

198. Use of the pill electrode for transesophageal atrial pacing. Jenkins JM, Dick M, Collins S, O'Neill W, Campbell RM, Wilber DJ. Pacing Clin Electrophysiol 1985 Jul;8(4):512-27.

199. Sitdikov FG, Gil'mutdinova RI, Minnakhmentov RR, Gizzatullin AR. Effect of electrical stimulation of vagus nerves on cardiac activity in sympathectomized rats during postnatal ontogeny. Bull Exp Bio Med 2003;6:534-6.

200. Lewis ME, Al-Khalidi AH, Bonser RS, Clutton-Brock T, Morton D, Paterson D, Townend JN, Coote JH. Vagus nerve stimulation decreases left ventricular contractility in vivo in the human and pig heart. J Physiol. 2001 Jul 15;534(Pt. 2):547-52.

201. Dehghani: UCL Medical Physics: Construction of simple finite element representation.

202. Donaldson N de N and Donaldson P E K 1986 Performance of platinum stimulating electrodes, mapped on the limit-voltage plane. Part 2: corrosion *in vitro. Med. Biol. Eng. Comput.* 24 424–30

203. Impedance Characterization and Modeling of Electrodes for Biomedical Applications Wendy Franks, Iwan Schenker, Patrik Schmutz, and Andreas Hierlemann IEEE Transactions on Biomedical Engineering, Vol. 52, No. 7, July 2005 1295-1302

204. Fricke, H. The theory of electrolytic polarization. *Phil. Mag.* 14:310-318, 1932.

205. Zimmerman, E. C. The influence of temperature on polarization capacity and resistance. *Phys. Rev.* 35:543-555, 1930.

206. Randles, E. B. Rapid electrode reactions. *Discuss. Faraday Soc.* 1:11-19, 1947.

207. Geddes, L. A., and L. E. Baker. *Principles of Applied Biomedical Instrumentation,* 1 st Ed. New York: John Wiley and Sons, 1968, 479 pp.

208. Sluyters-Rehbach, M., and J. H. Sluyters. Sine wave methods in the study of electrode processes. *Electro-anal. Chem.* 4:1-121, 1970.

209. B. Onaral and H. P. Schwan, "Linear and nonlinear properties of platinum electrode polarization. I. Frequency dependence at very low frequencies," *Med. Biol. Eng. Comput.*, vol. 20, pp. 299–306, 1982.

210. E. T. McAdams and J. Jossinet, "Physical interpretation of Schwan's limit voltage of linearity," *Med. Biol. Eng. Comp.*, vol. 32, pp. 126–30, 1994.

211. G.T.A. Kovacs "Introduction to the theory, design and modelling of thin-film microelectrodes for neural interfaces", in Enabling Technologies for Cultured Neural Networks, D.A.Stenger and T.M. McKenna, Eds. London U.K.: Academic, 1994, pp. 121-165.

212. Ragheb, T., and L. A. Geddes. The polarization impedance of common electrode metals operating at low current density. *Ann. Biomed. Eng.* 19:151-163, 1991.

213. Schwan H.P. Determination of biological impedance. In: Nastuk, W., ed. Physical techniques in biological research, New York: New York Academy of Sciences; 1963: pp. 323-407.

214. Geddes, LA: Electrodes and the measurement of Bioelectric events. New York: Wiley Interscience; 1972

215. MacDonald, JR. Impedance spectroscopy. New York Wiley Interscience; 1987

216. Speden, R. N. (1965), The Effect of Some Volatile Anaesthetics on The Transmurally Stimulated Guinea-Pig Ileum. British Journal of Pharmacology and Chemotherapy, 25: 104–118

217. Crosby WH and Kugler HW: Intraluminal biopsy of the small intestine: the intestinal biopsy capsule. The American Journal of Digestive Diseases, May 1957, 2 (5): 236–241.

218. Swain CP, Mosse CA, Burke P, et al. Remote propulsion of wireless capsule endoscopes. Gastrointest Endosc 2002; 55: AB88

219. Fritscher-Ravens A, Burke P, Mills T, Mosse CA, Mylonaki M, Swain P: Development and testing of an electrically propelled capsule endoscope in man. Gastrointest Endosc, 2003; 57(5): AB84.

220. Paul Swain, Tim Mills, Brian Kelleher, Loren Schmitz, Sandy Mosse, Paul Burke, Keitch Ikeda, Annette Fritcher-Ravens, Radio-controlled Movement of a Robotic Endoscope in the Human Gastrointestinal Tract, Gastrointest Endosc 2005; 61(5): AB101.

Picture references
(All images from 2012)

2.1 http://www.encognitive.com/images/digestive-system-2.jpg
2.2 http://www.baileybio.com/plogger/images/anatomy___physiology/12._powerpoint_-_digestive_system/wall_of_gi_tract.jpg
2.3 http://www.patient.co.uk/images/OM1207a.jpg
2.4 http://www.ganfyd.org/images/thumb/9/95/Oesophagitis_endoscopy.jpg/180px-Oesophagitis_endoscopy.jpg
2.5 http://1.bp.blogspot.com/_bzOQIIUFKBE/TTNujL2XjjI/AAAAAAAAARU/-ozADzWXt2U/s1600/chron-s-disease2.JPG
2.6 http://trialx.com/curetalk/wp-content/blogs.dir/7/files/2011/05/diseases/Adenocarcinoma_Of_The_Esophagus-1.jpg
2.7 http://gastrolab.1g.fi/ja/ja1017/slides/1.jpg
2.8 http://trialx.com/curetalk/wp-content/blogs.dir/7/files/2011/05/diseases/Gastric_Adenocarcinoma-1.jpg
2.9 http://www.medgadget.com/archives/img/crohn.jpg
2.10 http://www.gastrointestinalatlas.com/JejunalLymphoma5.jpg
2.11 http://www9.biostr.washington.edu/hubio511/RadAbdo/frames.htm
2.12 http://www.mtbakerimaging.com
2.13 http://www.mr-tip.com/exam_gifs/mr_colonography_gadolinium_per_rectum_1.gif, http://radiology.rsna.org/content/223/1/248/F2.small.gif
2.14 http://www.rbmedical.co.uk, http://www.generalmanual.com , http://www.zgrum.com/, http://img.medicalexpo.com, http://www.suatozden.com/
2.15 www.givenimaging.com

3.1 http://faculty.etsu.edu
3.2 http://www.ncbi.nlm.nih.gov/pmc/article/PMC2544441/figure/f4
3.3 PhD of Mosse

B. (All Pictures); F Netter M.D. © CIBA